UNIVERSIDAD DE CHILE
FACULTAD DE CIENCIAS FÍSICAS Y MATEMÁTICAS
DEPARTAMENTO DE INGENIERÍA QUÍMICA, BIOTECNOLOGÍA Y MATERIALES

DESIGN OF A SOLAR-BIOGAS HYBRID ENERGY SYSTEM FOR A MINING PROCESS IN CHILE CONSIDERING TECHNICAL, ECONOMIC AND ENVIRONMENTAL ASPECTS

TESIS PARA OPTAR AL GRADO DE MAGÍSTER EN CIENCIAS DE LA INGENIERÍA, MENCIÓN QUÍMICA

MEMORIA PARA OPTAR AL TÍTULO DE INGENIERA CIVIL QUÍMICA

JAVIERA ANDREA VERGARA ZAMBRANO

PROFESOR GUÍA:
FELIPE DÍAZ ALVARADO

PROFESOR CO-GUÍA:
WILLY KRACHT GAJARDO

MIEMBROS DE LA COMISIÓN:
FRANCISCO GRACIA CAROCA
MARÍA ELENA LIENQUEO CONTRERAS
LINE ROALD

Este trabajo ha sido parcialmente financiado por:
ADVANCED MINING TECHNOLOGY CENTER (AMTC)

SANTIAGO DE CHILE
2021

Abstract

RESUMEN DE LA TESIS PARA OPTAR AL TÍTULO DE:
INGENIERA CIVIL QUÍMICA Y GRADO DE MAGÍSTER EN CIENCIAS DE LA INGENIERÍA, MENCIÓN QUÍMICA
POR: JAVIERA ANDREA VERGARA ZAMBRANO
FECHA: 25/11/2021
PROF. GUÍA: FELIPE DÍAZ ALVARADO

DESIGN OF A SOLAR-BIOGAS HYBRID ENERGY SYSTEM FOR A MINING PROCESS IN CHILE CONSIDERING TECHNICAL, ECONOMIC AND ENVIRONMENTAL ASPECTS

One of the main challenges of the mining industry from an environmental prospect is the growing increase in energy consumption. Over the next ten years, energy demand is expected to increase by 41% since mines are getting older and deeper, a change in the copper production structure and the increase in seawater consumption. Within the energy demand of a mining process, final energy consumption and electricity generation are the primary sources of greenhouse gas (GHG) emissions. Thus, decreasing energy consumption and studying new energy sources with a lower environmental impact becomes necessary. In this context, the use of hybrid renewable energy systems has proven to be an attractive option regarding costs, operability, and environmental impact. Besides, they are more resilient than single energy systems.

The interest of this research is to design a hybrid renewable energy system to supply the electrical demand of a mining process and evaluate the possible trade-offs that may exist. For this purpose, a multi-objective optimization problem has been formulated considering two objectives: minimizing annual costs and minimizing GHG emissions. The calculation of GHG emissions includes direct emissions associated with fuel combustion and indirect emissions associated with electricity purchase. The proposed energy system considers solar energy and biogas generated from organic waste as primary energy sources, two energy storage systems (lithium-ion batteries and hydrogen storage), and a connection to the electrical grid. The approach is applied to a case study that considers a typical mine located in the North of Chile. The model has been implemented in the computational program Julia and solved using Gurobi.

In the first instance, the problem has been solved considering each objective function separately, and then the multi-objective problem has been solved using the ϵ-constraint method. Finally, a sensitivity analysis has been performed, considering the variation in energy demand, biogas availability, costs, and grid emissions factor. The results show that biogas and solar energy are attractive options to reduce costs and emissions in the mining industry. However, the biogas does not have the potential to cover the demand as it is limited by the biomass available. Regarding the system configuration, all the proposed technologies were selected in the simulations. The energy was primarily stored in batteries; nonetheless, there is no preference between storage systems considering GHG emissions. The use of energy storage systems showed to increase the costs. However, these systems are needed to use more renewable energy and reduce emissions. A trade-off between costs and emissions was observed. Therefore, the prioritization of one criterion will significantly impact the other. Lastly, a second environmental criterion is suggested to evaluate the impact of renewable energy and energy storage systems such as abiotic depletion or the use of land.

Resumen

RESUMEN DE LA TESIS PARA OPTAR AL TÍTULO DE:
INGENIERA CIVIL QUÍMICA Y GRADO DE MAGÍSTER EN CIENCIAS DE LA INGENIERÍA, MENCIÓN QUÍMICA
POR: JAVIERA ANDREA VERGARA ZAMBRANO
FECHA: 25/11/2021
PROF. GUÍA: FELIPE DÍAZ ALVARADO

DESIGN OF A SOLAR-BIOGAS HYBRID ENERGY SYSTEM FOR A MINING PROCESS IN CHILE CONSIDERING TECHNICAL, ECONOMIC AND ENVIRONMENTAL ASPECTS

Uno de los principales desafíos de la industria minera desde el punto de vista medioambiental es el aumento en el consumo de energía. Se espera que en los próximos diez años la demanda de energía aumente en un 41% debido a que las minas son cada vez más antiguas, a un cambio en la estructura de producción y a un aumento en el uso de agua de mar. Dentro de la demanda energética de un proceso minero, el consumo de energía final y la generación de electricidad son las principales fuentes de emisiones de gases de efecto invernadero (GEI). Así, es necesario disminuir el consumo de energía y estudiar nuevas fuentes con un menor impacto ambiental. En este contexto, el uso de sistemas híbridos de energía renovable ha demostrado ser una opción atractiva en cuanto a costos, operatividad e impacto ambiental. Además, son más resilientes que los sistemas de energía renovable en solitario.

El objectivo de esta investigación es diseñar un sistema híbrido de energía renovable para abastecer la demanda eléctrica de un proceso minero y evaluar los diferentes *trade-offs* que pueden existir. Para esto, se formuló un problema de optimización multi-objetivo considerando la minimización de los costos anuales y las emisiones de GEI. El cálculo de este último incluye las emisiones directas asociadas al proceso de combustión y las emisiones indirectas por la compra de electricidad. El sistema propuesto considera energía solar y el biogás generado a partir de residuos orgánicos como principales fuentes de energía, dos sistemas de almacenamiento (baterías de ión-litio y almacenamiento de hidrógeno) y conexión a la red eléctrica. El modelo es aplicado a un caso de estudio que considera a una mina típica ubicada en el norte de Chile.

El modelo se implementó en Julia y se resolvió utilizando Gurobi. Primero se resolvió el problema monoobjetivo y luego el problema multiobjetivo utilizando el método ϵ-*contraint*. Por último, se realizó un análisis de sensibilidad, variando 4 parámetros: demanda eléctrica, disponibilidad de biogás, costos del almacenamiento de hidrógeno y el factor de emisiones de la red eléctrica. Los resultados confirman que existe un *trade-off* entre los costos y las emisiones, y que la priorización de un criterio afectará significativamente al otro. El uso de sistemas de almacenamiento podría ayudar a reducir las emisiones de GEI, sin embargo los costos aumentarían. En todas las simulaciones, las configuración del sistema considera todas las tecnologías propuestas, y la mayor parte de la energía es almacenada en baterías, aún cuando no existe una preferencia entre los sistemas de almacenamiento en cuanto a emisiones de GEI. Se sugiere incluir un segundo criterio medioambiental para evaluar el impacto de las energías renovables y los sistemas de almacenamiento. Por último, el biogás y la energía solar muestran ser opciones atractivas para reducir los costos y las emisiones en la minería. No obstante, el biogás no tiene el potencial para cubrir la demanda, ya que está limitado por la biomasa disponible.

A mi Lela, por su cariño, enseñanzas y apoyo

Agradecimientos

Quiero partir agradeciendo a mi comisión. Felipe, gracias por tu apoyo, por enseñarme que siempre hay otra manera de ver las cosas y por tu disposición a escucharme y resolver mis dudas. Willy, gracias por el apoyo durante este proceso y por las oportunidades que me has dado. Profesor Francisco Gracia, gracias por incentivarme a buscar mi área de investigación, por su apoyo y las oportunidades a lo largo de estos años y por enseñarme una mirada diferente de la docencia universitaria. A la profesora Line Roald le agradezco su disposición y motivación para ser parte de este desafío. Finalmente, agradezco a la profesora María Elena por aceptar ser parte de mi comisión.

Gracias a mi familia, por incentivarme a estudiar y apoyarme a lo largo de este camino. Especialmente agradezco a mi mamá y mis abuelos Graciela y Sergio por siempre preocuparse por que no me faltara nada. Gracias a mi hermano por apoyarme siempre. Gracias a Lidia por estar con nosotros todos estos años. Finalmente, no puede dejar afuera a Pablito. Gracias por todas las veces que me fuiste a dejar y a buscar en todos estos años, y por preocuparte de mi.

Gracias a mis amigas de la vida. Javi, gracias por tu eterna amistad, por creer en mi, entenderme y escucharme. Montse, gracias por todas las aventuras, por haber vivido esta etapa universitaria juntas y por estar ahí siempre.

Gracias a mi grupo de taller. Ami y Consu que les puedo decir. Agradezco infinito haberlas conocido y espero que nuestra amistad dure mucho tiempo más. Javier, mi eterno compañero de trabajos. Agradezco que el destino nos pusiera juntos en primer año. Gracias por la paciencia y tu preocupación.

Gracias a mis amigos de plan común: Camilo, Cata, Iván, Javi, Jipi, Maca, Mandiola, Ojeda, Pauli, Sofi, Tata y Vale por su amistad todos estos años. Plan común y mi paso por la universidad no hubiese sido lo mismo sin ustedes. Gracias también a la Tita por haber sido mi primera amiga en la universidad y por todo su apoyo.

Gracias a la UVM, por darme la oportunidad de crecer y desarrollarme y por todos los momentos que vivimos como grupo.

Gracias Willy por tu apoyo, por resolver mis infinitas dudas, y por incentivarme en este proceso.

Por último, quiero agradecer a todas las personas con las que compartí de alguna manera durante estos años. Especialmente a la Gina y toda la gente de IQBT.

Contents

List of Tables

List of Figures

Chapter 1

Introduction

1.1. Background

The mining industry in Chile and its challenges

Mining, specifically copper mining, is the most significant economic activity in Chile [1]. It represents 12% of the country's GDP[1], approximately 56% of the exports, and 16% of the foreign investment [2]. The sector has steadily grown in the past decades, reaching a production of 5.7 million metric tons of copper in 2020. Consequently, Chile is the world's leading copper producer, accounting for 28% of the production [2].

Nowadays, the mining industry faces many challenges and problems. From an environmental perspective, one of the main issues is the steady increase in energy consumption [3]. It is expected that in the next ten years, the energy demand will increase by 41% [4] due to three main reasons. Firstly, mines are getting older and deeper, leading to lower ore grades, harder rock, and longer material transportation distances [5]. This situation has caused the extraction and processing of larger volumes of ore to maintain the same production, which increases the use of energy in crushing and grinding processes. Secondly, there is a change in the copper production structure in Chile. A majority production of copper concentrates is expected over electrowinning cathodes due to the gradual depletion of copper oxide deposits. Consequently, more concentrator plants are used, which are a highly intensive process in electrical energy [3]. Thirdly, the use of seawater has increased since the restrictions on water supply through continental sources and the preponderance in the production of concentrates, which is also intensive in water resources [4]. The desalination of seawater and its pumping is a high-intensity energy process [5].

The energy demand of a mining process depends on the primary energy in fuels directly used during production, the primary energy needed to produce the electricity used, and the primary energy requirements for the materials and infrastructure needed [6]. From this, the final consumption of energy and electricity generation are the primary source of Greenhouse Gas (GHG) emissions into the atmosphere [7]. In fact, in 2019, the copper mining industry in Chile was responsible for 16,366 thousand tons of CO_2-eq, which corresponds to approximately 15% of the national GHG emissions [8]. Therefore, it is necessary to decrease energy consumption and study new sources with lower environmental impact [9; 10].

[1] GDP: Gross Domestic Product.

Integration of renewable energy in mining

In Chile, the mining industry is one of the country's primary energy consumers. Actually, according to the Chilean Copper Commission (COCHILCO), the total amount of energy consumed by the mining sector in 2018 was 176,745 TJ (including electricity and fuels), which accounts for 14% of the country's total energy consumption that year [11]. Broken down the data by type of energy, electricity consumption in the same period was 33% of the national consumption. Meanwhile, diesel consumption, the primary fuel used in this sector, accounted for 14%.

The electricity used in copper mines across Chile is supplied by the National Electrical System (SEN) [4], mainly relying on fossil fuels, as seen in Figure 1.1. However, in the last few years, the Chilean power sector has been transitioning from fossil fuels to renewable energy sources such as solar, wind, biomass, and small hydro [12]. These have some benefits as lower carbon emissions and the reduction of air pollution. Nonetheless, there is still a dependence on fossil fuels as renewable energy has an intermittency nature [13].

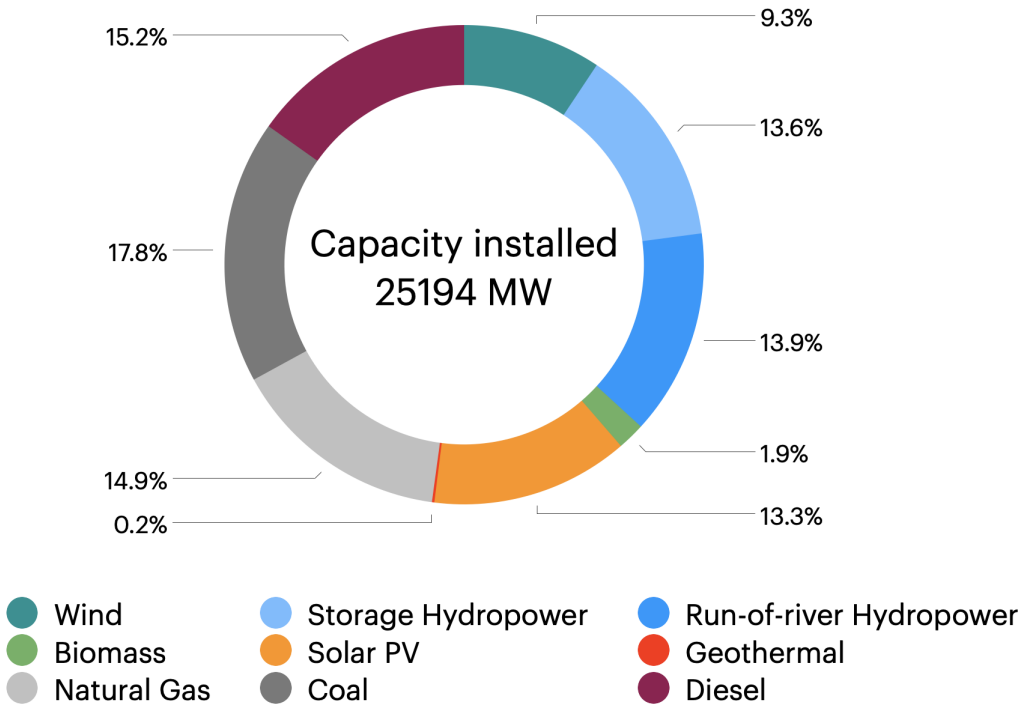

Figure 1.1: Power capacity installed of the National Electrical System (SEN) by fuel and technology. Source: Own elaboration based on the data obtained from [14].

Some mines worldwide have started incorporating renewable energy, and several projects are planned for the following years. In Chile, the *Gabriela Mistral* division of CODELCO uses solar thermal energy in the electrowinning operation, replacing about 80% of the fossil fuel used in this stage [15]. Also, *Minera Los Pelambres*, belonging to Antofagasta Minerals, uses solar photovoltaic energy to supply around 40% of its energy requirements [16].

In the literature, there is ongoing research on the use of renewable energy in mining. For instance, Castillo et al. [17] presented different photovoltaic power configurations as an alternative to partially feed the electrorefining process. Also, the feasibility of using solar energy for rock grinding has been studied by Pamparana et al. [18], showing that its implementation is profitable by complementing the photovoltaic (PV) panels with external batteries. The storage system is included to increase the reliability of the system. In later studies, Pamparana et al. [19; 20] analyzed the effect that the uncertainty of rock hardness has on the performance of the PV-battery system, finding that uncertainty and variability of the ore impact the size of all components.

Other studies consider more than one renewable energy source in the design of energy systems for copper production. For example, Amusat et al. [21] studied a system containing two solar energy generation alternatives and three energy storage alternatives (Pumped Hydraulic, Adiabatic Compressed Air, and Molten Salt) to supply the electrical and thermal demands of a mine in Chile. This study was extended in [22] and [23], including variability, costs, and reliability in the design. The results suggested that significant cost savings are possible for minor loss in reliability and performance, and oversizing is often required to guarantee energy security. In another study found in this context, Vyhmeister et al. [24] explored a solar-wind system combined with hydrogen energy storage. The findings showed that the system could partially supply the energy mining requirements in Chile and, at the same time, improve the overall environmental sustainability of the copper mining industry. Finally, Moreno-Leiva et al. [9] provide recommendations for developing methods to design renewable energy systems for copper production. The first recommendation is to improve the energy demand models by considering the effect of the geography and location of the mines on both the demand itself and the availability of renewable resources.

Use of Hybrid Renewable Energy Systems

Energy systems that include more than one type of renewable energy are known as hybrid renewable energy systems (HRES). They can improve the performance over what could be achieved by each renewable energy system working separately [25]. Among the studies about HRES design, few consider biogas [26–28] and almost non-applied in the mining sector. However, this biofuel has several advantages, presenting the potential to provide diversified energy services such as electricity and heating and reduce GHG emissions [29].

In this context, the interest of this research is to assess the potential of a hybrid renewable energy system that includes solar energy and the use of biogas for a mining process in Chile. Given that most mines are located in the Atacama Desert, one choice for renewable energy is solar power, using photovoltaic technology [24]. On the other hand, biogas energy is independent of climate conditions, and it is highly predictable as it depends on the availability of biomass [29]. In particular, organic wastes can be used as a feedstock, which production in cities is highly stable and constitutes around 50% of the Municipal Solid Wastes [30]. These reasons make the combination of solar energy with biogas a potential solution to supply the energy mining requirements in Chile.

This study also pretends to contribute to the evaluation of different energy storage systems like hydrogen, as it is expected to have a key role in the decarbonization of the mining sector [31]. In addition, this work shows how renewable energy's variability and its intermittency nature can be considered in the preliminary stage of the design of energy systems and provides an insight into how these factors impact the cost, size, configuration, and performance of hybrid renewable energy systems.

1.2. Research Questions and Goals

The main goal of this thesis is to design and evaluate a solar-biogas hybrid energy system for a mining process in the north of Chile, considering technical, economic, and environmental aspects. More precisely, this study pretends to answer the following research questions:

- **RQ1:** How can an energy requirement of a mining process in Chile be supplied with solar energy and biogas?
- **RQ2:** What is the optimal configuration of a solar-biogas hybrid energy system that minimizes costs and environmental impacts when used to satisfy a given energy requirement in a mining process?
- **RQ3:** Which trade-offs can be found?

In order to answer each question and achieve the primary goal, this thesis has the following specific goals:

- **SG1:** Characterize the energy demand of a mining process in Chile and define the components of a solar-biogas hybrid energy system to satisfy the electric energy requirements of a mining process.
- **SG2:** Formulate and solve a multi-objective optimization problem to find the best configuration of a solar-biogas hybrid energy system to reduce economic costs and GHG emissions in an applied case for the mining industry in Chile.
- **SG3:** Analyze possible trade-offs that can exist and their impacts.

1.3. Research scopes

This study is focused on the preliminary design and sizing of a grid-connected hybrid renewable energy system to supply the electrical demand of a mining process in Chile. It is supposed that the mine is situated in the Antofagasta Region, where the world's largest copper reserves and the principal mining processes of Chile are located [32]. Besides, the solar radiation level is high [33]. The mining activities are not modeled, and the energy efficiency of the mining operations is not considered.

The electrical load estimation takes into account all the electrical requirements of the mine operations. The system considers solar energy and biogas as the primary energy sources. Solar energy has a great potential to provide energy in the area, and biogas is a controllable energy source that can compensate for the intermittency of solar energy. On the other hand,

lithium batteries and hydrogen storage are evaluated for energy storage. The effect of daily, seasonal, and climate-based variability on the sizing of the energy generation and storage units is also considered.

The sizes and capacities for each technology are modeled through the minimization of a multi-objective optimization problem. Two aspects are evaluated: economic and environmental. The economic objective involves the costs of installing each technology and fixed operation and maintenance costs per year. The environmental objective function considers direct GHG emissions associated with fuel combustion and indirect GHG emissions associated with the purchase of electricity (emissions scope 1 and 2 defined by the GHG Protocol [34]). An environmental analysis from a life cycle perspective is not included.

1.4. Thesis structure

This thesis is composed of 5 main chapters. In chapter 1, a brief introduction of the work is presented. Also, the research questions, goals, and scopes of the present study are included. Chapter 2 presents a literature review on hybrid renewable energy systems and optimization techniques for designing and sizing them. Chapter 3 describes the research methodology used in this work, including a description of the case study, the data collected, and the optimization problem formulation. Chapter 4 presents and discusses the results obtained for the optimization problem considering different scenarios. Chapter 5 summarizes the main findings and conclusions. Besides, the answers to the research questions of this study are provided.

Chapter 2

Theoretical Framework

This chapter presents the theoretical framework to describe the current knowledge on hybrid renewable energy systems and their design. Firstly, a background on hybrid renewable systems is provided, describing the main characteristics of their components. Then, different configurations and considerations for the design of these systems are presented. The chapter ends with a summary of optimization techniques used for the design of hybrid renewable energy systems.

2.1. Hybrid Renewable Energy Systems

Hybrid renewable energy systems (HRES), also known as hybrid energy or power systems, are the combination of two or more renewable energy sources integrated with power control equipment and optional storage systems. They can increase the system efficiency and optimize production and energy management [35; 36].

HRES are attractive configurations that can be used in different applications. In particular, they can compensate for the unreliability of single renewable energy sources such as solar or wind, which do not deliver constant power. Through their complementarity, their combination can provide a continuous electrical output, improving the system's performance and making it more resilient [35]. However, a disadvantage of these systems is that they are more complex than single-source systems because they include different sources and devices, needing a more sophisticated control system, which also makes the global system costs higher [37].

Hybrid renewable energy systems have different components. Their main characteristics are presented in the next section.

2.1.1. Components

The main components of a HRES are energy sources, energy storage systems, converters, and loads.

Energy sources

Energy can be classified into two categories based on the source's replacement: renewable and non-renewable [38]. On the one hand, renewable energy comes from sources that cannot run out or can be naturally replaced in a human timescale [39]. The five main sources are:

- Hydropower: Also known as water power, is generated using the mechanical energy of flowing water by forcing it to pass through a penstock, which turns a turbine and generates electricity [40]. Hydropower generation has many advantages. It has a high level of reliability, high efficiency, and low operating and maintenance costs. In contrast, the main disadvantages are high investment costs and dependence on water availability [38].

- Wind energy: Wind is used to produce electricity by converting the kinetic energy of air in motion to mechanical energy using a turbine [41]. Wind energy has economic and environmental advantages since it reduces GHG emissions and can diminish electricity costs. However, its intermittency and unpredictable nature limit its use unless large-scale energy storage or access to the grid is available [38].

- Solar energy: It corresponds to the sun's energy converted into thermal or electrical energy. There are three ways in which solar energy can be harnessed: Photovoltaics (PV), where sunlight is directly converted to electricity by electronic devices called solar cells; Concentrated Solar Power (CSP), which uses mirrors to concentrate solar rays to produce steam, which drives a turbine and generates electricity; and Solar Heating and Cooling (SHC), which collects the thermal energy from the sun and uses this heat to provide hot water, heating, and cooling [42; 43]. Solar energy is one of the most abundant renewable resources on earth. Nevertheless, the main problem is its intermittency, as it depends on the sunshine. Like in wind energy, this results in high operational costs [38].

- Geothermal energy: It corresponds to thermal energy generated and stored within the earth, caused by the temperature difference between the earth's core and surface [44]. For electricity production, wills are drilled into underground reservoirs to tap steam and hot water that drive turbines linked to electricity generators [45]. One of the main advantages of geothermal energy is low emissions and that it depends on an abundant and reliable energy source. Nonetheless, the drawback is that the geothermal plant's locations are limited [38].

- Bioenergy: It is a form of energy generated from organic matter known as biomass [46]. Examples of biomass are waste of plants and animals, agriculture and forest residues, and organic components of municipal and industrial wastes. Biomass stores the energy of sunlight into chemical bonds and releases it when these bonds are broken [47]. There are different methods of harnessing bioenergy: "traditional methods," which refers to the combustion of biomass, commonly used for heating, and "modern methods," which includes bio-refineries, biogas produced through anaerobic digestion, wood pellet heating systems, among others. One of the significant advantages of bioenergy is its flexibility. It can generate electricity, heat, or transport fuels, and also it can be stored as a solid, liquid, and gaseous energy carrier. Although its combustion produces carbon dioxide, it can significantly reduce GHG emissions as bioenergy sources absorb CO_2 during their growth. Despite this, one of its withdraw is that it is not as efficient as fossil fuels [38; 48].

On the other hand, non-renewable energy is based on sources that will run out and will not be replaced in a human timescale [39]. Most non-renewable energy sources are fossils fuels such as coal, petroleum, and natural gas [38]. As this work focuses on renewable energy, it will not be detailed on this topic.

Energy Storage Systems

Energy storage systems (ESS) are devices that capture the energy produced at one time and release it later when it is needed. They are essential for energy systems' operation as they ensure the continuity of energy supply and improve the system's reliability [49]. Besides, they can be used as an alternative to backup generators such as diesel-based systems, reducing contaminating gas emissions.

ESS can be classified according to the type of energy they store, as seen in Figure 2.1. Each one has different cost, performance, and scalability characteristics that have to be considered when selecting a suitable storage technology [49]. For instance, for short-term applications, energy storage systems have the primary goal of supporting the excess/deficit of energy and guaranteeing the system's security and power load. Conventional batteries are used in most cases since they are energy efficient and have lower costs than other technologies. In contrast, energy storage systems aim to provide the demand for a more extended period for larger applications. One of the most suitable technology is pumped hydro, but only in specific locations (where the source is available). It is important to note that the correct energy management strategy's choice should guarantee optimum performance for the whole hybrid energy system.

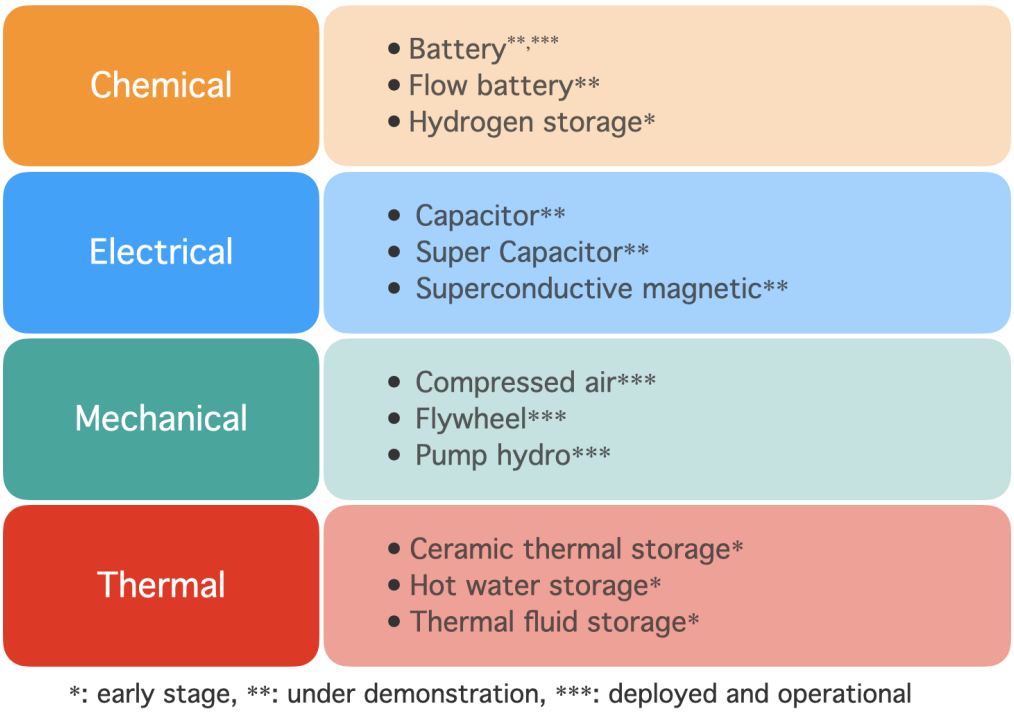

Figure 2.1: Type of energy storage system. Own elaboration based on [50; 51].

Recently hydrogen storage has appeared as a promising technology to be used as a backup for hybrid energy systems since fuel cells have higher efficiency, lower maintenance, and lower emissions than diesel systems [52]. Furthermore, hydrogen is an energy vector that can be produced renewably. Nonetheless, this technology needs more control, security, and

associated equipment for proper operation [53].

Converters

Converters or power converters are devices for adapting the source of electrical energy to a given receiver by converting it [35]. They can convert direct current (DC) into alternating current (AC) or vice versa, change the current voltage or frequency, or do a combination of these. Based on the form (frequency) on the two sides, converters can be divided into four categories, as seen in Figure 2.2. Commonly, it is called rectifier to a converter when the average power flow is from the AC to the DC side, and inverter when the average power flow goes from the DC to the AC side [54]. The other two converters do not have a specific name.

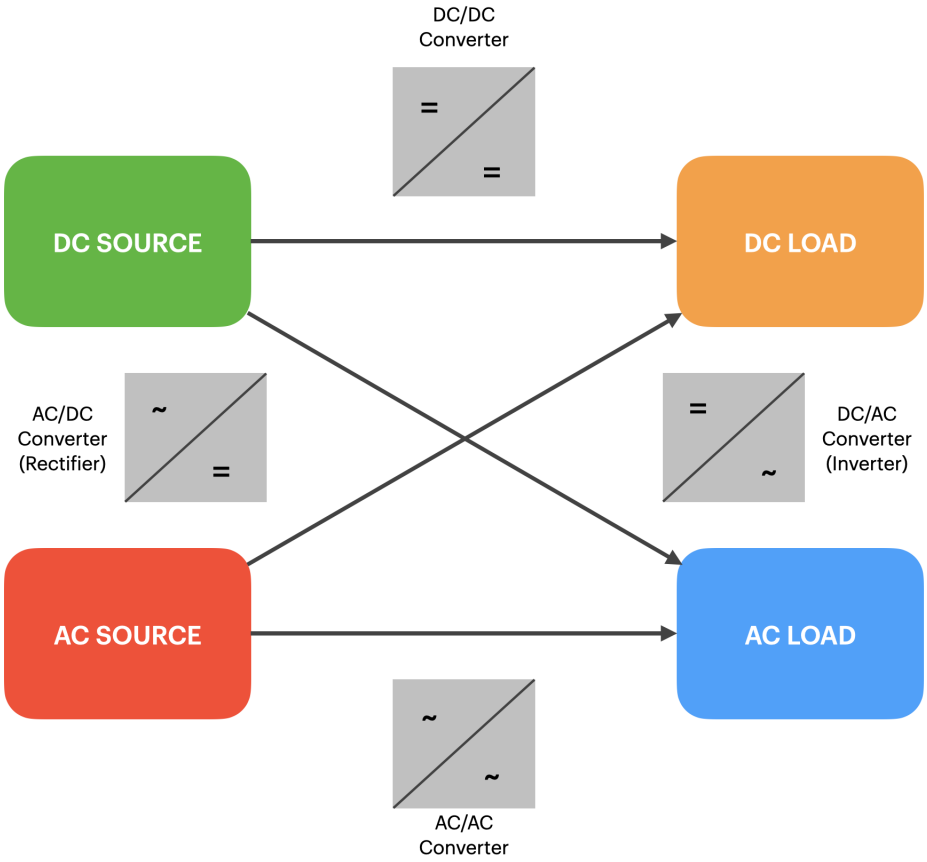

Figure 2.2: Sources and loads supplied by various converters. Source: Own elaboration based on [35].

Loads

An electrical load is a device that converts electrical energy into other forms of energy like heat, light, or mechanical energy [55]. Depending on the type of bus, loads are classified into AC or DC loads. The energy demand by a load at a particular time is represented in an electrical load profile. The profile varies according to the time of the day, weather, seasons, and customer load types [56]. An example of an electrical load for an industrial consumer is shown in Figure 2.3. For this type of consumer, relatively minor variations in the demand are observed from hour to hour.

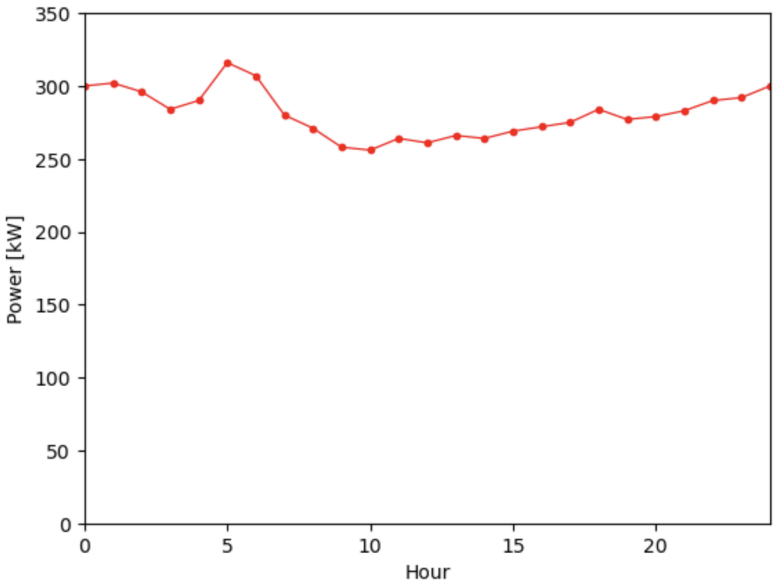

Figure 2.3: Average load curve for an industrial consumer. Own elaboration based on [57].

2.1.2. Configuration

The configuration of a HRES can be classified in different ways. The most common ones are based on the grid connection and its components integration method [52]. In the first categorization, HRES are distinguished according to their stand-alone or grid-connected operation. When a system is connected to the grid is called on-grid system. This configuration ensures that the demand is provided in energy deficit situations and increases the system's performance by taking advantage of the energy excess. Otherwise, when a system is isolated from the grid is called isolated system. This configuration has problems related to reliability and performance since there are limited resources available, and it has to discharge the energy excess. For these reasons, isolated systems are generally used when the connection to the grid is impossible or very expensive.

On the other side, concerning the integration method of its components, a HRES is classified depending on the internal connection bus's nature. Three types can be distinguished: direct current (DC), alternating current (AC), or hybrid. The DC buses are commonly used for low power as they are simpler to use and reduce losses, avoiding technical problems related to power quality. However, they require a large number of conversion elements as most loads are supplied in AC. Conversely, AC buses are preferred in medium and high production applications due to the technical simplicity of operating at higher voltages than DC, reducing the system's internal losses. The disadvantage is that it requires more elements for power quality correction, increasing the system's complexity and cost. Finally, a hybrid bus uses both buses (AC and DC), interconnecting generation and consumption of the same type. It has the advantage of reducing the number of converters, but the system's control is more complicated than using only one type of bus.

2.1.3. Design

Designing a hybrid renewable energy system consists mainly of finding each component's proper sizing since it is a fundamental aspect of its techno-economic feasibility [58]. Usually, one or more performance criteria should be evaluated like economic, reliability, and environmental, subject to different constraints, such as operational and technological [59]. For this, optimization techniques have shown to be useful tools [60].

In order to design a HRES, the following perspectives should be considered [36]:

- Load characterization: To describe the load is necessary to estimate the energy demand through time, identify if it is critical or not, and determine the reliability that the system requires.
- Potential of renewable and conventional energy: Renewable source's potential can be estimated from statical data considering the location, weather conditions, and environmental variables. On the other side, the potential of conventional technologies is defined by the possibility of connection to the grid and available fuel-based technologies.
- Restrictions of the system: Along with the restrictions of each component, there should also be considered other aspects such as the size of the facilities, the stability conditions of loads, and the losses of the system.
- Aspects to be optimized: The optimization principles might include not only economic aspects but also technical variables and environmental factors as continuity of supply, meeting the demand, system reliability, carbon dioxide emissions, among others.

Moreover, some of these factors are not static through time, and different scenarios should be studied to analyze the sensibility of the model.

2.2. Optimization in Hybrid Renewable Energy Systems

Optimization algorithms are ways of computing a maximum or minimum of mathematical functions [61]. Different methods have been used to size, plan, and operate HRES [60; 62; 63]. The three commonly used modeling and optimization techniques for hybrid systems are classical algorithms, metaheuristic methods, and hybrid of two or more optimization techniques.

Classical techniques

Classical optimization algorithms help find solutions to differentiable and continuous functions [61]. These methods are analytical and use differential calculus techniques to locate the optimum points [64]. One of the most used and developed branches is mathematical programming (MP), which has supplied the energy sector with methods for solving decision problems of diverse sizes and complexities [65]. The formulation of a typical mathematical programming model consists of three main elements as shown in Equation 2.1: an objective function ($F(x, y)$) which is mathematically formulated based on a set of decision variables that

can be continuous or integer ($x \in R^n$ and $y \in Z^m$ respectively); and constraints ($h_i(x,y) = 0$ and $g_j(x,y)$), which are the equations to model the problem [66]. Decisions may depend on multiple criteria in real problems, and a multi-objective formulation approach should be considered. In a single-objective optimization, the objective function correspond to a scalar value ($F(x,y) \in \mathbb{R}$), while in multi-objective optimization it is a vector of objective functions, i.e, $F(x,y) = (f_1(x,y), f_2(x,y), ..., f_p(x,y)) \in \mathbb{R}^n$.

$$\begin{aligned} \min_{x,y} \quad & F(x,y) \\ \text{s.t.} \quad & h_i(x,y) = 0 \quad \forall i = 1,2,...,I \\ & g_j(x,y) \leq 0 \quad \forall j = 1,2,...,J \\ & x \in \mathbb{R}^n \\ & y \in \mathbb{Z}^m \end{aligned} \tag{2.1}$$

Mathematical programming models can be classified into different categories depending on the decision variables and the nature of their equations: Linear Programming (LP), Mixed-Integer Linear Programming (MILP), Nonlinear Programming (NLP), and Mixed-Integer Nonlinear Programming (MINLP). The optimization techniques review presented below focuses on linear and nonlinear programming as it is the main difference in the energy models found in the literature. Additionally, most of the studies found used integer variables to model renewable energy.

Linear programming (LP) studies cases where all dependencies between the current decision variables are linear, that is said, the function $F(x,y)$ and all the constraints ($h_i(x,y)$ and $h_i(x,y)$) are linear [67]. LP has the advantage that it can be easily solved computationally. However, a significant limitation of these methods is that they cannot accurately represent physical systems [7]. Linear programming has been used in several studies for HRES optimization. For instance, Saif et al. [68] formulated a LP model of a PV-wind-diesel-battery hybrid power system. The problem considered two objective functions: minimizing costs and minimizing carbon dioxide emissions. The results showed that a multi-objective optimization problem is a useful tool in designing and planning the operation of hybrid power systems as it allows the decision-maker to set its priorities and select the solution that realizes them. Pereira [59] presented a multi-objective optimization model for selecting and sizing components of a HRES composed of wind turbines, photovoltaic, diesel generators, and batteries. Three criteria were evaluated: techno-economic, environmental, and social. The author also concludes that a multi-objective approach is a helpful tool for decision-making. In another study, Vafaei and Kazerani [69] studied a MIP optimization model to optimally-sized a micro-grid[1] composed of a wind turbine, a diesel generator, and a hydrogen-based energy storage system. The results showed that hybrid systems could reduce the adverse environmental impacts of burning fossil fuels.

[1] **Microgrid**: A localized group of distributed generation sources (technologies that generate electricity at or near where it will be used), energy storage devices, and loads that can operate connected to the centralized power network and function autonomously as physical or economic conditions dictate [70].

Nonlinear programming (NLP) studies cases were either the objective function $F(x, y)$ or the constraints $h_i(x, y)$ and $h_i(x, y)$ contain nonlinear parts. It can be applied in large-scale systems, and they can represent more accurately physical systems than LP. For example, some characteristics of storage systems like operation costs and storage efficiency cannot be modeled only with linear functions [7]. However, this method's drawback is its high computational burden [71]. Some authors have applied nonlinear programming techniques to account for these characteristics. For example, Das et al. [72] developed a NLP optimization problem for the optimal sizing problem of two storage systems (battery and pumped hydro), considering various operational constraints to get the minimum total cost of the system. The results showed that different energy storage systems have diverse operational parameters, and selecting an appropriate energy storage system for the service requirements is crucial. Alternatively, Kongnam wt al. [73] used a MINLP model to determine the optimum capacity of wind farms. The optimization problem was formulated to select the optimal technological type and size concerning operation costs, maintenance costs, and available area. The simulation results indicated that the uncertainty of renewable resources has a significant impact on the investment decision.

Another method used is Dynamic Programming (DP). It studies cases in which the optimization strategy is based on splitting the problem into smaller subproblems [61]. It helps solve sequential or multistage problems by optimizing each stage, reducing the computational time to determine the optimal solution. Nevertheless, DP requires many recursive functions, making the coding and implementation complex [71]. Several studies have used this algorithm to determine the optimal capacity size of energy systems. For instance, An et al. [74] used DP to find the optimal energy management of a hybrid system that combines wind turbines, photovoltaic, diesel generators, and a battery system. The problem was transformed into a multistage decision procedure concerning the battery's state of charge (SOC), resulting in the minimum system cost. The results showed that the method could minimize the operation cost of the hybrid system and CO_2 emissions while satisfying the technical conditions. Alternatively, Li et al. [75] determined the optimal system configuration of a hybrid system concerning costs and efficiency. The system included PV panels, hydrogen fuel cells for long-term storage, and battery banks for short-term storage. The proposed PV/FC/Battery hybrid system had lower cost, higher efficiency, and fewer PV modules than a single storage system. Besides, a trade-off between costs and efficiency was found.

Metaheuristic techniques

Metaheuristic methods are based on nature's behaviour. They have been used to solve complex optimization problems of HRES due to their capabilities to give efficient, accurate, and optimal solutions [61]. Examples of these methods are genetic algorithm and particle swarm optimization.

Genetic algorithm (GA) is an evolutionary population-based algorithm that includes different operations to find an optimal solution such as initiation, mutation, crossover, and selection [61]. GA has proved to be a good method for solving large-scale and combinatorial optimization problems [76]. However, its main disadvantage is that it tends to converge to locally optimal solutions [77]. Several studies use GA to optimize and design a HRES. For example, Jin Ko et al.[78] used GA to determine the configuration and sizing of a HRES

composed of nine different energy conversion devices (renewable and fossil fuels) considering economic, technical, and environmental objective functions. The authors concluded that it could be helpful to select the best design of a HRES by comparing the values of the objective functions of the Pareto-optimal solutions obtained. In another research, Dufo-López et al. [79] proposed a control strategy of a PV–diesel–battery–hydrogen system using GA. The strategy optimizes how the excess energy is used while minimizing the total cost throughout its lifetime. If the energy demanded by the load is higher than the one produced by the renewable sources, the control strategy determines the most economical way to meet the energy deficit.

Particle swarm optimization (PSO) is an iterative algorithm that simulates the social behavior of how swarms move to find food in a particular area. The primary shortage of PSO is that it requires several modifications due to its complex and conflicted nature [71]. It has been applied in some studies for HRES optimization. For example, Avril et al. [80] studied a multi-objective design of a hybrid system based on PSO. The problem simultaneously minimizes the total levelized cost and the connection to the grid while fulfilling a constraint of consumer satisfaction. The results showed that the best economical solution is to use batteries for the short term; meanwhile, hydrogen storage is preferred for a midterm. In another study, Kashefi Kaviani et al. [81] presented an advanced variation of the PSO algorithm to optimize a reliable hydrogen-based stand-alone wind–PV generating system to minimize the hybrid system's annualized cost. The results indicate that the costs of the system directly depend on its components' reliabilities.

Hybrid techniques

A hybrid algorithm is a combination of two or more optimization techniques. It can overcome the limitations of individual methods, providing more effective and reliable solutions for HRES. Nonetheless, they can have high computational costs and are hard to implement [61]. Some studies have used them to optimize a HRES [82; 83], but the results have shown certain limitations. For instance, suboptimal solutions were obtained in the work of Khatib et al. [82].

Chapter 3

Research methodology and data

This chapter focuses on the research methodology and the data collected and used in the model. First, an overview of the optimization model is provided. Then, the energy system proposed is described, and the main mathematical equations and optimization constraints are given. Next, the objective functions considered in this study are described, and the model implementation and solution strategy are explained. Lastly, the case study is presented, including the load demand, resources estimation, and the input data needed for the model.

3.1. Optimization Problem Overview

In this study, a multi-objective optimization problem is formulated and solved to design and evaluate a hybrid renewable energy system to supply the electrical demand of a mining process. In Figure 3.1, an overview of the optimization model is depicted. It includes the inputs and outputs of the model, the main constraints, and the objective functions considered.

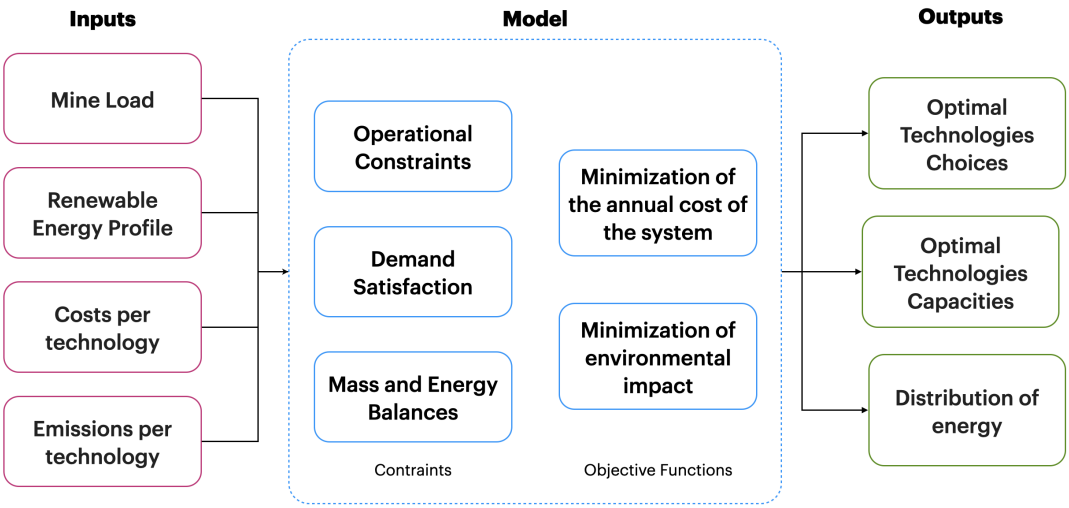

Figure 3.1: An overview of the optimization model. Source: Own elaboration.

The model considers the minimization of two objective functions: the system's annual cost and GHG emissions. On the one hand, the system's annual cost considers the annual investment costs and each technology's annual operation and maintenance costs. On the

other hand, the environmental impact consists of calculating the GHG emissions associated with fuel combustion and the purchase of electrical energy. The main constraints of the model are: satisfying the load demand, the operational restrictions of each technology, such as efficiencies, conversions, and capacities, and the mass and energy balances.

The model's inputs are the electrical mine load curve, the profile of the renewable energy sources studied, the costs of each technology, and their environmental impacts. Meanwhile, the outputs obtained are the optimal sizes and choice of the generation and storage technologies and the energy distribution at each time step.

The optimization model is described and explained in detail in the following sections: the superstructure, the mathematical equations and constraints, the objective functions considered, and the data used as input parameters. The outputs and results of the model are shown in Chapter 4.

3.2. Superstructure Description

Figure 3.2 shows the superstructure of the energy system proposed given the available renewable generation options and the selected storage alternatives. The system includes a PV array and a generator fueled with biogas as the primary energy sources, two options for energy storage (battery bank and an electrolyzer-hydrogen storage-fuel cell system), the mine load, and inverters and converters when it is needed. Besides, the system is connected to the grid as the principal mines in Chile are grid-connected [33], and this configuration of operation increases the system's performance [52].

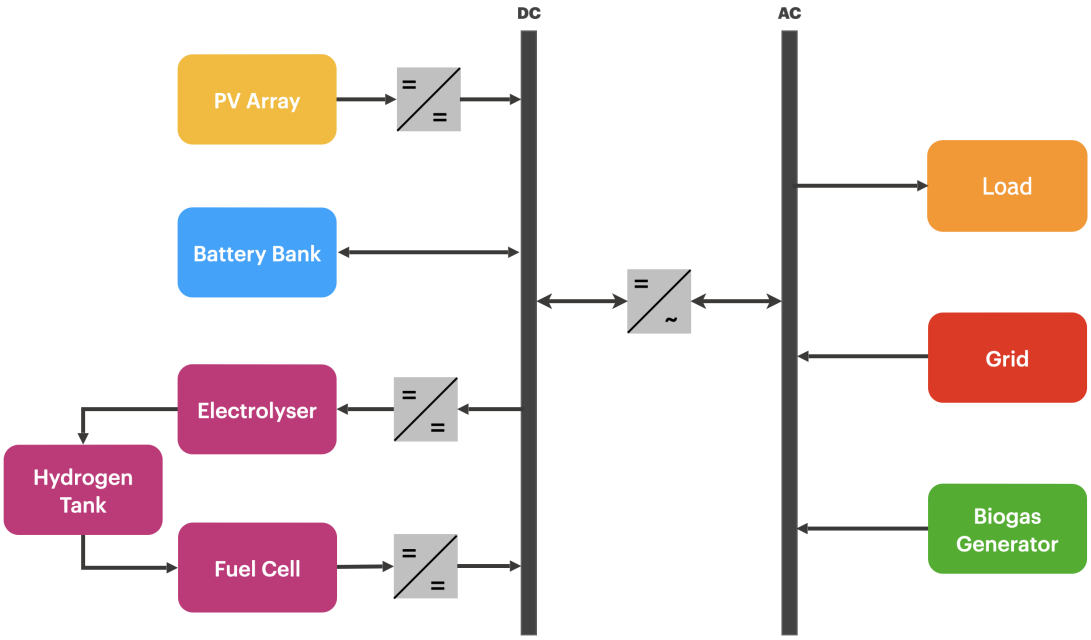

Figure 3.2: Schematic diagram of the biogas-PV hybrid energy system proposed. Source: Own elaboration.

The PV array converts the solar energy into electricity; meanwhile, the generator produces electricity by the combustion of the fuel (biogas in this case). The available energy from renewable sources is directly delivered to the load to provide the load demand. The energy excess or deficit is saved in or supplied by the energy storage systems when needed. The grid is used if the options cannot cater to the system's requirements or is economically convenient.

The system is optimized regarding its components quantity and size, which means that not all the resources and components in Figure 3.2 are part of all the energy systems modeled. In the following section, the model of each system component is described.

3.3. Modelling of HRES

The following section summarizes and describes the mathematical equations used for modeling the different components of the HRES in this thesis. First, the generation and storage technologies models are explained, and then specific constraints of the problem are presented. In the model, time is modeled discretely, assuming no significant changes during the time step.

3.3.1. Generation Models

PV Model

As mentioned before, the sunlight can be converted directly into electricity using PV panels. The power generated by a PV system at any time t, $P_{pv}^{g}(t)$, can be expressed as follows [84; 85]:

$$P_{pv}^{g}(t) = P_{pv}^{nom} \cdot \frac{G^{\theta}(t)}{G_{ref}} \cdot [1 + \alpha \cdot (T_c(t) - T_{ref})] \quad \forall\, t \in T \tag{3.1}$$

Where P_{pv}^{nom} is the nominal power of the PV system, $G^{\theta}(t)$ is the global irradiance incident on the tilted plane of slope θ at time t, G_{ref} is the global irradiance at reference conditions, α is the temperature coefficient of efficiency, $T_c(t)$ is the temperature of the PV cell at time t, and T_{ref} is the temperature of reference.

The nominal power of a PV system, P_{pv}^{nom}, depends on the number of panels, the area of each one, and its efficiency. It can be calculated by [86]:

$$P_{pv}^{nom} = N_{PV} \cdot A \cdot \eta_{ref} \cdot 10^{-3}\ [\frac{MW}{m^2}] \tag{3.2}$$

Where N_{PV} is the number of PV modules, A is the area of each panel, and η_{ref} is the efficiency of the PV panel under standard test conditions (1,000 Wh/m^2 and 25℃).

The temperature of the module is represented by the following equation [60]:

$$T_c(t) = T_a(t) + G^{\theta}(t) \cdot (\frac{\tau\beta}{U_L}) \quad \forall\, t \in T \tag{3.3}$$

Where $T_a(t)$ is the ambient temperature at time t, τ is the transmittance coefficient of PV cells, β is the absorbance coefficient of PV cells, and U_L is the overall heat loss coefficient.

It is difficult to measure the value of $\tau\beta/U_L$ directly; instead, manufacturers report the nominal operating cell temperature, T_c^{NOCT}, which is defined as the cell temperature that results at an incident radiation of 800 W/m^2 (G^{NOCT}), an ambient temperature of 20°C (T_a^{NOCT}) and no-load operation. The overall heat loss coefficient can be estimated from the nominal operating cell temperature (NOCT) as follows [60]:

$$\frac{\tau\beta}{U_L} = \frac{T_c^{NOCT} - T_a^{NOCT}}{G^{NOCT}} \tag{3.4}$$

Finally, the power available at any time t, $P_{pv}^{a}(t)$, depends on the losses caused by the system's operation, PT, as seen in Equation 3.5 [86]. The total losses are calculated based on the systems losses L_i by Equation 3.6.

$$P_{pv}^{a}(t) = P_{pv}^{g}(t) \cdot (1 - \frac{PT}{100}) \quad \forall\, t \in T \tag{3.5}$$

$$PT = 100 \cdot [1 - \prod_{i=1}(1 - \frac{L_i}{100})] \tag{3.6}$$

Biogas Generator Model

The fuel consumption of biogas in a generator at any time t, $f_{bg}(t)$, is estimated depending on each hour's rated and output power. It can be described as [87; 88]:

$$f_{bg}(t) = a_{bg} \cdot P_{bg}^{nom} + b_{bg} \cdot P_{bg}(t) \quad \forall\, t \in T \tag{3.7}$$

Where a_{bg} and b_{bg} are constants coefficients of the fuel consumption curve, P_{bg}^{nom} is the nominal power of the biogas generator, and $P_{bg}(t)$ is the output power of the biogas generator at time t.

Grid

The grid model considers that the mine has a contract with the electric company for a given power value P_{grid}^{con}. There is a cost associated with the power contracted, C_{grid}^{con}, and a cost for the energy consumed at any time, C_{grid}. Additionally, if the energy consumed is higher than the power contracted, there is a penalty for overconsumption with a cost C_{grid}^{over}. The proposed model is based on experts' knowledge since electricity contracts for non-regulated customers in Chile, such as mines, are private and case-specific.

A variable $P_{grid}^{over}(t)$ is used to calculate overconsumption at any time t. It is defined as zero if overconsumption does not occur, implying that the penalty is zero. Conversely, if overconsumption does happen, it is calculated as the difference between the energy consumed and the power contracted. The equations used are presented below.

First, a binary variable $y_g(t)$ is defined to indicate if there is overconsumption or not.

$$y_g(t) = \begin{cases} 1 & \text{if there is overconsumption at time t} \\ 0 & \text{if there is no overconsumption at time t} \end{cases} \tag{3.8}$$

Then the P_{grid}^{over} is calculated as the maximum between zero and the difference of the power contracted and consumed: $max\{0, P_{grid}(t) - P_{grid}^{con}\}$, where $P_{grid}(t)$ is the energy supplied by the grid at time t. The following equations can express it:

$$0 \leq P_{grid}^{over}(t) \quad \forall t \in T \tag{3.9}$$

$$P_{grid}^{over}(t) \leq M \cdot y_{grid}(t) \quad \forall t \in T \tag{3.10}$$

$$P_{grid}(t) - P_{grid}^{con} \leq P_{grid}^{over}(t) \quad \forall t \in T \tag{3.11}$$

$$P_{grid}^{over}(t) \leq (P_{grid}(t) - P_{grid}^{con}) + M \cdot (1 - y_{grid}(t)) \quad \forall t \in T \tag{3.12}$$

3.3.2. Storage Models

Battery Model

Figure 3.3 shows a schematic of a battery system considering the efficiency losses during the charging and discharging processes and that some energy is lost due to self-discharge. The battery bank is made up of a series and parallel connections of individual batteries.

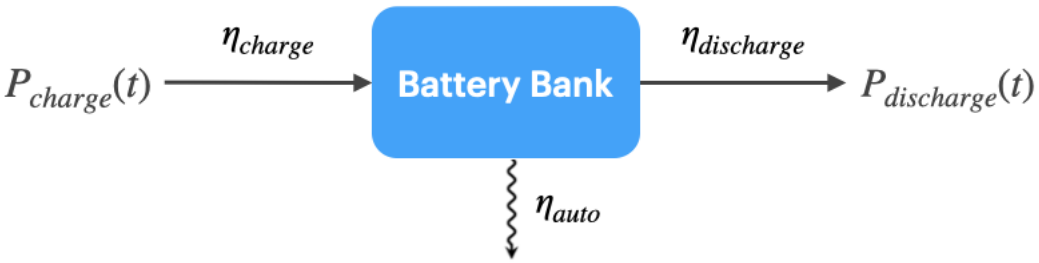

Figure 3.3: Schematic of a battery system showing system losses. Source: Own elaboration based on [22].

Based on the schematic, the amount of energy stored in the battery bank at any time t, $P_b(t)$, can be expressed by an energy balance on the battery system [18; 89]:

$$P_b(t) = P_b(t-1) \cdot (1 - \eta_{auto}) + P_{charge}(t) \cdot \eta_{charge} - \frac{P_{discharge}(t)}{\eta_{discharge}} \quad \forall\, t \in T \tag{3.13}$$

Where $P_b(t-1)$ is the amount of energy stored in the battery at time t-1, η_{auto} is the hourly self-discharge rate, $P_{charge}(t)$ is the energy that is charged in the battery at time t, η_{charge} is the charge efficiency of the battery, $P_{discharge}(t)$ is the energy discharged from the battery to the system at time t, and $\eta_{discharge}$ is the discharge efficiency of the battery.

There is another way of measuring the energy of a battery: the State of Charge (SOC). It is defined as the ratio between the battery's current capacity, $P_b(t)$, and its nominal capacity, P_b^{nom}, as shown in Equation 3.14 [90]. The SOC of a battery will range from 0% to 100% (battery fully discharged and charged respectively) [22].

$$SOC(t) = \frac{P_b(t)}{P_b^{nom}} \quad \forall\, t \in T \tag{3.14}$$

The amount of energy that a battery can supply or store is bound to avoid gassing and over-charging the battery [88]. It can supply energy to a load until the lower limit of Minimum State of Charge, SOC_{min}, and can be charged until the Maximum State of Charge, SOC_{max}, is reached [91]. Equation 3.15 represents this constraint.

$$SOC_{min} \leq SOC(t) \leq SOC_{max} \quad \forall\, t \in T \tag{3.15}$$

Considering the boundaries of the SOC, Equation 3.14 can be rewritten in a linear form in terms of the energy stored in a battery as follows [18]:

$$SOC_{min} \cdot P_b^{nom} \leq P_b(t) \leq SOC_{max} \cdot P_b^{nom} \quad \forall\, t \in T \tag{3.16}$$

The SOC_{min} is determined by the Depth of Discharge (DoD), which is a measure of how deeply a battery can be discharged [22]. Given a maximum depth of discharge DOD_{max}, the minimum level of discharge of the battery will be [22]:

$$SOC_{min} = (1 - DoD_{max}) \tag{3.17}$$

Typically, battery manufacturers provide information on the recommended lower limit the battery bank should not exceed when discharging to preserve battery life. Also, the SOC_{max} is provided by manufacturers.

Additionally, a battery has the characteristic that it cannot charge and discharge simultaneously [18]. A binary variable $z_b(t)$ is defined to indicate the state of the battery at any time.

$$z_b(t) = \begin{cases} 1 & \text{if the battery is discharging at time t} \\ 0 & \text{if the battery is charging at time t} \end{cases} \tag{3.18}$$

- Discharging: If the battery is discharging ($z_b(t) = 1$), the energy charged to the battery is zero.

$$P_{charge}(t) \leq M \cdot (1 - z_b(t)) \quad \forall t \in T \tag{3.19}$$

- Charging: If the battery is charging ($z_b(t) = 0$), the energy discharged by the battery is zero.

$$P_{discharge}(t) \leq M \cdot z_b(t) \quad \forall t \in T \tag{3.20}$$

Hydrogen Storage Model

Figure 3.4 shows a schematic of the hydrogen storage model with its components and the notation used in this study. The system has three components: an electrolyzer, which produces hydrogen through water electrolysis, a hydrogen tank that stores the hydrogen produced, and a fuel cell that uses the hydrogen to produce electricity when it is needed. The model of each component is shown below.

Figure 3.4: Schematic of a hydrogen storage system. Source: Own elaboration.

Electrolyzer Model

The electrolyzer's hydrogen mass flow, $q_{H_2}(t)$, is modeled as dependent on electrical consumption and its efficiency, as shown in Equation 3.21 [87]:

$$\eta_{el} = \frac{q_{H_2}(t) \cdot HHV_{H_2}}{P_{el}(t)} \quad \forall t \in T \tag{3.21}$$

Where η_{el} is the efficiency of the electrolyzer, HHV_{H_2} is the higher heat value of hydrogen, and $P_{el}(t)$ is the electrolyzer electrical consumption at time t.

On the other hand, although electrolyzers can operate over their nominal power capacity, P_{el}^{nom}, for design, it would consider that the nominal power capacity of this technology is calculated as the maximum electrical consumption as seen in Equation 3.22 [92].

$$P_{el}(t) \leq P_{el}^{nom} \quad \forall t \in T \tag{3.22}$$

Hydrogen Tank

The expression used to calculate the current hydrogen level is based on a mass balance between the input and the hydrogen output flow in the tank and can be expressed as follows [88]:

$$L_{H_2}(t) = L_{H_2}(t-1) + q_{H_2}(t) - \frac{f_{H_2}(t)}{\eta_{tank}} \quad \forall t \in T \tag{3.23}$$

Where $L_{H_2}(t)$ is the hydrogen level of the tank at time t, $L_{H_2}(t-1)$ is the hydrogen level of the tank at time t-1, $q_{H_2}(t)$ is the hydrogen flow mass produced by the electrolyzer at time t, $f_{H_2}(t)$ is the fuel cell hydrogen consumption at time t, and η_{tank} is the efficiency of the tank as it may present losses resulted from leakage or pumping.

There are lower and upper limits for the hydrogen stored. It is not possible to store more hydrogen than the rated capacity of the tank. On the other hand, a fraction of hydrogen may not be extracted because of technical problems such as hydrogen pressure drop [87]. The following equation represents these boundaries:

$$H_2{}^{min} \cdot H_2nom \leq L_{H_2}(t) \leq H_2{}^{max} \cdot H_2nom \quad \forall t \in T \tag{3.24}$$

Where the upper and lower limits are expressed as a percentage of the rated capacity of the tank (H_2^{min} and H_2^{max}, respectively).

Fuel Cell

The hydrogen consumption of the fuel cell, $f_{H_2}(t)$, is modeled as dependent on the output power and its efficiency. It is defined by the following equation [87]:

$$\eta_{fc} = \frac{P_{fc}(t)}{f_{H_2}(t) \cdot LHV_{H_2}} \quad \forall t \in T \tag{3.25}$$

Where η_{fc} is the efficiency of the fuel cell, $P_{fc}(t)$ is the output power of the fuel cell at time t, and LHV_{H_2} is the lower heat value of hydrogen.

Considering most fuel cells operate between 90 and 100% load fraction of rated capacity and may be sized for near peak load, the nominal capacity of this technology is calculated as the maximum output power as seen in Equation 3.26 [93]. However, it is important to note that some fuel cells may even be operated significantly above the rated capacity.

$$P_{fc}(t) \leq P_{fc}^{nom} \quad \forall t \in T \tag{3.26}$$

3.3.3. Optimization Model Constraints

In addition to the equations related to the behavior of the generation and storage units presented above, several physical constraints are placed on the model so it may be used for the case proposed.

Power Balance and Converters

The electricity supplied by the energy system must be sufficient to meet the electrical demand of the mine $P_{load}(t)$ at any time. Considering the superstructure proposed in Section 3.2, the energy balance of the system is:

$$P_{load}(t) - P_{bg}(t) - P_{grid}(t) - (P_{pv}(t) \cdot \eta_{con} + P_b^{charge}(t) - P_b^{discharge}(t) - \frac{P_{ele}(t)}{\eta_{con}} + P_{fc}(t) \cdot \eta_{con}) \cdot \eta_{inv} \; \forall t \in T \tag{3.27}$$

Where η_{inv} is the efficiency of the inverter and η_{con} is the efficiency of the converters. It is supposed that all the converters DC/DC have the same efficiency.

Boundary value constraints

The initial and final conditions of the storage systems were defined to avoid designs with significant differences in the amounts of energy stored at the start and the end of the process. The energy available at the start of the process has no cost. Thus, the optimal solution may have a large amount of "free" energy at the start of the process, reducing the need to generate such energy, making the design unrealistic. Precisely for this study, it is imposed that each storage option's initial and final states are the same, as expressed in Equations 3.28 and 3.29. It is important to note that this can be used for large simulation periods like a year but may not be accurate for shorter periods and should be evaluated in every case its pertinence.

$$P_b(t = t_i) = P_b(t = t_f) \tag{3.28}$$

$$L_{H_2}(t = t_i) = L_{H_2}(t = t_f) \tag{3.29}$$

Where t_i is the initial time of the simulation, and t_f is the final time of the simulation.

Capacity constraints

Constraints were placed on the nominal capacities of the batteries, electrolyzer, and fuel cell to avoid having technologies with large capacities that do not exist in reality. For each case, the maximum nominal capacity was defined based on that technology's currently largest capacity. Equations 3.30, 3.31, and 3.32 represent these constraints.

$$P_b^{nom} \leq P_b^{max} \tag{3.30}$$

$$P_{el}^{nom} \leq P_{el}^{max} \tag{3.31}$$

$$P_{fc}^{nom} \leq P_{fc}^{max} \tag{3.32}$$

Where P_b^{max}, $P_f l^{max}$ and $P_f c^{max}$ are the maximum nominal capacity of the batteries, electrolyzer, and fuel cell, respectively.

On the other hand, the amount of biogas consumed by the generator, $f_{bg}(t)$, was limited by the biogas available in the zone, f_{bg}^{max}, as shown in Equation 3.33.

$$f_{bg}(t) \leq f_{bg}^{max} \tag{3.33}$$

3.4. Optimization Process Criteria

The objective functions considered in this study are minimizing the system's annual cost and minimizing GHG emissions. They are explained as follows.

Annual costs

The total annual costs, C_T, consist of the annual capital costs, $C_{Capital}$, the annual operation and maintenance costs, $C_{O\&M}$, and the costs of energy purchase from the grid, C_E, as seen in Equation 3.34 [89]. Using the annualized costs allows considering the differences between the lifetimes of each technology in the model.

$$C_T = C_{Capital} + C_{O\&M} + C_E \tag{3.34}$$

The annual capital costs of the system are given as:

$$C_{Capital} = C_{pv}^{Cap} + C_{bg}^{Cap} + C_{b}^{Cap} + C_{el}^{Cap} + C_{tank}^{Cap} + C_{fc}^{Cap} \tag{3.35}$$

Where C_{pv}^{Cap}, C_{bg}^{Cap}, C_{b}^{Cap}, C_{el}^{Cap}, C_{tank}^{Cap} and C_{fc}^{Cap} are the annual capital cost of the PV system, biogas generator, battery bank, electrolyzer, hydrogen tank, and fuel cell, respectively.

The initial capital costs of each technology are converted into annual capital costs, using the Capital Recovery Factor (CRF) as shown in Equation 3.36 [89].

$$C_j^{Cap} = C_j^{Inv} \cdot CRF_j \quad \forall j \in \{pv, bg, b, el, tank, fc\} \tag{3.36}$$

Where C_j^{Inv} is the investment costs of the technology j.

The Capital Recovery Factor is defined as [89]:

$$CRF_j = \frac{i \cdot (1+i)^{n_j}}{(1+i)^{n_j} - 1} \quad \forall j \in \{pv, bg, b, el, tank, fc\} \tag{3.37}$$

Where i is the interest rate, and n_j is the lifetime of the technology j. In this study, it was assumed an interest rate of 7% for all technologies [94].

The operation and maintenance costs, $C_{O\&M}$, are defined as the sum of each component's operation and maintenance costs, as shown in Equation 3.38. In order of appearance, they represent the PV system, biogas generator, batteries, electrolyzer, hydrogen tank, and fuel cell operational and maintenance costs.

$$C_{O\&M} = C_{pv}^{O\&M} + C_{bg}^{O\&M} + C_{b}^{O\&M} + C_{el}^{O\&M} + C_{tank}^{O\&M} + C_{fc}^{O\&M} \tag{3.38}$$

The grid costs, C_E, are calculated based on the model proposed in Section 3.3.1. There is a cost associated with the power contracted, C^{con}_{grid}, a cost for the energy consumed at any time, C_{grid}, and there is a penalty if overconsumption occurs, with a cost C^{over}_{grid}. It can be expressed as:

$$C_E = C^{con}_{grid} \cdot P^{con}_{grid} \cdot m + \sum_{t \in T} C_{grid} \cdot P_{grid}(t) + \sum_{t \in T} C^{over}_{grid} \cdot P^{over}_{grid}(t) \tag{3.39}$$

Where m is the number of months in a year, as the power contracted is paid monthly [95].

The costs and economic parameters used for each technology are shown in Table 3.1. For the grid, the costs were defined based on the information on regulated customers in Chile and different expert's knowledge [95; 96]. The values used are 60 USD/MWh for the energy purchase (C_{grid}), 7.4 $kUSD/MW/month$ for the contracted power (C^{con}_{grid}) and 103 USD/MWh for the energy overconsumption (C^{over}_{grid}). It is important to note that these values are highly variable in time and are case-specific.

Table 3.1: Economic parameters of all considered technologies.

Technology	**Parameter**	**Value**	**Reference**
PV System	Investment Costs	970 USD/kW	[95]
	O&M Costs*	2%	[95]
	Lifetime	25 years	[97]
Biogas Generator	Investment Costs	3500 USD/kW	[95]
	O&M Costs*	2%	[95]
	Lifetime	25 years	[94]
Battery System	Investment Costs	350 USD/kWh	[98]
	O&M Costs*	2%	[99]
	Lifetime	10 years	[100]
Electrolyzer	Investment Costs	784 USD/kW	[101]
	O&M Costs*	2%	[101]
	Lifetime	25 years	[102]
Hydrogen Tank	Investment Costs	1000 USD/kg	[103]
	O&M Costs*	2%	[104]
	Lifetime	25 years	[102]
Fuel Cell	Investment Costs	600 USD/kW	[102]
	O&M Costs*	1.8%	[105]
	Lifetime	20 years	[104]

* The O&M costs are expressed as a percentage of the Investment Costs.

GHG emissions

The emissions considered in this study are the direct GHG emissions associated with fuel combustion and indirect GHG emissions associated with the purchase of electricity (emissions scope 1 and 2 defined by the GHG Protocol [34]). So, except for the biogas generator and the electrical grid, the operational emissions of all other components of the system proposed can be neglected [68]. The unit used to estimate the system's pollution is kg of $CO_2 - eq$.

The GHG emissions of the hybrid energy system, E_T, can be calculated by using Equation 3.40:

$$E_T = \sum_{t \in T} E_{grid} \cdot P_{grid}(t) + E_{bg} \cdot P_{bg}(t) \tag{3.40}$$

Where E_{grid} is the emission factor of the grid and E_{bg} is the emission factor of the biogas generator. They take the value of 383.4 $kg\ CO_2 - eq/MWh$ and 0.21 $kg\ CO_2 - eq/MWh$ respectively [106; 107].

The complete nomenclature of indices, parameters, and variables used in this thesis are detailed in Appendix A.

3.5. Model implementation and solution strategy

The present optimization problem is classified as a MILP problem as it contains linear expressions and integer variables in its constraints and objective functions. Table 3.2 displays the total number of variables and constraints of the model.

Table 3.2: Number of variables and constraints used in the model.

Variables and Constraints	**Number**
Continuous variables	113886
Integer variables	17522 (17520 binary)
Constraints	192726

The model is implemented in the programming language Julia [108], using the package JuMP [109], and its solution is obtained using Gurobi [110], a commercial solver for MILP problems. It was designed to simulate and optimize the energy system for one year, considering hourly time steps. The time step chosen allows studying the differences in the level of renewable energy available and the behavior of the storage systems throughout the day. Smaller steps would increase the size of the problem without providing substantially more information. Meanwhile, larger steps would lead to the loss of some information, increasing the possibility of obtaining an unrealistic design.

In a preliminary phase, the problem is solved considering each criterion proposed in Section 3.4 separately to analyze how its optimal values changed when making a multi-objective optimization and get the utopia and nadir points. Then, the multi-objective optimization

problem is solved using the ϵ-constraint method. Lastly, a post-optimal analysis is done to analyze the sensibility of the model. Each phase and its formulation are explained below.

Preliminary phase: Mono-objective optimization

In this preliminary phase, the optimization problem is solved considering the minimization of one objective function. The formulation of each mono-objective optimization problem is:

- Minimization of annual costs

$$\begin{array}{lll} \min & C_T & \\ \text{s.t.} & h_j(x,y,z) = 0 \quad \forall j = 1,2,...,J & \left\{ \begin{array}{l} \text{Demand satisfaction} \\ \text{Mass and energy balances} \\ \text{Operational Constraints} \end{array} \right. \\ & g_i(x,y,z) \leq 0 \quad \forall i = 1,2,...,I & \\ & x \in \mathbb{R}^n, y \in Y = \{0,1\}^m, z \in \mathbb{Z}^+ & \end{array} \tag{3.41}$$

- Minimization of GHG emissions

$$\begin{array}{lll} \min & E_T & \\ \text{s.t.} & h_j(x,y,z) = 0 \quad \forall j = 1,2,...,J & \left\{ \begin{array}{l} \text{Demand satisfaction} \\ \text{Mass and energy balances} \\ \text{Operational Constraints} \end{array} \right. \\ & g_i(x,y,z) \leq 0 \quad \forall i = 1,2,...,I & \\ & x \in \mathbb{R}^n, y \in Y = \{0,1\}^m, z \in \mathbb{Z}^+ & \end{array} \tag{3.42}$$

Solution phase: Multi-objective optimization

The multi-objective problem is solved by implementing the ϵ-constraint method, a multi-objective optimization technique for generating Pareto optimal solutions [111]. In this method, one objective function is minimized, and the others are used as constraints. For transforming the multi-objective problem into several single-objective problems with constraints, the following procedure is used:

$$\begin{array}{lll} \min & f_p(x) & \\ \text{s.t.} & f_q(x) \leq \epsilon_q \quad \forall q = 1,2,...,Q, q \neq p & \\ & x \in S & \end{array} \tag{3.43}$$

Where S is the feasible region, defined by any equality and inequality constraints, and the vector of upper bound, $\epsilon = (\epsilon_1, \epsilon_2, ..., \epsilon_q)$, represents the maximum value that each objective can have. To obtain a subset of the Pareto optimal set, the vector of upper bounds must be varied and make a new optimization process for each new vector.

The optimization problem proposed considering multi-criteria can be formulated in a more concise manner as follows:

$$
\begin{aligned}
\min \quad & C_T \\
\text{s.t.} \quad & E_T \leq \epsilon_{ET} \\
& \left.\begin{aligned} & h_j(x,y,z) = 0 \quad \forall j = 1,2,...,J \\ & g_i(x,y,z) \leq 0 \quad \forall i = 1,2,...,I \\ & x \in \mathbb{R}^n, y \in Y = \{0,1\}^m, z \in \mathbb{Z}^+ \end{aligned}\right\} \begin{aligned} & \text{Demand satisfaction} \\ & \text{Mass and energy balances} \\ & \text{Operational Constraints} \end{aligned}
\end{aligned} \tag{3.44}
$$

Where ϵ_{emi} is the maximum value that the GHG emissions can reach. For this problem, it is defined considering equidistant points of the distance between the nadir and utopia points (E_T^N and E_T^U respectively) [112; 113]. Mathematically it can be expressed as follows:

$$\epsilon_{ET} = E_T^N - w \cdot (E_T^N - E_T^U) \tag{3.45}$$

Where w is the relative weight importance between both objective functions and takes a value between 0 and 1.

Sensibility Analysis

Finally, a sensibility analysis is performed to study the sensibility of different parameters to the developed model. The sensitivity variables considered included the load demand, biogas availability, hydrogen storage costs, and the grid emissions factor. The sensitivity analysis was performed considering the same importance weight for each function ($w = 0.5$), and the parameters were changed one at a time. Table 3.3 shows the scenarios considered.

Table 3.3: Scenarios considered in the sensibility analysis.

# Scenario	Variation
Scenario 0	Case Base
Scenario 1	Increase in energy demand by 20%.
Scenario 2	Increase in energy demand by 41%.
Scenario 3	Increase in biogas available by 100%.
Scenario 4	Increase in biogas available by 300%.
Scenario 5	Decrease in hydrogen storage costs by 20%
Scenario 6	Decrease in hydrogen storage costs by 50%
Scenario 7	Decrease in the grid emissions by 33%
Scenario 8	Decrease in the grid emissions by 78%

A change in the load demand was considered, as energy consumption is expected to increase in the following years. The 20% and 41% increase were chosen based on the projections for the years 2025 and 2030, respectively [4]. It is important to note that this projected variation is aggregated and may differ from the mine variation by itself. On the other hand, biogas availability is selected for the analysis to study the potential of this

energy source. The percentages were arbitrarily selected. Hydrogen storage costs were selected for the analysis, among other costs, as energy storage systems are fundamental for incorporating renewable energy, and they are currently more expensive than batteries. The scenarios proposed were arbitrarily chosen. Finally, a variation on the grid emissions coefficient is evaluated as it will tend to decrease as more renewable energy is incorporated into the electrical grid [106]. The variation was chosen based on the coefficients of the European Union (EU) grid (E_{grid}=255 kg CO_2-eq/MWh) and Lithuania grid (E_{grid}=83 kg CO_2-eq/MWh). Around 35% of the electricity consumed comes from renewable sources in the EU grid; meanwhile, Lithuania has the lowest GHG emissions coefficient compared to the rest of the European countries without having nuclear power plants for the generation of electricity [114; 115]. Nuclear power plants were a critical criterion as the Chilean grid does not have this energy type.

3.6. Case of study

For the case of study, a mine located in the Antofagasta Region in Chile is proposed. The location was chosen based on principal mines of the country are located in that zone, and that solar radiation level is high [33]. There is access to electricity in the region through the National Electric System (SEN) [106]. Figure 3.5 shows the location of the study on the map, including the transmission lines and stations available.

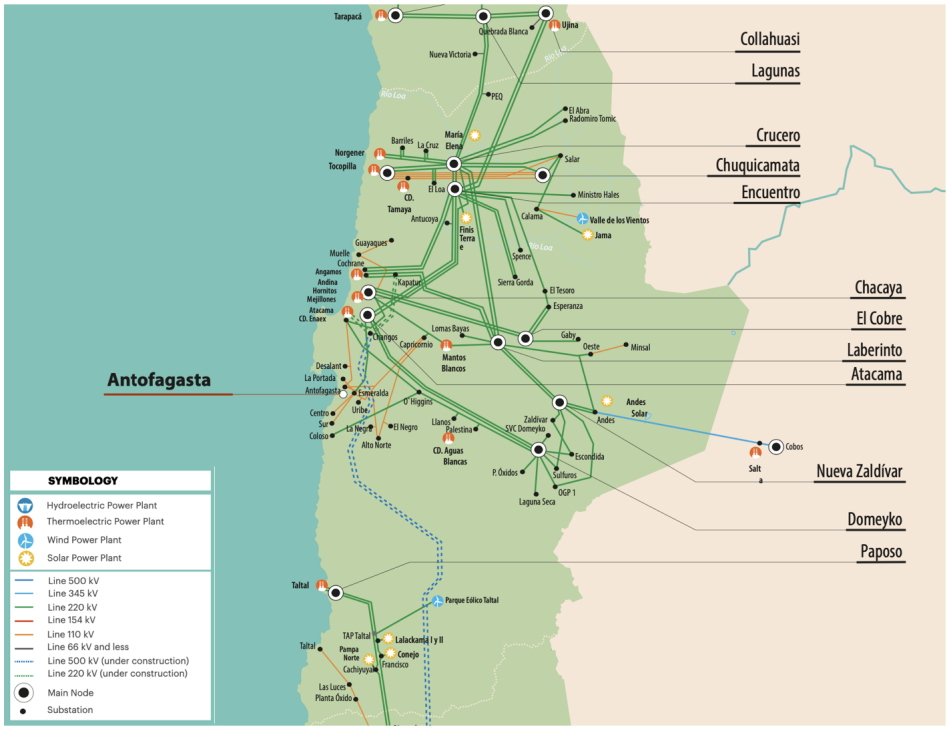

Figure 3.5: Electricity transmission lines in Antofagasta Region. Adapted from [116].

For the model, it was necessary to estimate the electrical load of the mine and the renewable sources available. They are detailed as follows.

3.6.1. Load Profile of the mine

The annual electrical load profile used for the simulations was estimated using data representing a mine in the North of Chile. As the original data presented some outliers, data analysis was done. It is explained in Appendix B.

Figure 3.6 shows the annual and daily demand patterns used in the model. It can be noticed that the electrical demand does not have a daily or seasonal variation which matches with a mining process being a continuous process that, in theory, should demand the same energy at every moment [7]. Two assumptions were made to estimate the load: the load remains constant every time step, and maintenance and breakdown interruptions are not considered. Therefore the power is assumed to be supplied without interruption.

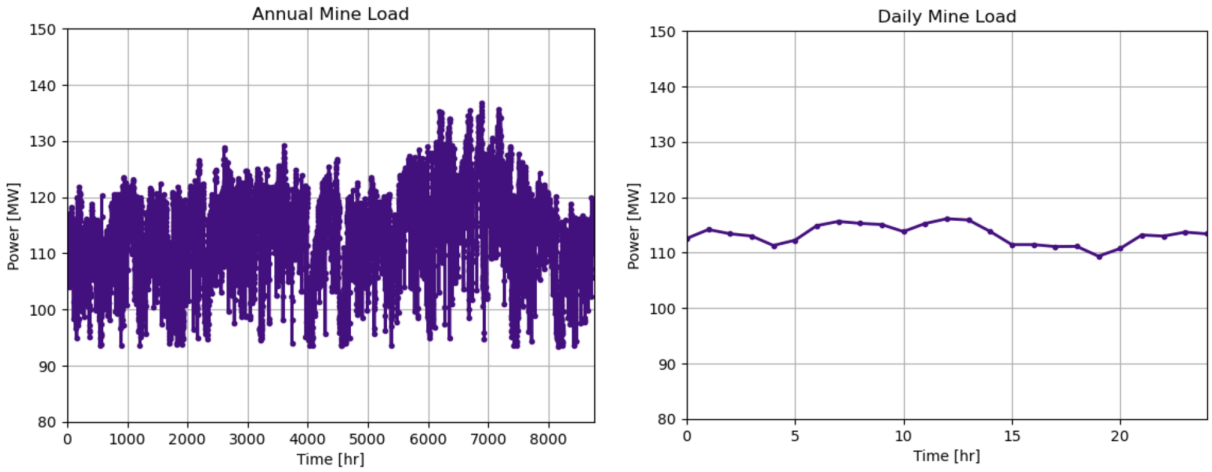

Figure 3.6: Annual and daily power demand of a copper mine. Source: Own elaboration.

3.6.2. Resources data of the studied area

The resource assessment of biomass and solar available in the zone is explained below.

Solar resource

The solar resource input data were obtained from the online solar explorer tool (*Explorador Solar*) developed by the University of Chile and the Ministry of Energy of Chile [117]. The radiation database and its accuracy are explained in reference [118].

The records contain Chile's global horizontal irradiance (GHI) data over ten years (2006–2016) recorded at hourly intervals. Based on this data, the tool calculates the hourly solar global irradiance incident on a tilted plane based on the Liu and Jordan model described in Appendix C [119; 120]. For the estimation, the values shown in Table 3.4 were used. The position was chosen based on the location of mines and the electrical transmission lines, the level of radiation, the space available, the landfills location, and other solar plants' location. On the other side, the azimuth angle and the tilted plane's angle are optimized values given by the solar explorer tool to maximize the PV generation [117].

Table 3.4: Parameter used for the estimation of the global irradiance incident on a tilted plane.

Parameter	**Value**
Latitude	-23.22
Longitude	-69.72
Angle of the tilted plane	23°
Azimuth angle	2°

The annual average solar radiation was found to be 7.23 $kWh/m^2/day$. Figure 3.7 displays the average monthly solar radiation of the selected zone. A seasonal variation can be observed: the solar irradiation is higher from October to March (spring-summer) and lower from April to September (autumn-winter).

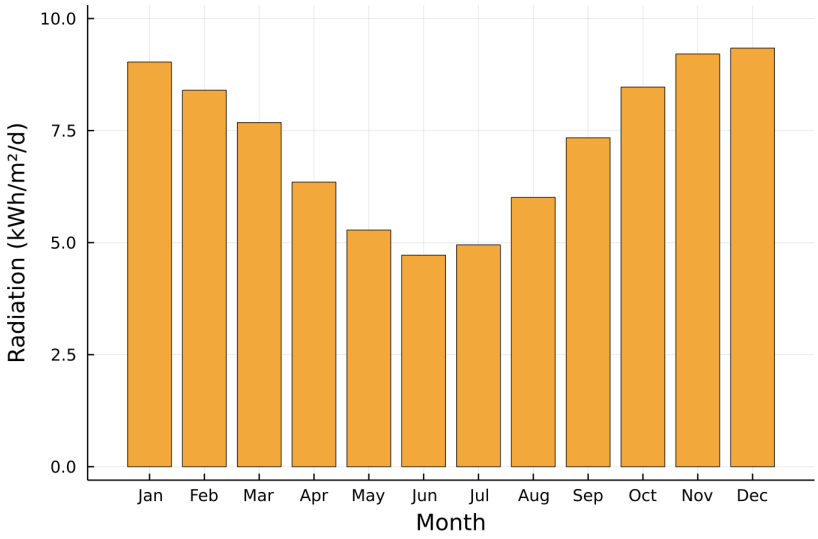

Figure 3.7: Monthly average solar radiation at the study area. Source: Own elaboration based on [117].

Figure 3.8 shows the daily global irradiation on a tilted surface of slope 23° on a typical summer and winter day. It is seen higher irradiation in summer than in winter. Additionally, in both cases, the peak radiation occurs between 12:00 pm and 3:00 pm; meanwhile, between 8:00 pm to 6:00 am, it is almost zero. This behavior coincides with daytime and nighttime, respectively.

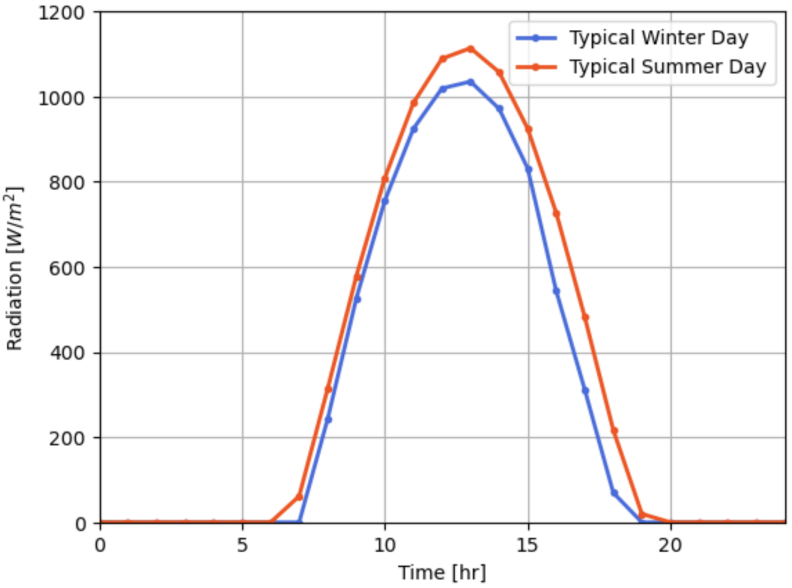

Figure 3.8: Daily global irradiation on a tilted surface of slope 23º from the horizontal on a typical summer and winter day. Source: Own elaboration based on [117].

Biomass resource & Biogas production

For this study, the biomass considered for biogas production is organics from Municipal Solid Waste (MSW). The selection was made considering the problems associated with MSW effective disposal and that landfill sites are becoming scarce [121].

The organic municipal waste flow was estimated to be 254 ton/day. The calculation was done considering the wastes that the landfill of Antofagasta City collects and the percentage of organics in wastes in Chile. On the other hand, for the biogas potential, a biogas yield of 105 m^3/ton of organic waste was used based on the work of Seruga Et-al. [122], which analyzed municipal solid wastes with a similar organic fraction as Chile. The biogas flow estimated is 26,670 m^3/day. In Appendix D, the biomass and biogas potential calculations are detailed.

3.6.3. System component inputs

For the simulation of the different components of the HRES, several technical parameters were necessary, such as efficiency, capacities, among others. The properties of the modeled components and all the applied technical parameters are provided in Appendix E.

Chapter 4

Results and Discussion

This chapter presents and discusses the results obtained for the different simulations done. It is organized into three sections: Single objective function design, Multi-objective function design, and Sensibility Analysis. The implementation of the model in Julia can be found in Appendix F.

4.1. Single objective function design

First, the optimization problem was solved considering the two criteria proposed separately. Case 1 considers the minimization of the annual costs; meanwhile, case 2 involves minimizing the system's emissions. The results and analysis for both cases are detailed as follows.

Objective functions

The economic objective chosen was the annual costs of the system as it allows considering the lifetime of the technologies into the model. The costs considered for the calculation were obtained from different sources, mainly from literature, and may vary from the actual costs in Chile. Market research is needed to have more precise values.

For the environmental function, the criterion taken was GHG emissions. The calculation considered the direct GHG emissions associated with fuel combustion and indirect GHG emissions associated with the purchase of electricity (scope 1 and 2 of the GHG protocol). Scope 3 emissions were not considered as there are challenging to estimate. They include indirect emissions resulting from value chain activities, and more precise information about a company is needed. Besides, the reports from COCHILCO about direct and indirect GHG emissions in the mining industry in Chile do not consider them either [8]. The selection of this environmental criterion implies that the storage technology's impact cannot be compared. For comparison, a third criterion should be included. In general renewable energy does not produce GHG emissions but does have other impacts like the use of land and resources. So, the criteria proposed are the use of land and abiotic depletion, which considers the depletion of nonliving resources such as fossil fuels and minerals [123]. A more accurate analysis should include the calculation of the impact of all technologies.

The optimal values obtained for each case are presented in Table 4.1. It can be concluded that a priori, the two objective functions considered, have an opposing character. Minimizing

costs involves an increase in emissions, and decreasing emissions requires increasing the costs. Additionally, the results show that the ideal scenario would be to have an energy system that costs 70.4 MUSD, and its emissions are 276.6 kton CO_2-eq, but it is mathematically unfeasible.

Table 4.1: Objective function results considering a single objective function.

Results	**Case 1: Minimizing costs**	**Case 2: Minimizing emissions**
Costs	70.4 MUSD	161.1 MUSD
Emissions	276.6 kton CO_2-eq	82.8 kton CO_2-eq

Configuration & Capacities

Figure 4.1 shows the configurations obtained when considering single objective functions for the design of the HRES. In case 1, the system consists of a PV array, a biogas generator, the grid, and the load. Renewable energies were chosen as they delivered cheaper energy than the grid, as seen in Table 4.2. Nonetheless, their energy is not enough to satisfy the load, and the grid is also needed. Additionally, no energy is stored as it will imply additional costs, showing that it is cheaper to use the grid than to store the energy excess. This matches with what is found in literature about ESS costs [124; 125].

In case 2, the configuration obtained considered all the proposed technologies: the PV array, the biogas generator, batteries, hydrogen storage system, and the grid. Both renewable options were chosen as solar energy does not have GHG emissions associated, and biogas emissions are lower than the grid. Moreover, the system prefers to store the energy excess as it does not produce emissions and implies using less the grid, consequently lowering the emissions. There is no preference between storage technologies as neither has emissions associated, so both are chosen.

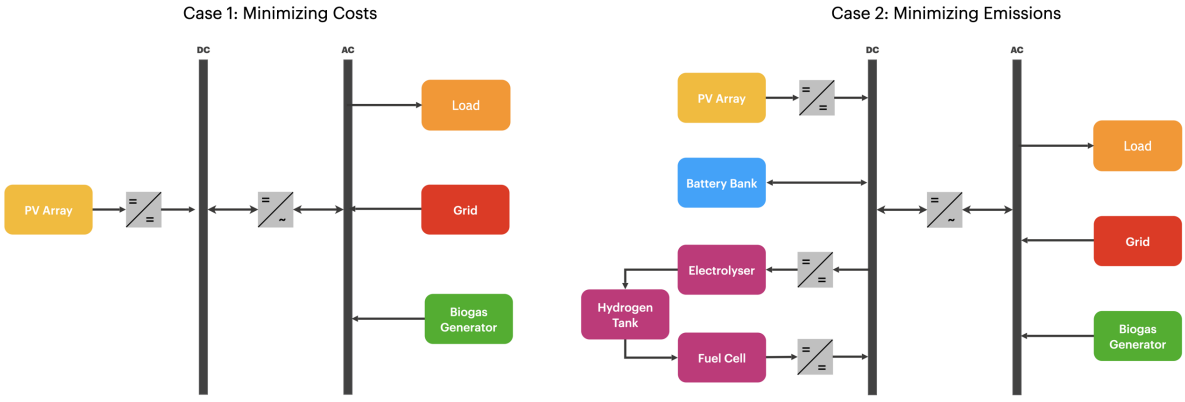

Figure 4.1: Resulting configuration of the HRES when considering a single objective function for the design.

Table 4.2: Costs of energy produced by different technologies Case 1 and 2.

Technology	Grid	Solar PV	Biogas
Costs/Energy delivered*	60 USD/MWh	49 USD/MWh	42 USD/MWh

* The costs obtained for cases 1 and 2 are the same.

The capacities of each technology are presented in Table 4.3. Regarding renewable energies, in case 1, the capacity of the solar PV plant is 140 MW, which is similar to the capacities of plants currently installed in Chile [126]. In case 2, the capacity is nearly quadrupled. It could still be possible to install as projects are planned for approximately 500 MW in the Region of Antofagasta [127]. For the biogas generator, its capacity is 3 MW in both cases. It can be attributed to the amount of biogas available as there are no technological restrictions. It is important to note that the biogas availability constraint is active, so a change in the amount of biogas available will affect the model results and the system's performance.

Concerning the storage systems, the capacities obtained for the batteries, electrolyzer, and fuel cell in case 2 are the actual world's largest capacities for each technology, which were the constraints imposed to avoid having an unrealistic model. As neither of the technologies has emissions associated, more energy is stored to avoid using the grid when the objective function is minimizing emissions. Consequently, both storage systems reached the maximum value possible. The capacities constraints for these technologies are also active, so renewable energies would be boosted if the technologies increase their capacity, and more GHG emissions can be reduced.

The power contracted from the grid is similar in both cases, but the value may not be optimum in the second case. The proposed grid model only considers economic aspects, implying that the same objective value could have been obtained only by overconsumption and non-contracting power from the grid. The model should be improved to avoid these cases, and for this, more details about energy contracts in needed.

Table 4.3: Capacities of each component of the HRES considering a single objective function for the design.

Technology	**Case 1: Minimizing costs**	**Case 2: Minimizing emissions**
Solar PV	140 MW	522 MW
Biogas Generator	3 MW	3 MW
Grid	131 MW	133 MW
Batteries	-	1200 MWh
Electrolyzer	-	100 MW
Hydrogen Tank	-	14 ton
Fuel Cell	-	59 MW

Variability & Seasonality

The typical energy generation profiles for both configurations are shown in Figures 4.2, 4.3, and 4.4 to analyze the variability and seasonality of energy sources and storage systems. It can be noticed that solar energy presents variability throughout the day, which is explained by the sunlight availability and coincides with the behavior of solar radiation presented in Figure 3.8. Solar energy generation occurs mainly between 10:00 am and 5:00 pm, and almost nonenergy is produced at nighttime. Concerning the seasonality of solar energy, there is a slight difference between the energy produced during summer and winter. However, it does not impact the system's operation.

Regarding biogas energy, no change is observed in the consumption of biogas during the day or throughout the year. This behavior is a consequence of assuming that the biomass and the biogas available are the same every hour, which could not be accurate. The biomass available and consequently the biogas generated will depend on the amount of wastes collected by the municipalities, which may vary day to day since they are not collected daily in every location. On the other hand, the organic fraction in wastes could have a seasonality explained by fruit and vegetables' availability throughout the year.

Concerning the energy storage systems, in Figure 4.4 the energy storage profiles for the electrolyzer and the batteries used in case 2 are depicted. The charging process occurs during the daytime when an excess of solar energy is produced, and both technologies proposed store a considerable amount of energy. It can be seen that the electrolyzer is used first, then the batteries. This tendency could be explained by the auto-discharge rate considered by the battery model. Using the electrolyzer first could result in a minor energy loss in the battery. Although it is more probable that the strategy used is random as there is no preference between both technologies considering GHG emissions. In the future, the model should consider the difference between both storage systems in terms of environmental impact and operability.

The discharging process of storage systems shown in Figure 4.3 shows that the batteries can fully supply the load during the first hours of the night, and then the fuel cell is used. After all the energy store is used, the grid is used to supply the load. The fuel cell cannot fully supply the load as its capacity limits it. If larger fuel cells are developed during the following years, hydrogen storage could be enhanced as it can also store energy for long periods than batteries. Additionally, the fuel cell only supplies energy for a few hours. Although it would be preferable as there would be less GHG emissions, it may not be the best option operationally as a more complex control system would be needed.

Finally, for both cases, the system cannot operate stand-alone (without the grid). In the first case, the grid is cheaper than storing energy, so the grid is used to supply energy at night when solar energy is unavailable or to complement during the day, as seen in Figure 4.2. For the second case, although the two options of storage energy are available, their capacity is not enough to supply the demand at all times. For this case, the grid mostly complements at night and after the storage technologies discharge at it can be seen in Figure 4.3.

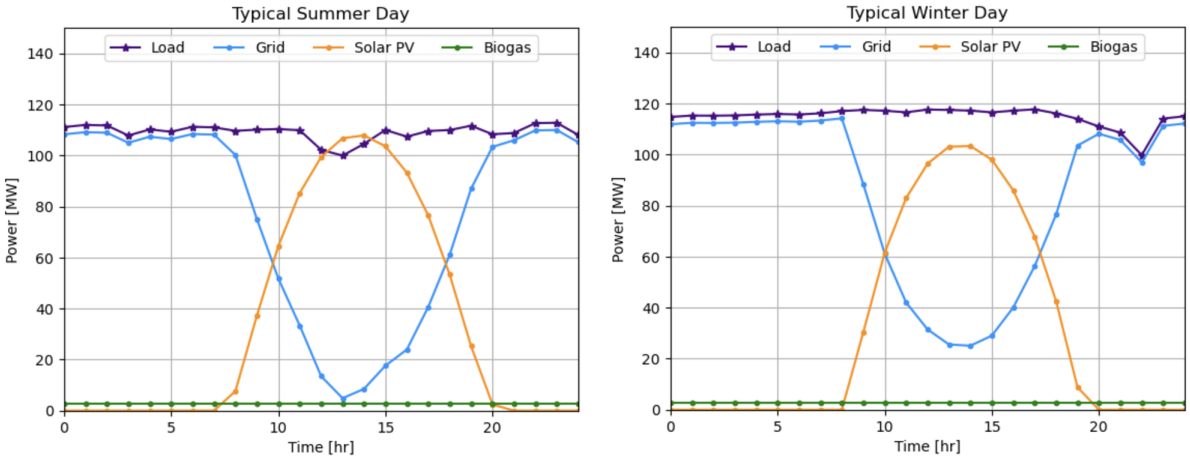

Figure 4.2: Typical energy profile on a summer and winter day considering the minimization of annual costs.

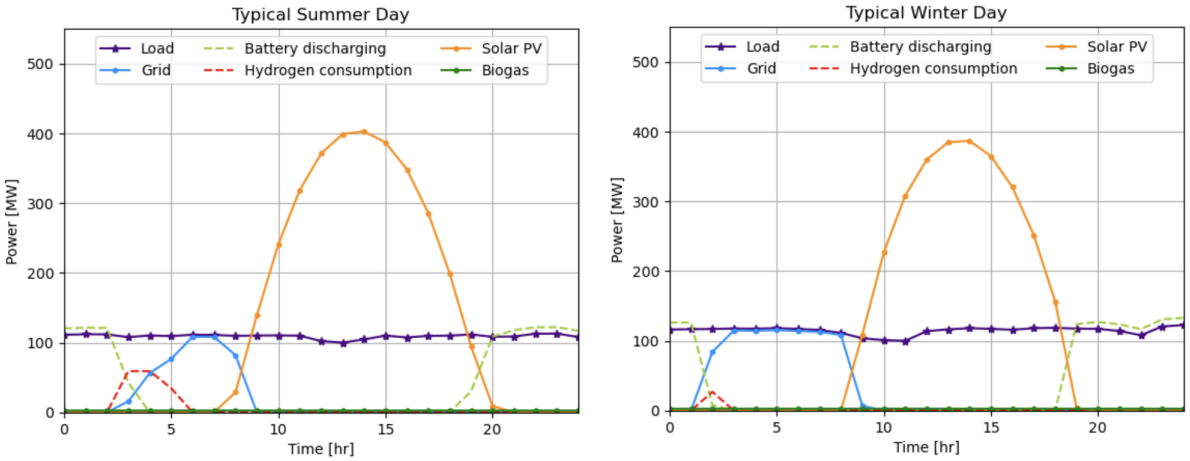

Figure 4.3: Typical energy profile on a summer and winter day considering the minimization of GHG emissions.

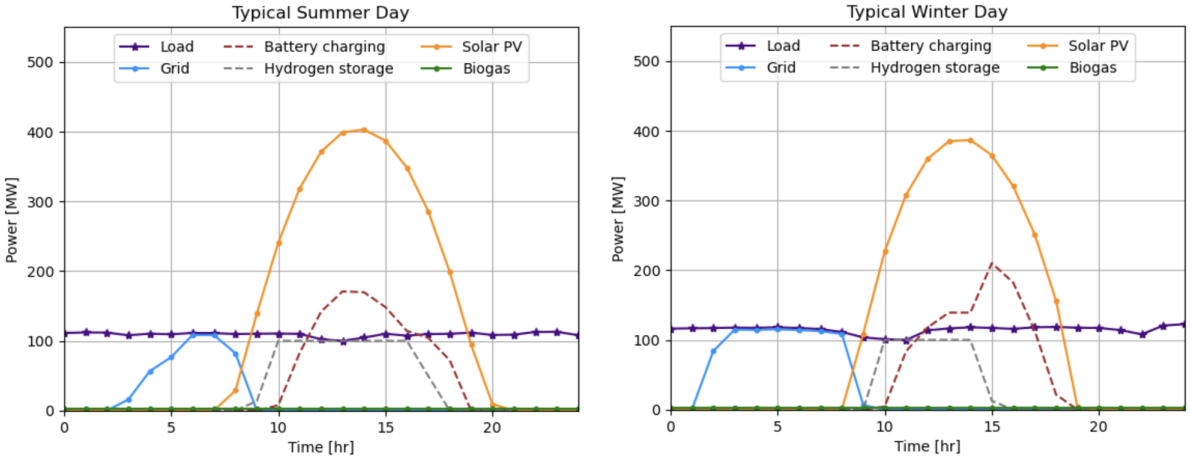

Figure 4.4: Typical energy charging profile on a summer and winter day considering the minimization of GHG emissions.

The role of renewable energies

Energy production from biogas seems to be an attractive option to reduce emissions, as it produces fewer emissions than fossil fuels and the electrical grid [106; 107]. Moreover, the results show that it can also deliver cheaper energy than the grid. Nonetheless, from Figure 4.5, it can be noticed that only around 3% of the energy is produced from biogas. It is attributed to the amount of biomass available in the zone for biogas production. Thus, while biogas would be a preferred option to reduce costs and emissions of a mining process, at least the use of organic from municipal wastes as feedstock does not have the potential to do it. The study of other biomass available in the area for biogas production is recommended.

The results also show that solar energy can produce cheaper energy than the grid (See Table 4.2) and can contribute to reducing the mining emissions as it does not have GHG emissions associated. Indeed, Figure 4.5 shows that almost 85% of the energy could come from the sun. Therefore, solar energy has a great potential to replace fossil fuels and the grid. However, due to its intermittency nature, it is necessary to use storage systems in a complementary way.

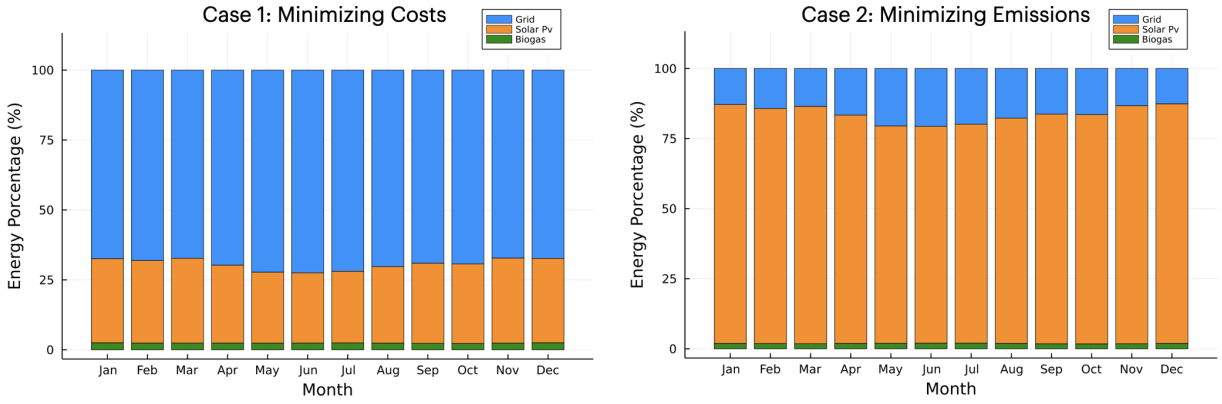

Figure 4.5: Monthly energy production obtained considering single objective functions.

4.2. Multi-objective function design

In a second stage, the problem was solved considering a multi-objective function: minimizing costs and minimizing the system's GHG emissions. Different relative importance weights were considered to obtain a subset of the Pareto front. The configuration of the energy system is also analyzed.

Pareto front

Figure 4.6 presents the set of possible trade-offs between the two objective functions. The Pareto front divides the solution space into the feasible solution zone (above the curve), where the solution points are feasible but not optimum, and the infeasible solution zone (below the curve). The Pareto front points are optimal solutions associated with certain relative importance weights of the two objective functions.

The Pareto curve obtained confirms the opposing character of the proposed economic and environmental functions: minimizing costs implies increasing emissions and vice versa. A more significant variation can be seen in the emissions compared to the costs as it varies by 70% versus 56%. The behavior of the curve shows that the costs tend to increase with a more significant step when the minimization of emissions takes primary importance; meanwhile, the emissions tend to decrease significantly. This result is interesting in the context of the system design, as it points that prioritizing one function will significantly impact the other. Additionally, the nonlinear form of the curve is a consequence of having integer variables, and that the system does not have the same configuration in every scenario.

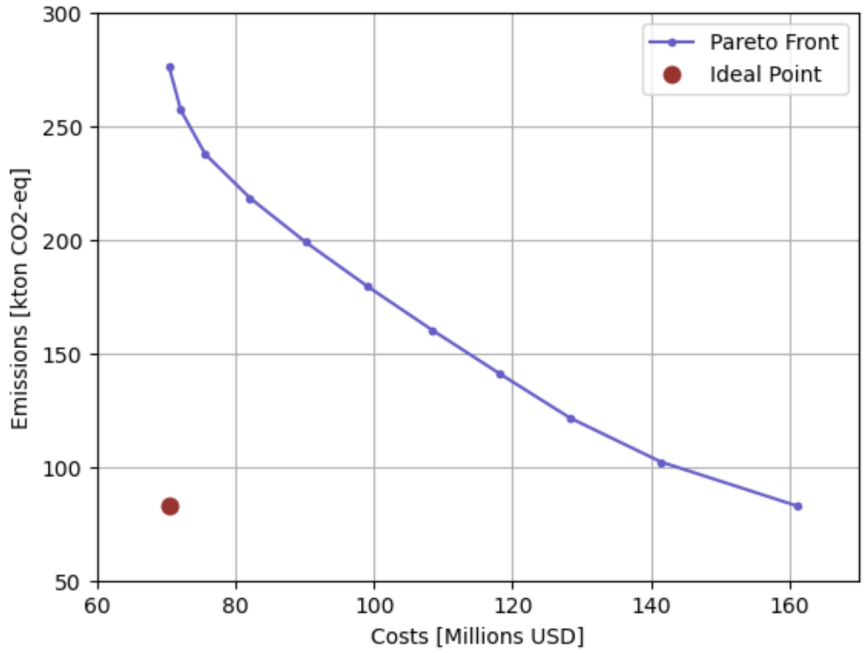

Figure 4.6: Pareto front between the annual cost versus the GHG emissions of the energy system.

From the Pareto front, it can be concluded that a carbon tax between 100 and 1,000 USD/CO_2-eq is needed to promote the minimization of emissions in the energy system proposed. These values differ significantly from the actual carbon taxes in Chile (around 5 USD/CO_2-eq) and other developed countries [128; 129]. It means that to promote the reduction of GHG emissions, not only are carbon taxes needed, but it is also necessary to reduce the investment costs of technologies.

Configuration & Capacities

The results considering different relative weights are shown in Table 4.4 to analyze the configuration and capacities of the multi-objective optimization problem. When the environmental function takes more importance (w near to 1), the solar PV plant capacity increases and the power contracted from the grid decreases. This tendency was expected, as to reduce GHG emissions, less energy from the grid must be used, and more renewable energy is needed. The biogas generator capacity remains the same in the three cases, and it is supported by the limited amount of biogas available in the study zone, as discussed before.

Concerning the storage systems, the battery bank capacity increases as the environmental function becomes more important than the economic function, which is expected as storing energy does not have GHG emissions associated. Despite this, the hydrogen storage system has similar capacities for the three cases. The non-preference between both technologies and the lower hydrogen storage capacities in contrast to batteries may explain it. Besides, the costs of hydrogen storage are higher than in batteries.

Table 4.4: Capacities of each component of the HRES considering a multi-objective function and different relative weights for the design.

Technology	**Case 3: Minimizing costs & emissions (w=0.3)**	**Case 4: Minimizing costs & emissions (w=0.5)**	**Case 5: Minimizing costs & emissions (w=0.7)**
Solar PV	244 MW	308 MW	372 MW
Biogas Generator	3 MW	3 MW	3 MW
Grid	119 MW	101 MW	82 MW
Batteries	110 MWh	440 MWh	788 MWh
Electrolyzer	45 MW	45 MW	49 MW
Hydrogen Tank	3 ton	4 ton	5 ton
Fuel Cell	3 MW	3 MW	4 MW

The results show that the optimal configuration to minimize costs and emissions should consider all the technologies. However, the role of the hydrogen storage system and the biogas generator are questionable, as they can only supply about 3% of the mine load each one. From an operational perspective, the load could be supplied using only solar energy and the grid. Besides, it could be preferable to store the energy only in batteries, considering that, currently, hydrogen storage is more expensive and less developed than batteries. Therefore, the model should be used as a tool for decision-making, and other aspects should be taken into account to decide the system's final configuration. For instance, it is recommended to evaluate other environmental impacts since GHG emissions are not the only impact energy systems have. Specifically, it is suggested to include as a criterion the use of non-renewable resources (abiotic depletion) to compare the different storage technologies.

Multi-objective optimization & the method used

The application of a multi-objective optimization problem has the advantage that more than one aspect can be considered in the design of a HRES and improves the decision-making process. However, one critical point is to decide the relative importance weights among the objective functions. In this problem, in particular, the configurations obtained considering different importance weights are similar. However, a trade-off exists between both objective functions, and prioritizing one function will significantly impact the other. It is suggested to discuss the values among the different stakeholders involved in the project to have a more representative opinion and reduce subjectivity. As the decision-making process can be complex multicriteria tools can be used as they are helpful to assess the judgments of individual decision-makers or multiple stakeholders.

The method selected for solving the multi-objective optimization problem was the ϵ-constraint method, as its results are not affected by the scaling of the objective functions [130]. Additionally, with this method, almost every run produces a different efficient solution, avoiding having redundant runs. In this problem, the ϵ-constraint method showed to solve the multi-optimization problem in a reasonable CPU time. However, the solving time was highly incremented compared to the mono-objective problem (4000 s versus 60 s). It may be attributed to the upper bound considered for the environmental function, but no further analysis was done. It is recommended to do additional analysis if more objective functions are considered [130].

4.3. Sensibility Analysis

The sensibility analysis performed considered the variation in the load demand, the biogas availability, the hydrogen storage costs, and the grid emissions factor. The Pareto fronts, the configurations, and the capacities are analyzed as follows. It is important to notice that the sensibility analysis performed considered the variation of one parameter to study the effect that each one has in the model. Nonetheless, the parameters would probably vary simultaneously.

Pareto fronts

Figure 4.7 shows the Pareto fronts of each scenario. When more energy is demanded, both costs and emissions increase, and the curve shape remains the same. The increase in both criteria is almost proportionally, and it is because the renewable energy potential is the same, so if more energy is demanded implies using more the grid, which costs and emissions associated are linear. The results also show that the model could be used to evaluate different energy scenarios. In particular, the two proposed scenarios can probably occur in Chile as is expected a steady increase in the energy demand in the following years [4].

If more biogas is available, both the costs and the emissions decrease and are explained by the fact that the energy produced from biogas is cheaper (as discussed in Section 4.1) and has fewer GHG emissions associated in comparison to the grid. The results also suggest that more energy from biogas should be produced to reduce costs and GHG emissions. Therefore, the potential of biogas production along Chile should be deeply studied as its use could also benefit other industries.

Regarding a reduction in the hydrogen storage costs, the same objective values were obtained in both scenarios, which means that more than an economic incentive is needed to use hydrogen storage. The results may also be attributed to the non-preference between energy storage systems concerning GHG emissions; hence, other environmental impacts should be incorporated into the model.

The last scenarios studied considered a variation on the grid emission coefficient, which supposes that the electrical grid will be cleaner in the future, supported by incorporating renewable energy in place of fossil fuels. A reduction of 33% on the grid emissions is considered

a possible scenario in Chile considering the Chilean decarbonization plan; meanwhile, the second case (reduction of 78% of the grid emissions) is a best scenario. The results show that renewable energy significantly impacts the system as it reduces the GHG emissions associated. Therefore, it is important to incorporate renewable energy into the electrical grid or through hybrid energy systems. On the other hand, almost no changes are seen about the costs as it is supposed that the grid and technology costs remain constant.

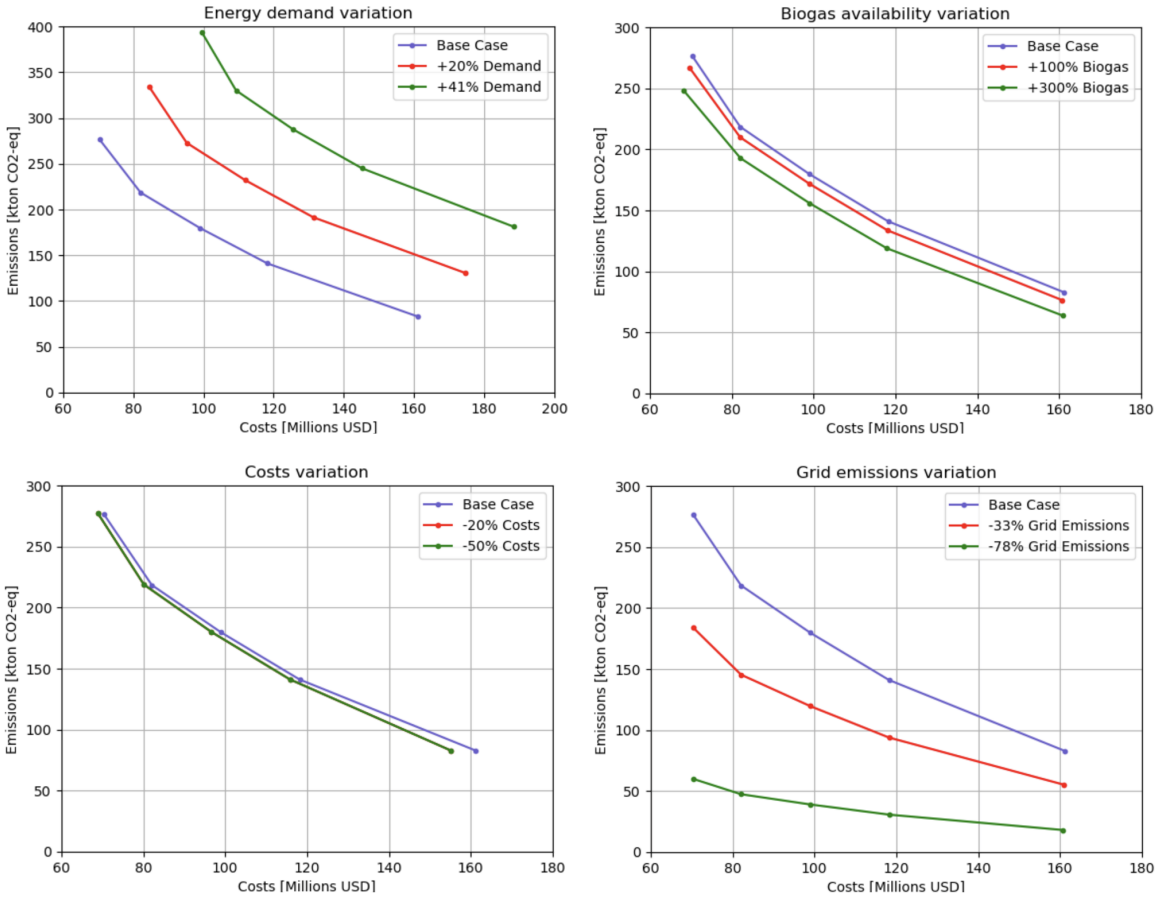

Figure 4.7: Pareto fronts under different scenarios.

Configuration & Capacities

Concerning the energy system configuration, the same technologies were selected in every scenario, and the capacities of each one do not significantly change compared to the case base, as seen in Table 4.5. There is a slight increase in the PV system capacity and the power contracted from the grid as the energy demand increases because more energy is needed to supply the load.

A variation in biogas availability confirms the potential of biogas to reduce emissions and costs, as the biogas generator has the maximum possible capacity considering the biogas limit of each scenario. The results also suggest that the system prefers to use biogas instead of solar energy, which is supported by the fact that biogas energy is more stable since it does

not depend on climatic factors. In addition, no energy storage systems are needed, which reduces costs. Because the biogas available in each hour is limited, and its value remains constant throughout the day, increasing the amount of biogas means that more energy can be stored during the day and thus reduce the use of the grid at night. However, a better strategy might be to take full advantage of solar energy during the day and limit biogas only to the night. It is important to note that the proposed scenarios are arbitrary, and the potential for biogas generation needs to be studied in depth for these scenarios to be possible.

As for energy storage systems, a decrease in hydrogen storage costs will encourage their use. However, it is also necessary to increase the capacities of electrolyzers and fuel cells in parallel. In this model, the storage system capacities were restricted by the largest capacity of each technology developed to date, but this does not mean that these technologies could not have a larger capacity in the future. In the two scenarios proposed, the fuel cell and the electrolyzer have the same capacities. It may be associated because the model does not prefer a storage system in terms of emissions. Finally, regarding the batteries capacities, they do not vary in the majority of the scenarios analyzed. The only exception is when the available biogas doubles, as the power from the grid decreases and more energy must be stored to supply the load.

Table 4.5: Capacity of each technology in different scenarios.

Technology	**Solar PV**	**Biogas Generator**	**Grid**	**Batteries**	**Electrolyzer**	**H2 Tank**	**Fuel Cell**
Scenario 0 (Base Case)	308 MW	3 MW	101 MW	440 MWh	45 MW	4 ton	3 MW
Scenario 1 (+20% Energy)	341 MW	3 MW	128 MW	409 MWh	51 MW	4 ton	4 MW
Scenario 2 (+41% Energy)	384 MW	3 MW	158 MW	347 MWh	66 MW	5 ton	5 MW
Scenario 3 (+100% Biogas)	370 MW	6 MW	79 MW	798 MWh	46 MW	5 ton	4 MW
Scenario 4 (+300% Biogas)	301 MW	11 MW	90 MW	496 MWh	34 MW	4 ton	3 MW
Scenario 5 (-20% Costs)	315 MW	3 MW	95 MW	408 MWh	53 MW	30 ton	13 MW
Scenario 6 (-50% Costs)	315 MW	3 MW	95 MW	408 MWh	53 MW	30 ton	13 MW
Scenario 7 (Grid EU)	307 MW	3 MW	101 MW	439 MWh	45 MW	3 ton	4 MW
Scenario 8 (Grid Lithuania)	307 MW	3 MW	101 MW	439 MWh	45 MW	3 ton	4 MW

Chapter 5

Conclusion

This chapter summarizes the work and contributions of this thesis and provides the findings to each research question. Also, future recommendations are presented.

5.1. Summary of Thesis and Key Contributions

The main purpose of thesis work has been to design and evaluate a solar-biogas hybrid renewable energy system for a mining process considering technical, economic, and environmental aspects. This goal has been accomplished with the following results.

A hybrid renewable energy system was proposed to supply the electrical demand of a mining process. It included a PV array, a biogas generator, a battery bank, a hydrogen storage system, and access to the electrical grid. A multi-objective optimization problem was formulated to find the optimal configuration of the HRES considering the minimization of the annual costs and GHG emissions. The main constraints of the model were the operational restrictions of each technology, the demand satisfaction, and the mass and energy balances.

The model was applied to a case study that considered a hypothetical mine located in the Antofagasta Region in Chile. The solar radiation profile was obtained from the solar explorer tool, and it was assumed that biogas was produced from the organic fraction of municipal solid wastes. The mine load profile was estimated using data of a mine located in the North of Chile. The model was simulated for one year with an hourly step to consider the variability of renewable resources, and the implementation was done in the computational program Julia.

The optimization problem was first solved considering each objective function separately, and then the multi-objective optimization problem was solved using the ϵ-constraint method. The results showed that the two objective functions considered have an opposing character as minimizing the costs implies increasing the emissions and vice versa. Moreover, the behavior of the Pareto front showed that prioritizing one function will significantly impact the other.

The findings also indicate that renewable energy could help reduce emissions, but storage systems are needed in a complementary way, which increases the system's costs. In all simulations, most of the energy was stored in batteries, although there is no preference between storage systems considering GHG emissions. A deeper evaluation of

the environmental impact of energy systems is suggested as GHG emissions are not the only impact that energy systems have. Particularly the use of land or resources (abiotic depletion) should be considered.

From the renewable sources studied, solar energy can supply the demand of a mining process but not the biogas, as it is limited by the biomass available in the zone. Nevertheless, electricity production from biogas seems to be an attractive option if more biomass is available since it can bring economic and environmental benefits. It produces cheaper energy than other sources and has lower GHG emissions associated than the electrical grid.

Lastly, a sensibility analysis was performed considering a variation in the load demand, the biogas availability, the hydrogen storage costs, and the grid emissions factor. The analysis showed that the model developed could be used to evaluate future energy demand scenarios. Also, more biogas should be used for energy production. The constraint of the biogas availability was active in all the scenarios proposed, which means that a change in the amount of biomass available for biogas production will affect the model results and the system's performance. On the other hand, incorporating renewable energy into the electrical grid or though hybrid energy systems could be a key factor for decreasing GHG emissions. Finally, an economic incentive and the development of larger electrolyzer and fuel cells are needed to enhance hydrogen storage.

5.2. Summary of findings

The following are the answers to the research questions posed in this work.

Research question 1: How can an energy requirement of a mining process in Chile be supplied with solar energy and biogas?

This study analyzed the potential of using solar energy and biogas to supply the electrical demand of a mining process. The results showed a great potential to use solar energy in the North of Chile as it can almost supply 85% of the mine load, and no seasonality is presented. Besides, it brings economic and environmental benefits by producing cheaper energy than the grid and reducing the mining emissions as it does not have GHG emissions associated. Nonetheless, due to its intermittent nature, it is necessary to use storage systems in a complementary way.

On the other hand, the electricity generation from biogas proved to be an attractive option to reduce emissions. Besides, it could also have economic benefits. However, its use is subject to the availability of biomass. In particular, organics from municipal solid wastes as a feedstock can only supply approximately 3% of the load.

The proposed HRES appears to be an attractive option to supply an energy requirement of a mining process using solar energy and biogas. It can reduce the use of the electrical grid while providing economic and environmental benefits. Nevertheless, biomass availability for biogas production needs to be studied further to evaluate the potential of the HRES fully.

Research question 2: What is the optimal configuration of a biogas-PV hybrid energy system that minimizes costs and environmental impacts when used to satisfy a given energy requirement in a mining process?

Several simulations were done to analyze the optimal configuration of the HRES and the capacities of its components. Based on them, the optimal configuration of the energy system to minimize both costs and the environmental impact considers a PV array and biogas as primary energy sources and batteries and hydrogen storage to store or supply energy when needed. Besides, the system is connected to the electrical grid as it cannot operate stand-alone. The capacity of each component is depicted in Table 5.1.

Table 5.1: Capacities of each component of the HRES considering the optimal configuration that minimizes costs and the environmental impact.

Technology	Capacity
Solar PV	308 MW
Biogas Generator	3 MW
Grid	101 MW
Batteries	440 MWh
Electrolyzer	45 MW
Hydrogen Tank	4 ton
Fuel Cell	3 MW

The configuration obtained is a Pareto optimal solution but may not be the best option in terms of operability. The system would require a more complex control system as it includes different energy sources and storage systems. Moreover, the biogas generator and a fuel cell would have a limited capacity to supply the load. On the other hand, having more technologies could make the system more resilient. Hence, the design of a HRES should also include criteria concerning stability and operability.

In this study, the HRES was designed considering an economic and environmental objective function, where the environmental criterion selected was GHG emissions. Its calculation considered direct GHG emissions associated with fuel combustion and indirect GHG emissions associated with the purchase of electricity. Consequently, non of the energy storage systems has an environmental impact and cannot be compared with the model. This non-preference between both technologies impacts the capacities results. It is suggested to incorporate another environmental impact in the model that primes the comparison of the energy storage systems. In general, renewable energy does not produce GHG emissions but has other impacts like land and resources. So, the criterion proposed is abiotic depletion, which considers the depletion of nonliving resources such as fossil fuels and minerals.

Lastly, the configuration presented considered that both objective functions have the same importance. However, the decision of relative importance weight is a critical point in decision making as prioritizing one criterion could significantly impact the other. It is recommended to discuss the value among the different stakeholders involved to have a more representative opinion and reduce subjectivity. Besides, as the decision-making process can be complex, the

use of multicriteria tools is suggested as they are helpful to assess the judgments of different stakeholders.

Research question 3: Which trade-off can be found?

The results show that a trade-off exists between costs and GHG emissions, and the prioritization of one criterion will significantly impact the other. Therefore, it is not possible to reduce GHG emissions without increasing the costs and vice versa. It is essential to consider the trade-off that exists and the interest of all the stakeholders for decision-making.

From the Pareto front obtained between the annual costs and GHG emissions, it can be concluded that carbon tax should have a cost between 100 and 1,000 USD/CO_2-eq to promote the minimization of emissions in the HRES proposed. These values are significantly different from the actual prices of carbon taxes. Thus, to promote the reduction of GHG emissions, not only are carbon taxes needed, but it is also necessary to reduce the investment costs of technologies.

5.3. Future recommendations

A potential direction for this work is a tri-criteria design that includes a second environmental criterion to evaluate the impact of renewable energy and energy storage systems as generally they do not have GHG emissions associated. In particular, the model did not have a preference regarding storage systems which impacted the results obtained. The third objective function could consider the use of land or resources (abiotic depletion). The resolution method should be evaluated if another objective function is considered, as the solving time was highly incremented in the multi-objective problem.

Finally, in future works, it is recommended to study operation strategies considering the availability and characteristics of renewable sources. For instance, biogas could be limited to being used only at night to take full advantage of solar energy during the day.

Glossary

AC	Alternating Current
AD	Anaerobic Digestion
COCHILCO	Chilean Copper Commission
CNE	National Commission of Energy
CO_2-eq	Carbon Dioxide Equivalent
CODELCO	Chilean National Copper Corporation
CPU	Central Processing Unit
CRF	Capital Recovery Factor
c-Si	Crystalline Silicone
CSP	Concentrated Solar Power
DC	Direct Current
DoD	Depth of Discharge
DP	Dynamic Programming
ESS	Energy Storage System
EU	European Union
GA	Genetic Algorithm
GDP	Gross Domestic Product
GHG	Greenhouse Gas
HRES	Hybrid Renewable Energy System
INE	National Institute of Statistics
kWh	Kilowatt-hour
ILP	Integer Linear Programming
LP	Linear Programming
MAD	Median Absolute Deviation
MILP	Mixed-Integer Linear Programming
MINLP	Mixed-Integer Nonlinear Programming
MIP	Mixed Integer Programming
MP	Mathematical Programming
MSW	Municipal Solid Waste
MWh	Megawatt-hour
NLP	Nonlinear Programming
NOCT	Nominal Operating Cell Temperature
O&M	Operation and Maintenance
PEM	Proton Exchange Membrane
PSO	Particle Swarm Optimization
PV	Photovoltaic
SEN	National Electrical System
SHC	Solar Heating and Cooling
SOC	State of Charge
WWTPs	Water Treatment Plants

Bibliography

[1] Comisión Nacional de Productividad. 2017. Productivity in the Chilean Copper Mining Industry. Tech. rep. Comisión Nacional de Productividad.

[2] Consejo Minero. 2021. Cifras actualizadas de la minería-Abril 2021. Tech. rep. Consejo Minero.

[3] Montes, C., and González, A. 2018. Consumo de energía y recursos hídricos en minería del cobre al 2017. Tech. rep. Comisión Nacional del Cobre.

[4] COCHILCO. 2019. Proyección del consumo de energía eléctrica en la minería del cobre 2019-2030. Tech. rep. Comisión Chilena del Cobre.

[5] Fundación Chile. 2016. From copper to innovation: Mining technology roadmap 2035. Tech. rep. Fundación Chile.

[6] Harmsen, J., Roes, A., and Patel, M. 2013. The impact of copper scarcity on the efficiency of 2050 global renewable energy scenarios. Energy, 50: 62-73.

[7] Guilbaud, J. 2016. Hybrid Renewable Power Systems for the mining industry: system costs, reliability costs and portafolio cost risks. Doctoral Thesis for the degree of Philosophiae Doctor. University College London.

[8] Comisión Chilena del Cobre. 2020. Emisiones de gases de efecto invernadero directos e indirectos en la minería del cobre al año 2019. Tech. rep. Ministerio de Minería.

[9] Moreno-Leiva, S., Haas, J., Junne, T., Valencia, F., Godin, H., Kracht, W., Nowak, W., and Eltrop, L. 2020. Renewable energy in copper production: A review on systems design and methodological approaches. Journal of Cleaner Production, 246.

[10] Moreno-Leiva, S., Díaz-Ferrán, G., Haas, J., Telsnig, T., Díaz-Alvarado, F., Palma-Behnke, R., Kracht, W., and Román, R., Chudinzow, D., and Eltrop, L. 2017. Towards solar power supply for copper production in Chile: Assessment of global warming potential using a life-cycle approach. Journal of Cleaner Production, 164: 242-249.

[11] COCHILCO. 2019. Informe de actualización del consumo energético de la minería del cobre al año 2018. Tech. rep. Comisión Chilena del Cobre.

[12] O'Ryan, R., Nasirov, S., and Álvarez-Espinosa, A. 2020. Renewable energy expansion in the Chilean power market: A dynamic general equilibrium modeling approach to determine CO2 emission baselines. Journal of Cleaner Production, 247.

[13] Zahedi, A. 2011. A review of drivers, benefits, and challenges in integrating renewable energy sources into electricity grid. Renewable and Sustainable Energy Reviews, 15(9): 4775-4779.

[14] Comisión Nacional de Energía. 2020. Capacidad total instalada Sistema Eléctrico Nacional. [Online]. Available in: http://energiaabierta.cl/visualizaciones/capacidad-instalada/ (Last accessed: 06/03/21)

[15] CODELCO. 2014. Pampa Elvira Solar de División Gabriela Mistral premiada por Fundación Recyclápolis y El Mercurio. [Online]. Available in: https://www.codelco.com/pampa-elvira-solar-de-division-gabriela-mistral-premiada-por-fundacion/prontus{_}codelco/2014-11-06/094222.html (Last accessed: 06/02/21)

[16] Antofagasta Minerals. 2015. Minera Los Pelambres suma la energía del sol. [Online]. Available in: https://www.aminerals.cl/comunicaciones/noticias/2015/minera-los-pelambres-suma-la-energia-del-sol/ (Last accessed: 06/02/21)

[17] Castillo, P., Kouro, S., Rojas, C, and Muller, N. 2015. Photovoltaic DC-DC converter for direct power interface to copper electrorefining process. IECON 2015 - 41st Annual Conference of the IEEE Industrial Electronics Society, 4388-4393.

[18] Pamparana, G., Kracht, W., Haas, J., and Díaz-Ferrán, G., Palma-Behnke, R., and Román, R. 2017. Integrating photovoltaic solar energy and a battery energy storage system to operate a semi-autogenous grinding mill. Journal of Cleaner Production, 165: 273-280.

[19] Pamparana, G., Kracht, W., Haas, J., Ortiz, J., Nowak, W., and Palma-Behnke, R. 2019. Studying the integration of solar energy into the operation of a semi-autogenous grinding mill. Part I: Framework, model development and effect of solar irradiance forecasting. Minerals Engineering, 137: 68-77.

[20] Pamparana, G., Kracht, W., Haas, J., Ortiz, J., Nowak, W., and Palma-Behnke, R. 2019. Studying the integration of solar energy into the operation of a semi-autogenous grinding mill. Part II: Effect of ore hardness variability, geometallurgical modeling and demand side management. Minerals Engineering, 137: 53-67.

[21] Amusat, O., Shearing, P., and Fraga, E. 2015. System Design of Renewable Energy Generation and Storage Alternatives for Large Scale Continuous Processes. Computer Aided Process Engineering, 37: 279-2284.

[22] Amusat, O., Shearing, P., and Fraga, E. 2016. Optimal integrated energy systems design incorporating variable renewable energy sources. Computers and Chemical Engineering, 95: 21-37.

[23] Amusat, O., Shearing, P., and Fraga, E. 2017. On the design of complex energy systems: Accounting for renewables variability in systems sizing. Computers and Chemical Engineering, 103: 103-115.

[24] Vyhmeister, E., Aleixendri, C., Bermúdez, J., Pina, J., Fúnez, C., Rodríguez, L., Godoy-Faúndez, A., Higueras, P., Clemente-Jul, C., Valdés-González, H., and Reyes-Bozo, L. 2017. A combined photovoltaic and novel renewable energy system: An optimized techno-economic analysis for mining industry applications. Journal of Cleaner Production, 149: 999-1010.

[25] Kantenbacher, J., and Shirley, R. 2017. Renewable Energy: Scaling Deployment in the United States and in Developing Economies. Scaling Deployment in the United States and in Developing Economies (Chap 5). In: Sustainable Cities and Communities Design Handbook: Green Engineering, Architecture, and Technology. Second Ed. Butterworth-

Heinemann. pages 89-109.

[26] Mandal, S., Yasmin, H., Sarker, M., and Beg, M. 2017. Prospect of solar-PV/biogas/diesel generator hybrid energy system of an off-grid area in Bangladesh. AIP Conference Proceedings.

[27] Singh, Anand and Baredar, Prashant and Gupta, Bhupendra. 2015. Computational Simulation & Optimization of a Solar, Fuel Cell and Biomass Hybrid Energy System Using HOMER Pro Software. Procedia Engineering, 127: 743-750.

[28] Vendoti, S., Muralidhar, M. and Kiranmayi, R. 2021. Techno-economic analysis of off-grid solar/wind/biogas/biomass/fuel cell/battery system for electrification in a cluster of villages by HOMER software. Environment, Development and Sustainability, 23(1): 351-372.

[29] Zhou, B., Xu, D., Li, C., Chung, C., Cao, Y., Chan, K., and Wu, Q. 2018. Optimal scheduling of biogas-solar-wind renewable portfolio for multicarrier energy supplies. IEEE Transactions on Power Systems, 33(3): 6229-6239.

[30] Koukosia, I., Makris, I., Mavropoulos, A., Mavropoulos, A., Mavropoulus, N., Psalida, A., and Tsakona, M. 2014. Waste Atlas b2013 Report. [Online]. Available in: http://www.atlas.d-waste.com/Documents/WASTEATLAS2013REPORT.pdf

[31] Ministerio de Energía de Chile. 2016. National Green Hydrogen Strategy. Tech. rep. Ministerio de Energía de Chile.

[32] Servicio Nacional de Geología y Minería (SERNAGEOMIN). 2021. Anuario de la mineria en Chile 2020. Tech. rep. Ministerio de Minería de Chile.

[33] Nasirov, Sh., and Agostini, C. 2018. Mining experts' perspectives on the determinants of solar technologies adoption in the Chilean mining industry. Renewable and Sustainable Energy Reviews, 95: 194-202.

[34] World Business Council for Sustainable Development World Resources Institute. 2015. The Greenhouse Gas Protocol: A Corporate Accounting and Reporting Standard. Tech. rep. World Business Council for Sustainable Development World Resources Institute.

[35] Zohuri, B. 2018. Hybrid Renewable Energy Systems (Chap 1). In: Hybrid Renewable Energy Systems. First Ed. Springer International Publishing. pages 1-38.

[36] Martínez, M. 2017. Stand-alone hybrid renewable energy systems (HRES). Ph. D. Thesis. Polytechnic University of Catalonia.

[37] Rekioua, Djamila. 2014. Wind Power Electric Systems (Chap 6). In: Wind Power Electric Systems. First Ed. Springer London. pages 163-184.

[38] Mohtasham, J. 2015. Review Article-Renewable Energies. Energy Procedia, 74: 1289-1297.

[39] Owusu, P., and Asumadu-Sarkodie, S. 2016. A review of renewable energy sources, sustainability issues and climate change mitigation. Cogent Engineering, 3(1).

[40] U.S. Energy information Administration (EIA). 2020. Renewable energy explained. [Online]. Available in: https://www.eia.gov/energyexplained/renewable-sources/ (Last accessed: 10/03/21)

[41] International Renewable Energy Agency (IRENA). 2020. Wind Energy. [Online]. Available in: https://www.irena.org/wind (Last accessed: 02/15/21)

[42] International Renewable Energy Agency (IRENA). 2020. Solar Energy. Online]. Available: https://www.irena.org/solar (Last accessed: 02/05/21)

[43] Wang, R., Xu, Z., and Ge, T. 2016. Introduction to solar heating and cooling systems (Chap 1). In: Advances in Solar Heating and Cooling. First Ed. Woodhead Publishing. pages 3-12.

[44] Archer, R. 2020. Geothermal energy (Chap 20). In: Future Energy: Improved, Sustainable and Clean Options for Our Planet. Third Ed. Elsevier. pages 431-445.

[45] U.S Departament of Energy. 2010. Geothermal Basics. [Online]. Available in: https://www.energy.gov/eere/geothermal/geothermal-basics (Last accessed: 02/05/21)

[46] Williams, C., Dahiya, A., and Porter, P. 2020.Introduction to bioenergy and waste to energy (Chap 1). In: Bioenergy: Biomass to Biofuels and Waste to Energy. Second Ed. Academic Press. pages 5-44.

[47] IRENA. 2020. BioEnergy. Tech. rep. International Renewable Energy Agency.

[48] Röder, Mirjam and Welfle, Andrew. 2018. Bioenergy (Chap 12). In: Managing Global Warming: An Interface of Technology and Human Issues. First Ed. Academic Press. pages 379-398.

[49] Novakovic, B., and Nasiri, A. 2016. Introduction to electrical energy systems (Chap 1). In: Electric Renewable Energy Systems. First Ed. Academic Press. pages 1-20.

[50] Cheng, M., Sami, S., and Wu, J. 2017. Benefits of using virtual energy storage system for power system frequency response. Applied Energy, 194: 76-385.

[51] Fathima, A., and Palanisamy, K. 2016. Energy Storage Systems for Energy Management of Renewables in Distributed Generation Systems (Chap. 7). In: Energy Management of Distributed Generation Systems. First Ed. InTech. pages 157-181.

[52] Vivas, F., De las Heras, A., Segura, F., Andújar, J. 2018. A review of energy management strategies for renewable hybrid energy systems with hydrogen backup. Renewable and Sustainable Energy Reviews, 82: 126-155.

[53] Segura, F. and Durán, E. and Andújar, J. M. 2009. Design, building and testing of a stand alone fuel cell hybrid system. Journal of Power Sources, 193(1): 276-284.

[54] Mohan, N., Undeland, T., and P.Robbins, W. 2003. Power Electronic Systems. In: Power Electronics: Converter, Application and Design. Third Ed. John Wiley & Sons. pages 3-15.

[55] Fardo, S., and Patrick, D. 2020. Power Systems Fundamentals (Chap 2). In: Electrical Power Systems Technology. Third Ed. River Publisher. pages 15-58.

[56] Asare-Bediako, B., Kling, W., and Ribeiro, P. 2014. Future residential load profiles: Scenario-based analysis of high penetration of heavy loads and distributed generation. Energy and Buildings, 75: 228-238.

[57] Mihai, C., Lepadat, I., and Helerea, E., and Călin, D. 2010. Load curve analysis for an industrial consumer. In: 2010 12th International Conference on Optimisation of

Electrical and Electronic Equipment (OPTIM). pages 1275-1280.

[58] Trifkovic, M., Sheikhzadeh, M., Nigim, K., and Daoutidis, P. 2014. Modeling and Control of a Renewable Hybrid Energy System With Hydrogen Storage, 22(1): 169-179.

[59] Pereira, M., Rego, E., and Nagano, M. 2018. A Multiobjective Optimization Model for the Design of Hybrid Renewable Energy Systems. IEEE Latin America Transactions, 16(3): 2925-2933.

[60] Kajela, D., and Manshahia, M. 2017. Optimization of Renewable Energy Systems : A Review. International Journal of Scientific Research in Science and Technology, 3(8): 769-795.

[61] Ghofrani, Mahmoud and Hosseini, Negar Niromand. 2016. Optimizing Hybrid Renewable Energy Systems: A Review (Chap 8). In: Sustainable Energy - Technological Issues, Applications and Case Studies. First Ed. IntechOpen.

[62] Fathima, A., and Palanisamy, K. 2015. Optimization in microgrids with hybrid energy systems - A review. Renewable and Sustainable Energy Reviews, 45:431-446.

[63] Upadhyay, S., and Sharma, M. 2014. A review on configurations, control and sizing methodologies of hybrid energy systems. Renewable and Sustainable Energy Reviews, 38: 47-63.

[64] Rao, S. 2019. Classical Optimization Techniques (Chap 2). In: Engineering Optimization Theory and Practice. Fifth Ed. Wiley. pages 57-108.

[65] Bradley, S., Hax, A., and Magnanti, T. 1977. Linear Mathematical Programming: an Overview (Chap 1). In: Applied Mathematical Programming. Addison-Wesley. pages 1-37.

[66] Balaman, Ş. 2019. Modeling and Optimization Approaches in Design and Management of Biomass-Based Production Chains (Chap 7). In: Decision-Making for Biomass-Based Production Chains. First Ed. Academic Press. pages 185-236.

[67] Huneke, F., Henkel, J., González, J., and Erdmann, G. 2012. Optimisation of hybrid off-grid energy systems by linear programming. Energy, Sustainability and Society, 2 (1).

[68] Saif, A., Elrab, K., Zeineldin, H., Kennedy, S., and Kirtley, J. 2010. Multi-objective capacity planning of a PV-wind-diesel-battery hybrid power system. In: 2010 EEE International Energy Conference and Exhibition. pages 217-222.

[69] Vafaei, M. and Kazerani, M. 2011. Optimal unit-sizing of a wind-hydrogen-diesel microgrid system for a remote community. In: 2011 IEEE PES Trondheim PowerTech: The Power of Technology for a Sustainable Society. pages 1-7.

[70] Hu, J., and Bhowmick, P. A consensus-based robust secondary voltage and frequency control scheme for islanded microgrids. 2020. International Journal of Electrical Power and Energy Systems, 116.

[71] Siddaiah, R., and Saini, R. 206. A review on planning, configurations, modeling and optimization techniques of hybrid renewable energy systems for off grid applications. Renewable and Sustainable Energy Reviews, 58: 376-396.

[72] Das, B., and Kumar, A. 2018. A NLP approach to optimally size an energy storage

system for proper utilization of renewable energy sources. Procedia Computer Science, 125: 483-491.

[73] Kongnam, C. and Nuchprayoon, S. and Premrudeepreechacharn, S. and Uatrongjit, S. 2009. Decision analysis on generation capacity of a wind park. Renewable and Sustainable Energy Reviews, 13(8): 2126-2133.

[74] An, L., and Tuan, T. 2018. Dynamic Programming for Optimal Energy Management of Hybrid Wind–PV–Diesel–Battery. Energies, 11.

[75] Li, C., Zhu, X., Cao, G., Sui, S and Hu, M. 2009. Dynamic modeling and sizing optimization of stand-alone photovoltaic power systems using hybrid energy storage technology. Renewable Energy, 32(3): 815-826.

[76] Alonso, M., Amaris, H., and Alvarez-Ortega, C. 2012. Integration of renewable energy sources in smart grids by means of evolutionary optimization algorithms. Expert Systems with Applications, 39(5): 5513-5522.

[77] Rocha, M., and Neves, J. 1999. Preventing premature convergence to local optima in genetic algorithms via random offspring generation. In: Multiple Approaches to Intelligent Systems, 12th International Conference on Industrial and Engineering Applications of Artificial Intelligence and Expert Systems.

[78] Ko, M., Kim, Y., Chung, M., and Jeon, H. 2015. Multi-objective optimization design for a hybrid energy system using the genetic algorithm. Energies, 8(4): 2924-2949.

[79] Dufo-López, R., Bernal-Agustín, J., and Contreras, J. 2007. Optimization of control strategies for stand-alone renewable energy systems with hydrogen storage. Renewable Energy, 32(7): 1102-1126.

[80] Avril, S., Arnaud, G., Florentin, A., and Vinard, M. 2010. Multi-objective optimization of batteries and hydrogen storage technologies for remote photovoltaic systems. Energy, 35(12): 5300-5308.

[81] Kashefi Kaviani, A., Riahy, G., and Kouhsari, S. 2009. Optimal design of a reliable hydrogen-based stand-alone wind/PV generating system, considering component outages. Renewable Energy, 34(11): 2380-2390.

[82] Khatib, T., Mohamed, A., and Sopian, K. 2012. Optimization of a PV/wind micro-grid for rural housing electrification using a hybrid iterative/genetic algorithm: Casestudy of Kuala Terengganu, Malaysia. Energy and Buildings, 47: 321–331.

[83] Sinha, S., and Chandel, S. 2015. Review of recent trends in optimization techniquesfor solar photovoltaic-wind based hybrid energy systems. Renewable and Sustain-able Energy Reviews, 50: 755–769.

[84] Singh, A., and Baredar, P. 2016. Techno-economic assessment of a solar PV, fuel cell, and biomass gasifier hybrid energy system. Energy Reports, 2: 254-260.

[85] Skoplaki, E., and Palyvos, J. 2009. On the temperature dependence of photovoltaic module electrical performance: A review of efficiency/power correlations. Solar Energy, 83(5): 614-624.

[86] Molina, A., and Martinez, F. 2017. Modelo de Generación Fotovoltaica. Tech. rep. Universodad de Chile-Ministerio de Energía.

[87] Dufo-López, R., Bernal-Agustín, J. 2008. Multi-objective design of PV-wind-diesel-hydrogen-battery systems. Renewable Energy, 33(12): 2559-2572.

[88] Eriksson, E., and Gray, E. 2019. Optimization of renewable hybrid energy systems – A multi-objective approach. Renewable Energy, 133: 971-999.

[89] Maleki, A., and Askarzadeh, A. 2014. Comparative study of artificial intelligence techniques for sizing of a hydrogen-based stand-alone photovoltaic/wind hybrid system. International Journal of Hydrogen Energy, 39(19): 9973-9984.

[90] Chang, W. 2013. The State of Charge Estimating Methods for Battery: A Review. ISRN Applied Mathematics.

[91] Sharafi, M., and ELMekkawy, T. 2014. Multi-objective optimal design of hybrid renewable energy systems using PSO-simulation based approach. Renewable Energy, 68: 67-79.

[92] Zarza, A. 2015. Dimensionado y análisis de modos de operación de una planta de producción de hidrógeno basado en energía eólica. Tesis de Pregrado. Universidad de Sevilla.

[93] Saur, G., Kurtz, J., Ainscough, C., Sprik, S., and Post, M. 2016. Stationary Fuel Cell Evaluation. Tech. rep. National Renewable Energy Laboratory (NREL).

[94] Badouard, T., and Moreira de Oliveira, D., Yearwood, J., and Torres, P., and Altmann, M. 2020. Final Report Cost of Energy (LCOE). Tech. rep. European Commission.

[95] CNE. 2020. Fijación de precios de nudo de corto. Tech. rep. Comisión Nacional de Energía.

[96] Comisión Nacional de Energía de Chile (CNE). 2021. Precio Medio de Mercado Sistema Eléctrico Nacional (PMM SEN). Tech. rep. Ministerio de Energia de Chile.

[97] IRENA. 2020.Renewable Power Generation Costs in 2019. Tech. rep. International Renewable Energy Agency.

[98] Cole, W., and Frazier, A. 2019. NREL Technical Report: Cost Projections for Utility-Scale Battery Storage. Tech. rep. National Renewable Energy Laboratory (NREL).

[99] U.S. Energy Information Administration. 2021. Cost and Performance Characteristics of New Generating Technologies, Annual Energy Outlook 2021. Tech. rep. US Energy Information Administration.

[100] Ahlen, J., Binet, T., Muhoro, P., and Seibert, B. 2019. Business & Technology Report: Battery Energy Storage Overview. Tech. rep. National Rural Electric Cooperative Association (NERECA).

[101] Yates, J., Daiyan, R., Patterson, R., Egan, R., and Amal, R., Ho-Baille, A., Chang, N. 2020. Techno-economic Analysis of Hydrogen Electrolysis from Off-Grid Stand-Alone Photovoltaics Incorporating Uncertainty Analysis. Cell Reports Physical Science, 1(10).

[102] Rezk, H., Alghassab, M., and Ziedan, H. 2020. An optimal sizing of stand-alone hybrid PV-fuel cell-battery to desalinate seawater at Saudi NEOM city. Processes, 8(4).

[103] Parks, G., Boyd, R., Cornish, J., and Remick, R. 2014. Hydrogen Station Compression, Storage, and Dispensing Technical Status and Costs: Systems Integration. Tech. rep.

National Renewable Energy Laboratory (NREL).

[104] Dursun, B., and Aykut, E. 2019. An investigation on wind/PV/fuel cell/battery hybrid renewable energy system for nursing home in Istanbul. Proceedings of the Institution of Mechanical Engineers, Part A: Journal of Power and Energy, 233(5): 616-625.

[105] Kharel, S., and Shabani, B. 2018. Hydrogen as a long-term large-scale energy storage solution to support renewables. Energies, 11(2825).

[106] Comisión Nacional de Energía de Chile (CNE). 2021. Factores de Emisión. [Online]. Available in: http://energiaabierta.cl/visualizaciones/factor-de-emision-sic-sing/ (Last accessed: 04/30/21)

[107] Departament of Industrial, Energy & Industrial Strategy. 2020. UK Government GHG Conversion Factors for Company Reporting. Tech. rep. United Kingdom Goverment.

[108] Bezanson, J., Edelman, A., Karpinski, S., and Shah, V. 2017. Julia: A fresh approach to numerical computing. SIAM Review, 59(1): 65-98.

[109] Dunning, I., Huchette, J., and Lubin, M. 2017. JuMP: A modeling language for mathematical optimization. SIAM Review, 59(2): 295-320.

[110] Gurobi Optimization, LLC. 2021. Gurobi Optimizer Reference Manual.

[111] Landa, R and Coello, C. 2006. Solving hard multiobjective optimization problems using ϵ-constraint with cultured differential evolution. Lecture Notes in Computer Science (including subseries Lecture Notes in Artificial Intelligence and Lecture Notes in Bioinformatics, pages 543-552.

[112] Grodzevich, O., and Romanko, O. 2006. Normalization and Other Topics in Multi-Objective Optimization. In: Proceedings of the fields-MITACS Industrial Problems Workshop.

[113] Chircop, K., and Zammit-Mangion, D. 2013. On Epsilon-Constraint Based Methods for the Generation of Pareto Frontiers. Journal of Mechanics Engineering and Automation, 3(5): 279-289.

[114] European Environment Agency. 2021. Greenhouse gas emission intensity of electricity generation in Europe. [Online]. Available in: https://www.eea.europa.eu/data-and-maps/indicators/overview-of-the-electricity-production-3/assessment-1 (Last accessed: 08/31/21)

[115] European Statistical System. 2021. What is the source of the electricity we consume?. [Online]. Available in: https://ec.europa.eu/eurostat/cache/infographs/energy/bloc-3b.html (Last accessed: 08/31/21)

[116] Cordinador Eléctrico Nacional. 2018. Sistemas Eléctricos de Chile 2017. [Online]. Available in: https://sic.coordinador.cl/wp-content/uploads/2017/03/Mapa-Coordinador-Electrico.pdf (Last accessed: 12/20/21)

[117] Universidad de Chile-Ministerio de Energia de Chile. 2017. Explorador Solar. [Online]. Available in: http://solar.minenergia.cl/inicio (Last accessed: 03/02/21)

[118] Molina, A., Falvey, M., and Rondanelli, R. 2017. A solar radiation database for Chile. Scientific Reports, 7.

[119] Shukla, K., Rangnekar, S., and Sudhakar, K. 2015. Comparative study of isotropic and anisotropic sky models to estimate solar radiation incident on tilted surface: A case study for Bhopal, India. Energy Reports, 1: 96-103.

[120] Liu, B., and Jordan, R. 1960. The interrelationship and characteristic distribution of direct, diffuse and total solar radiation. Solar Energy, 4(3).

[121] Mustafa, M., Calay, R., and Román, E. 2016. Biogas from Organic Waste - A Case Study. Procedia Engineering, 146: 310-317.

[122] Seruga, P., Krzywonos, M., Seruga, A., Niedzwiecki, L., Pawlak-Kruczek, H., and Urbanowska, A. 2020. Anaerobic Digestion Performance: Separate Collected vs. Mechanical Segregated Organic Fractions of Municipal Solid Waste as Feedstock. Energies, 13(15).

[123] van Oers, L., and Guinée, J. 2016. The abiotic depletion potential: Background, updates, and future. Resources, 5.

[124] IRENA. 2017. Electricity storage and renewables: Costs and markets to 2030. Tech. rep. International Renewable Energy Agency.

[125] da Rosa, A., and da Rosa, A. 2009. Hydrogen Storage (Chap. 11). In: Fundamentals of Renewable Energy Processes. Second Ed. Academic Press. pages 467-518.

[126] Generadoras de Chile. 2021. Centrales Energía Solar. [Online]. Available in: http://generadoras.cl/tipos-energia/energia-solar (Last accessed: 09/01/21)

[127] Servicio de Evaluación Ambiental. 2020. Ficha del Proyecto: Proyecto Solar Antofagasta. [Online]. Available in: https://seia.sea.gob.cl/expediente/ficha/fichaPrincipal.php?modo=normal{&}id{_}expediente=2145189301

[128] García, N. 2018. Implementación del Impuesto Verde en Chile. Tech. rep. Biblioteca del Congreso Nacional de Chile.

[129] Statista. 2021. Carbon taxes worldwide as of April 2021, by select country. [Online]. Available in: https://www.statista.com/statistics/483590/prices-of-implemented-carbon-pricing-instruments-worldwide-by-select-country/ (Last accessed: 10/01/21)

[130] Mavrotas, George. 2009. Effective implementation of the ϵ-constraint method in Multi-Objective Mathematical Programming problems. Applied Mathematics and Computation, 213:455-465.

[131] Jeswiet, J., and Szekeres, A. 2016. Energy Consumption in Mining Comminution. Procedia CIRP, 48: 140-145.

[132] Napier-munn, T. 2012. Comminution Energy and How to Reduce it. In: 2012 CEEC JkTech Workshop.

[133] The MathWorks Inc. 2021. Moving mean-Matlab. [Online]. Available in: https://www.mathworks.com/help/matlab/ref/movmean.html (Last accessed: 04/10/21)

[134] The MathWorks Inc. 2021. Isoutlier-Matlab. [Online]. Available in: https://www.mathworks.com/help/matlab/ref/isoutlier.html?searchHighlight=isoutlier{&}s{_}tid=srchtitle

[135] The MathWorks Inc. 2021. Filloutliers- Matlab. [Online]. Available in: https://www.mathworks.com/help/matlab/ref/filloutliers.html{#}bvlnf4n-1-fillmethod (Last accessed: 04/10/21)

[136] Khatib, T., and Elmenreich, W. 2016. Modelling of the solar source (Chap 1). In: Modeling of Photovoltaic Systems Using MATLAB ®. First Ed. Wiley. pages 1-37.

[137] Cooper, P. 1969. The Absorption of Radiation in Solar Stills. Solar Energy, 12(3): 333-346.

[138] Comisión Nacional de Energía de Chile (CNE) and GmbH, Deutsche Gesellschaft für Technische Zusammenarbeit (GTZ). 2007. Potencial de Biogás. IdentificaciÓn y Clasificación de los Distintos Tipos de Biomasa Disponible en Chile para la Generación de Biogás. Tech. rep. CNE/GTZ, Santiago.

[139] Office of Agricultural Studies and Policies (ODEPA). 2019. Panorama de la agricultura Chilena (Chilean agriculture overview). Tech. rep. Ministry of Agriculture of Chile.

[140] Stafford, W. 2020. WtE Best Practices and Perspectives in Africa (Chap 6). In: Municipal Solid Waste Energy Conversion in Developing Countries: Technologies, Best Practices, Challenges and Policy. First Ed. Elsevier. pages 185-217.

[141] Bünemann, A., and Brinkmann, J., and Löhle, S., Bartnik, S. 2020. Developing a legal framework for EPR in Chile. Tech. rep. Deutsche Gesellschaft für Internationale Zusammenarbeit (GIZ) GmbH, Bonn.

[142] Subsecretaria de Desarrollo Regional y Administrativo. 2019. Actualización de la situación por comuna y por región en materia de RSD y asimilables. Tech. rep. Ministerio del Interior y Seguridad Pública de Chile.

[143] Ministerio de Salud de Chile. 2019. Autoridades anunciaron cierre del vertedero La Chimba en Antofagasta. [Online]. Available in: https://www.minsal.cl/autoridades-anunciaron-cierre-del-vertedero-la-chimba-en-antofagasta/ (Last accessed: 03/05/21)

[144] National Institute of Statistics (INE). 2019. Regional Estimates and Projections of Chile's Population 2002-2035. Tech. rep. National Institute of Statistics (INE).

[145] Roddy, D. 2012. Volume 5: Biomass and biofuels - Introduction (Chap 5). In: Comprehensive Renewable Energy. First Ed. Elsevier. pages 1-9.

[146] Sangeetha, T., Rajneesh, C., and Yan, W. 2020. Integration of microbial electrolysis cells with anaerobic digestion to treat beer industry wastewater (Chap 15). In: Integrated Microbial Fuel Cells for Wastewater Treatment. First Ed. Butterworth-Heinemann. pages 313-346.

[147] Barragán-Escandón, A., Ruiz, J., Tigre, J., and Zalamea-León, E. 2020. Assessment of power generation using biogas from landfills in an equatorial tropical context. Sustainability, 12(7).

[148] Nyarko, F., Takyi, G., and Amalu, E. 2020. Robust crystalline silicon photovoltaic module (c-Si PVM) for the tropical climate: Future facing the technology. Scientific African, 8.

[149] Soley, S., and Dwivedi, A. 2019. Advances in high efficiency crystalline silicon homo junction solar cell technology. AIP Conference Proceedings, 2104.

[150] Lorenzo, José Alfonso Alonso. 2015. Rendimiento de Placas Solares. Available in: https://www.sfe-solar.com/paneles-solares/rendimiento/ (Last accessed: 03/05/2021)

[151] Eneria. 2018. Biogas generator sets from 100 kWe to 3,770 KWe- Product Data Sheet. Tech. rep. Eneria.

[152] Lilienthal, P and Lambert, T and Gilman, P. 2020. Homer Pro User Manual 3.14. Tech. rep. HOMER Energy LLC.

[153] IRENA. 2019. Utility-Scale Batteries Innovation Landscape Brief. Tech. rep. International Renewable Energy Agency.

[154] Pacific Gas and Electric Company (PG&E). 2018. PG&E Proposes Four New Cost-effective Energy Storage Projects to CPUC. [Online]. Available in: https://www.pge.com/en/about/newsroom/newsdetails/index.page?title=20180629_pge_proposes_four_new_cost-effective_energy_storage_projects_to_cpuc (Last accessed: 04/19/21)

[155] Yang, H., Lu, L., and Zhou, W. 2007. A novel optimization sizing model for hybrid solar-wind power generation system. Solar Energy, 81(1): 76-84.

[156] Tharani, K., and Dahiya, R. 2018. Choice of battery energy storage for a hybrid renewable energy system. Turkish Journal of Electrical Engineering and Computer Sciences, 26(2): 666-676.

[157] Bhandari, R., and Trudewind, C., and Zapp, P. 2014. Life cycle assessment of hydrogen production via electrolysis - A review. Journal of Cleaner Production, 85: 151-163.

[158] IRENA. 2020. Green Hydrogen Cost Reduction: Scaling up Electrolysers to Meet the 1.5ºC Climate Goal. Tech. rep. International Renewable Energy Agency.

[159] Brynolf, S., Taljegard, M., Grahn, M., and Hansson, J. 2018. Electrofuels for the transport sector: A review of production costs, 81: 1887-1905.

[160] Wulf, C., Linssen, J., and Zapp, P. 2018. Power-to-gas-concepts, demonstration, and prospects (Chap 9). In: Hydrogen Supply Chain: Design, Deployment and Operation. First Ed. Academic Press. pages 309-345.

[161] Tzimas, E., Filiou, C., Peteves, S., and Veyret, J. 2003. Hydrogen Storage : State-of-the-Art and Future Perspective. Tech. rep. European Commission.

[162] Salameh, Z. 2014. Energy storage (Chap 4). In: Renewable Energy System Design. First Ed. Academic Press. pages 201-298.

[163] Zhang, X. 2018. Current status of stationary fuel cells for coal power generation. Clean Energy, 2(2): 126-139.

[164] Mishra, S., Panigrahi, C., and Kothari, D. 2016. Design and simulation of a solar–wind–biogas hybrid system architecture using HOMER in India. International Journal of Ambient Energy, 37(2): 184-191.

Appendix A

Nomenclature

Indices

Symbol	Description	Unit
b	Batteries	-
bg	Biogas generator	-
fc	Fuel Cell	-
el	Electrolyzer	-
$tank$	Hydrogen tank	
pv	PV array	-

Parameters

Symbol	Description	Unit
A	Area of a solar panel	m^2
a_{bg}	Generator fuel curve intercept coefficient	$m^3/hr/MW$
b_{bg}	Generator fuel curve slope	$m^3/hr/MW$
C_{grid}	Cost energy from the grid	USD/MWh
C_{grid}^{con}	Cost grid power contacted	$USD/MW/month$
C_{grid}^{over}	Cost overconsumption	USD/MWh
C_j^{Cap}	Annual capital costs of technology j	USD
C_j^{Inv}	Investment costs of technology j	USD
CRF_j	Capital recovery factor of technology j	-
DoD_{max}	Maximum Depth of Discharge	%
E_{bg}	GHG emission factor of the biogas generator	kg $CO2$-eq
E_{grid}	GHG emission factor of the grid	kg $CO2$-eq
E_T^N	Nadir point environmental objective function	kg $CO2$-eq
E_T^U	Utopia point environmental objective function	kg $CO2$-eq
f_{bg}^{max}	Fuel available	m^3/hr
G^{NOCT}	Incident radiation NOCT	W/m^2
G_{ref}	Global irradiance at reference conditions	W/m^2
$G^{\theta}(t)$	Global irradiance incident on the tilted plane of slope θ at time t	W/m^2
H_2^{min}	Minimum level of hydrogen tank	%
H_2^{max}	Maximum level of hydrogen tank	%
HHV_{H_2}	Higher heat value of hydrogen	kWh/kg
i	Interest rate	%
L_i	Systems losses	%

Symbol	Description	Unit
LHV_{H_2}	Lower heat value of hydrogen	kWh/kg
M	Big M	-
m	Number of months in a year	-
n_j	Lifetime of technology j	%
P_b^{max}	Maximum battery capacity	MWh
P_{el}^{max}	Maximum electrolyzer capacity	MW
P_{fc}^{max}	Maximum fuel cell capacity	MW
PT	Losses caused by the operation of the system	%
SOC_{min}	Minimum State of Charge of the battery	%
SOC_{max}	Maximum State of Charge of the battery	%
$T_a(t)$	Ambient temperature at time t	℃
$T_c(t)$	Temperature of the PV cell at time t	℃
T_{ref}	Temperature of reference	℃
T_a^{NOCT}	Ambient temperature at NOCT	℃
T_c^{NOCT}	Cell temperature at NOCT	℃
t_i	Initial time of the simulation	hr
t_f	Final time of the simulation	hr
U_L	Overall heat loss coefficient	$(℃/W/m^2)^{-1}$
w	Relative weight importance between objective functions	-
α	Temperature coefficient of efficiency	K^{-1}
β	Absorbance coefficient of PV cells	-
ϵ_{ET}	Upper bound GHG emissions	kg CO_2-eq
η_{auto}	Battery hourly self-discharge rate	%
η_{charge}	Battery charge efficiency	%
η_{con}	Converter efficiency	%
$\eta_{discharge}$	Battery discharge efficiency	%
η_{el}	Electrolyzer efficiency	%
η_{fc}	Fuel cell efficiency	%
η_{in}	Inverter efficiency	%
η_{ref}	PV panel efficiency under standard test conditions	%
η_{tank}	Hydrogen tank efficiency	%
τ	Transmittance coefficient of PV cells	-

Variables

Symbol	Description	Unit
Continuous variables		
C_j^{Cap}	Annual capital costs of technology j	USD
$C_j^{O\&M}$	Annual operation and maintenance costs of technology j	USD
$C_{Capital}$	Annual capital costs of the system	USD
C_E	Annual costs of energy purchase from the grid	USD
$C_{O\&M}$	Annual operation and maintenance costs of the system	USD
C_T	Total annual costs	USD
E_T	GHG emissions of the hybrid energy system	kg CO_2-eq
$f_{bg}(t)$	Fuel consumption of biogas in a generator at time t	m^3/hr
$f_{h_2}(t)$	Fuel cell hydrogen consumption at time t	kg/hr
H_2nom	Hydrogen tank nominal capacity	kg
$L_{H_2}(t)$	Hydrogen tank level at time t	kg/hr

Symbol	Description	Unit
$P_b(t)$	Energy stored in the battery at time t	MWh
P_j^{nom}	Nominal capacity of the battery	MWh
$P_{bg}(t)$	Output power of the biogas generator at time t	MW
P_{bg}^{nom}	Nominal capacity of the biogas generator	MW
$P_{charge}(t)$	Energy charged in the battery at time t	MWh
$P_{discharge}(t)$	Energy discharged from the battery at time t	MWh
$P_{el}(t)$	Electrolyzer electrical consumption at time t	MWh
P_{el}^{nom}	Electrolyzer nominal power	MW
$P_{fc}(t)$	Output power of the fuel cell at time t	MW
P_{fc}^{nom}	Nominal capacity of the fuel cell	MW
$P_{grid}^{over}(t)$	Overconsumption Energy at time t	MWh
$P_{grid}(t)$	Energy supply by the grid at time t	MWh
$P_{pv}^{a}(t)$	Power available at by the PV system at time t	MW
$P_{pv}^{g}(t)$	Power generated by the PV system at any time t	MW
P_{pv}^{nom}	Nominal power of the PV system	MW
$q_{H_2}(t)$	Electrolyzer's hydrogen mass flow	kg/hr
$SOC(t)$	State of Charge of the battery at time t	%
Integer variables		
N_{PV}	Number of PV modules	-
P_{grid}^{con}	Grid power contracted	MW
Binary variables		
$y_g(t)$	Binary variable that defines if there is overconsumption or not	-
$z_b(t)$	Binary variable that defines if the battery is charging or not	-

Other symbols used in this worked

Symbol	Description	Unit
$\%organic$	Percentage of organic in municipal solid wastes	%
F_{MSW}	Municipal solid waste flow	$kg/day - person$
F_{OW}	Organic municipal waste flow	ton/day
$H_{solar}(t)$	Solar time at time t	-
$I_b(t)$	Direct solar radiation at time t	W/m^2
$I_b^{\theta}(t)$	Direct solar radiation on a tilted surface of slope θ at time t	W/m^2
$I_d(t)$	Diffuse solar radiation at time t	W/m^2
$I_d^{\theta}(t)$	Diffuse solar radiation on a tilted surface of slope θ at time t	W/m^2
$I_r(t)$	Reflected solar radiation at time t	W/m^2
$n(t)$	Number of days since the start of the year at time t	-
P_{2020}	Estimate Population attended by "La Chimba" landfill	$people$
$R_b(t)$	Ratio of the beam radiation on the tilted surface to beam radiation on the horizontal surface at time t	-
R_d	Ratio between diffuse solar energy on a horizontal surface and diffuse solar energy on a tilted surface	-
R_r	Factor of reflected solar energy on a tilted surface	-
γ	Azimuth angle	$^\circ$
$\delta(t)$	Solar declination angle at time t	$^\circ$
θ	Angle of the tilted plane	$^\circ$
ρ_g	Albedo	-
ϕ	Latitude	$^\circ$
$\omega(t)$	Hour angle at time t	$^\circ$

Appendix B

Mine Load Data Analysis

For estimating the mine load, data of a real mine located in the North of Chile were used. The data were obtained confidentially, so the mine name or its characteristics will not be mentioned. The data analysis done to the dataset is shown below.

The data obtained were the electrical demand of the comminution process from 2015 to 2019 hourly. This study considered that the mine load included the electrical demand of the whole mining process, so for its estimation, it was supposed that 50% of the mine energy consumption is associated with comminution, based on Jeswiet and Szekeres [131] and Napier-Munn [132]. The demand load curve estimated in the first instance is shown in Figure B.1. It can be noticed that the dataset had some outliers: in some hours, the demand was near 0 and in others almost four times the mean (Mean=123 MWh). This behavior was also present in the data from previous years and may be associated with the measurement equipment, maintenance, non scheduled plant shutdown, among other factors. In order to eliminate the outliers, data analysis was performed.

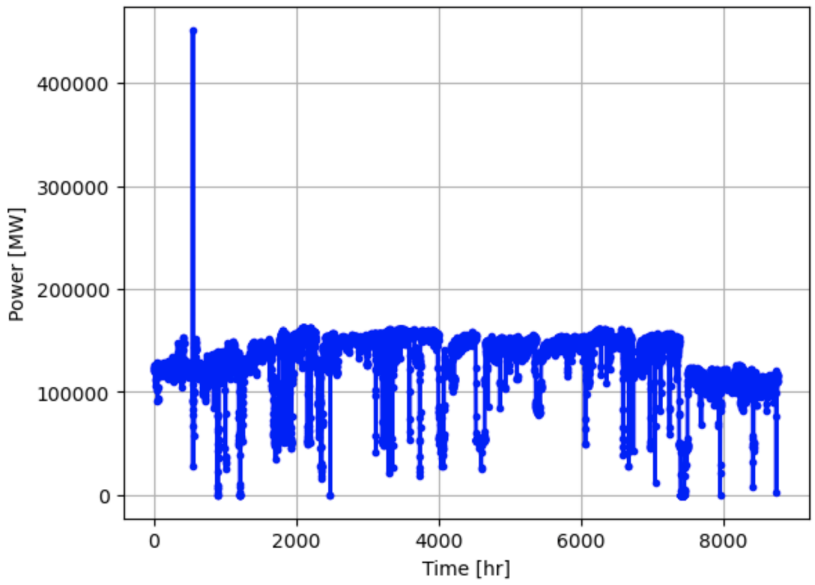

Figure B.1: Example of outliers in the mine load curve estimation. Source: Own elaboration.

In order to smooth the data, first, for each hour, the energy demand of the five years was averaged, and then two methods were studied: the moving average and the replacement of the outliers. Both methods were implemented in Matlab®.

1. Moving Average: The function used in Matlab® is called "movmean". This method returns an array of local mean values, where each mean is calculated over a sliding window of length k [133]. Figure B.2 shows the results obtained. It can be noticed that using this method smooth the data, but there still are some outliers.

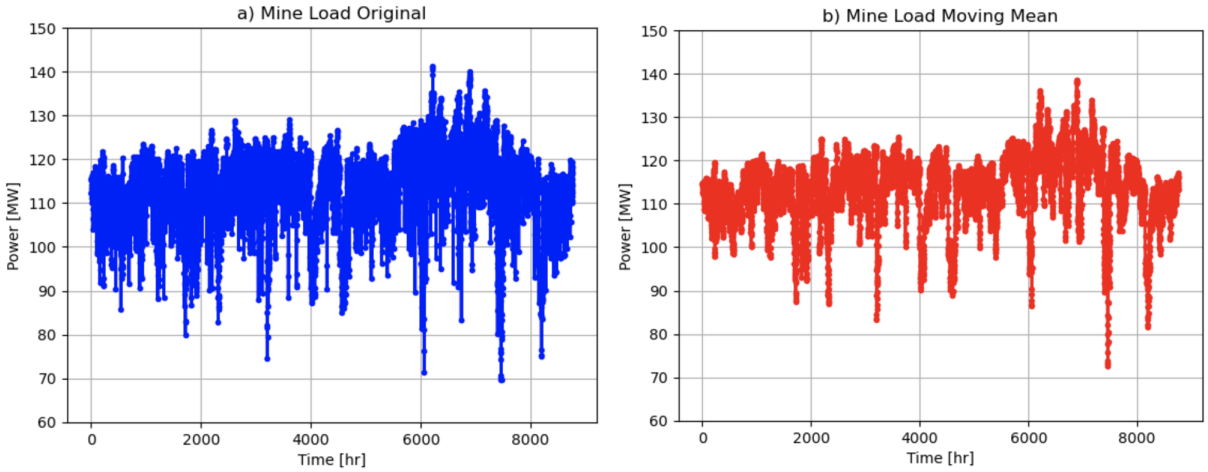

Figure B.2: Results obtained using Moving Average. Source: Own elaboration.

2. Replacement of outliers: The outliers were found with the function "isoutlier", which considers as an outlier a value that is more than three scaled median absolute deviations (MAD) away from the median [134]. Then, the outliers were replaced using the "filloutliers" function. The replacement methods studied were [135]:

   - Center: It fills the center value determined by the "findmethod".
   - Linear: It fills using linear interpolation of neighboring, non-outlier values.
   - Pchip: It fills using shape-preserving piecewise cubic spline interpolation.

   The three methods showed similar results, as seen in Figure B.3. Finally, the selected dataset was obtained with the linear method, as it was the simplest and more intuitive method.

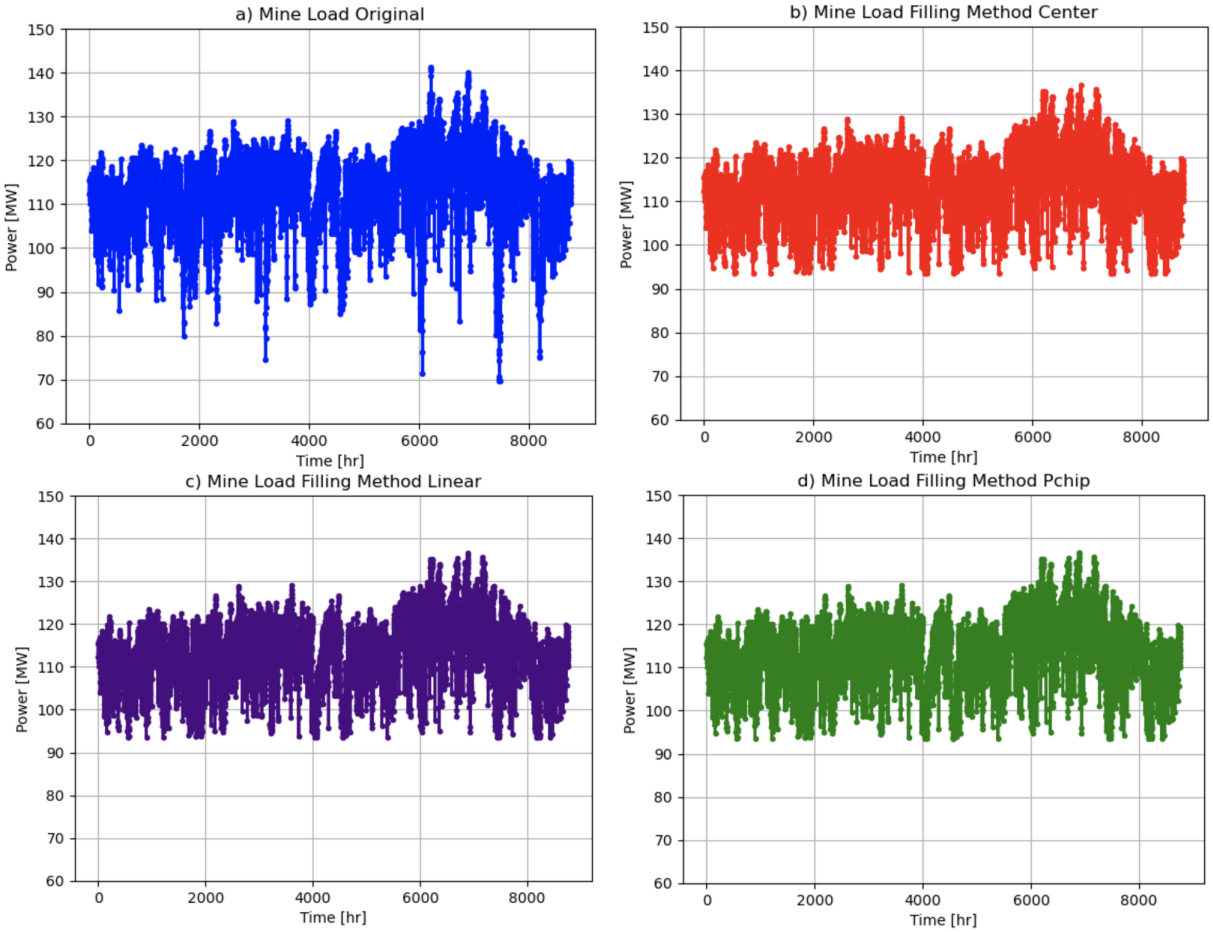

Figure B.3: Results obtained with the replacement of outlier methods. Source: Own elaboration.

Appendix C

Liu and Jordan Model

The solar explorer tool uses the Liu and Jordan equations to estimate the global irradiance incident on the tilted plane. Below the model is explained in detail.

Model Description

In the Liu and Jordan model [119; 120], the solar radiation on a tilted surface of slope θ from the horizontal at any time t, $G^{\theta}(t)$, is considered to be composed of three tree factors: the beam or direct solar radiation ($I_b^{\theta}(t)$), the diffuse solar radiation ($I_d^{\theta}(t)$) and the reflected solar radiation ($I_r(t)$). The components can be expressed by [136]:

$$G^{\theta}(t) = I_b^{\theta}(t) + I_d^{\theta}(t) + I_r(t) \; \forall t \in T \tag{C.1}$$

Equation C.1 can be rewritten in terms of solar energy components on a horizontal surface as follows [119; 120]:

$$G^{\theta}(t) = I_b(t) \cdot R_b(t) + I_d(t) \cdot R_d + I_i(t) \cdot \rho_g \cdot R_r \; \forall t \in T \tag{C.2}$$

Where $I_b(t)$ is the beam solar radiation at time t, $R_b(t)$ is the ratio of the beam radiation on the tilted surface to beam radiation on the horizontal surface at time t, $I_d(t)$ is the diffuse solar radiation at time t, R_d is the ratio between diffuse solar energy on a horizontal surface and diffuse solar energy on a tilted surface, $I_i(t)$ is the global horizontal solar radiation at time t, ρ_g is the albedo, and R_r is the factor of reflected solar energy on a tilted surface.

In the southern hemisphere, where Chile is located, the azimuth angle is 180° ($\gamma = 180°$), so the equation for the ratio of the beam radiation on the tilted surface to beam radiation on the horizontal surface, $R_b(t)$, is [119; 120; 136]:

$$R_b(t) = \frac{cos\ (\phi - \theta) \cdot cos\ \delta(t) \cdot cos\ \omega(t) + sin\ (\phi - \theta) \cdot sin\ \delta(t)}{cos\ \phi \cdot cos\ \delta(t) \cdot cos\ \omega(t) + sin\ \phi \cdot sin\ \delta(t)} \; \forall t \in T \tag{C.3}$$

Where ϕ is latitude, $\delta(t)$ is the solar declination angle at time t, and $\omega(t)$ is the hour angle at time t.

The solar declination angle is calculated from the equation of Cooper [137],

$$\delta(t) = 23.45 \cdot sin\ [360 \cdot (\frac{284 + n(t)}{365})]\ \forall t \in T \tag{C.4}$$

Where n is the number of days since the start of the year at time t.

The hour angle of the sun, measured from the solar noon, is [137]:

$$\omega(t) = (H_{solar}(t) - 12) \cdot 15^{\circ}\ \forall t \in T \tag{C.5}$$

Where $H_{solar}(t)$ is the solar time at time t.

Finally, the equations to calculated R_d and R_r, are the following [119; 120]:

$$R_d = \frac{1 + cos\ \theta}{2} \tag{C.6}$$

$$R_r = \frac{1 - cos\ \theta}{2} \tag{C.7}$$

Appendix D

Biogas Estimation

According to the study done by the National Commission of Energy (CNE) and *Deutsche Gesellschaft für Technische Zusammenarbeit* (GTZ) in 2007 [138], the most significant theoretical wastes potential for biogas projects in Chile is concentrated in poultry, pig, and cattle manure, seasonal crops, Municipal Solid Waste (MSW) and sludges from Water Treatment Plants (WWTPs). Considering that the case of study is located in the Antofagasta Region, where mainly due to climate conditions, agriculture, livestock, and forestry activities are not significantly developed, only MSW and sludge's from WWTPs have the potential to be used for biogas production [139]. In particular, in this thesis, biogas production from municipal organic wastes is studied, considering the problems associated with their effective disposal and that landfill sites are becoming scarce [121]. The estimation of the biomass and biogas potential is shown as follows.

Biomass Estimation

The Municipal Solid Wastes (MSW) are the wastes collected by the municipalities or disposed of at the municipal waste disposal site and include residential, industrial, commercial, municipal, and construction and demolition wastes [140]. In Chile, about 8 million tonnes of municipal solid waste are generated every year, and most of them are disposed of in landfills [141].

For the estimation of the MSW available, the information about disposal sites and facilities for the management of household and similar solid waste reported by the National Solid Waste Program of Chile in 2019 was used [142]. According to their report, in the Antofagasta Region, the primary landfill *La Chimba* collected the wastes of 446,315 people and received 176,528 tonnes of MSW per year, which means that a person generates approximately 1.1 kg of MSW per day as calculated in Equation D.1.

$$F_{MSW} = \frac{176.528 \ \frac{ton \ MSW}{year}}{446,315 \ people} \cdot \frac{1 \ year}{365 \ days} \cdot \frac{1,000 \ kg}{1 \ ton} = 1,1 \ \frac{kg \ MSW}{day - person} \tag{D.1}$$

The landfill *La Chimba* closed in December 2019, and landfill *Chaqueta Blanca* started its operation [143]. For this study, it would be considered that the population attended by the

landfill *Chaqueta Blanca* and the MSW received will be the same as the *La Chimba* landfill in the scenario analyzed.

To obtain the organic waste flow, first, the population in 2020 was estimated based on the report "Regional Estimates and Projections of Chile's Population 2002-2035" done by the National Institute of Statistics (INE) [144]. Then, considering that in Chile, about half of the municipal solids waste is organic and can be used to produce biogas, the organic municipal waste flow, F_{OW}, was calculated using Equation D.2 [30]. The results are shown in Table D.1.

$$F_{OW} = P_{2020} \cdot F_{MSW} \cdot \%organic \tag{D.2}$$

Table D.1: Results of organic waste estimation based on the population growth.

Parameters	**Value**	**Units**	**Reference**
% of organics in MSW	50	%	[30]
% Growth in comparison to 2019	3.48	%	[144]
Estimate Population attended by *La Chimba* landfill (P_{2020})	461,847	people	-
Organic municipal waste flow (F_{OW})	254	ton/day	-

Biogas Potential

In this study, it is supposed that biogas is produced by anaerobic digestion (AD). AD is a natural process through which bacteria break down organic matter in the absence of oxygen and produce biogas and digestate[1] [145]. The biogas produced consists of 50-75% of methane (CH_4), 25-50% of carbon dioxide (CO_2), and other components in smaller proportions like H_2S, H_2, N_2, and O_2 [146; 147]. The biogas potential for electricity production depends mainly on its methane content.

For the calculation of the biogas and methane generated, different factors were found in the literature. The value used is based on the work of Seruga Et.al. [122]. In their work, the authors estimated the biogas yield of municipal wastes with different compositions. In particular, one case analyzed had a similar organic wastes fraction with the Chilean case and is considered a probable scenario. The biogas yield estimated was 105 m^3 biogas/ton organic waste, with a methane proportion of 52%.

Finally, considering the biomass estimate and the biogas yield obtained in Seruga Et.al. [122], the biogas estimated is 26,670 m^3/day.

$$\text{Biogas estimated} = 254\ \frac{ton}{day} \cdot 105\ \frac{m^3}{ton} = 26,670\ \frac{m^3}{day} \tag{D.3}$$

[1] The material remaining after anaerobic digestion is called digestate. It can be used as fertilizer [145].

Appendix E

System component inputs

For the simulation of the HRES, different technical parameters were necessary to model the technologies selected accurately. The applied technical parameters are provided below, including the assumptions considered and their justification.

PV System

Table E.1 shows the technical parameters considered for the Solar PV System. It was assumed that the panels were of crystalline silicone (c-Si), as they are currently the most common solar cells in use [148; 149]. The area and efficiency of a solar panel were obtained from manufacturers. Meanwhile, reference and NOCT conditions were obtained from the literature. The total operational losses were calculated considering the system losses shown in Table E.2 [86]. The rest of the inputs, such as the panel's temperature, ambient temperature, and the global irradiance incident on the tilted plane, were obtained from the data provided by the Solar Explorer (explained in Chapter 3, Section 3.6.2).

Table E.1: Solar PV System Technical Parameters.

Parameter	**Value**	**Units**	**Reference**
PV Module Type	c-Si	-	[148; 149]
Area of a solar panel (A)	2	#	[150]
Efficiency of a PV panel under standard conditions (η_{ref})	18.5	%	[150]
Total operational losses (PT)	14	%	[86]
Temperature coefficient (α)	-0.0045	$℃^{-1}$	[85]
Temperature of reference (T_{ref})	25	℃	[84]
Global irradiance at reference conditions (G_{ref})	1000	W/m^2	[84]
Cell Temperature at NOCT (T_c^{NOCT})	48	℃	[62]
Ambient Temperature at NOCT (T_a^{NOCT})	20	℃	[60]
Incident Radiation at NOCT (G^{NOCT})	800	W/m^2	[60]

Table E.2: Systems losses consider in the model. Data were obtained from [86].

Loss Mechanism	**Default value**
Soiling	2%
Shading	3%
Snow	0%
Mismatch	2%
Connections	0.5%
Light-induced degradation	1.5%
Nameplate rating	1%
Age	0%
Availability	3%
Total losses	**14%**

Biogas Generator

Table E.3 shows the technical parameters considered for the biogas generator. The estimation of the biogas availability is detailed in Appendix D; meantime, the calculation of the fuel curve coefficients is shown below.

Table E.3: Biogas Generator Technical Parameters.

Parameter	**Value**	**Units**	**Reference**
Generator fuel curve intercept coefficient (a_{bg})	1.36	$m^3/hr/MW$	[151]
Generator fuel curve slope (b_{bg})	389	$m^3/hr/MW$	[151]
Fuel available (f_{bg}^{max})	1.111	m^3/hr	See estimation in Appendix D

The fuel curve used was obtained doing a linear curve fitting to data about generators fueled by biogas recovered from manufacturers. Other fuel curves for biogas were found in the literature. However, they were discarded because the generator's rated capacity was lower than the biogas potential (less than 400 W). In Figure E.1, the fuel curve is presented.

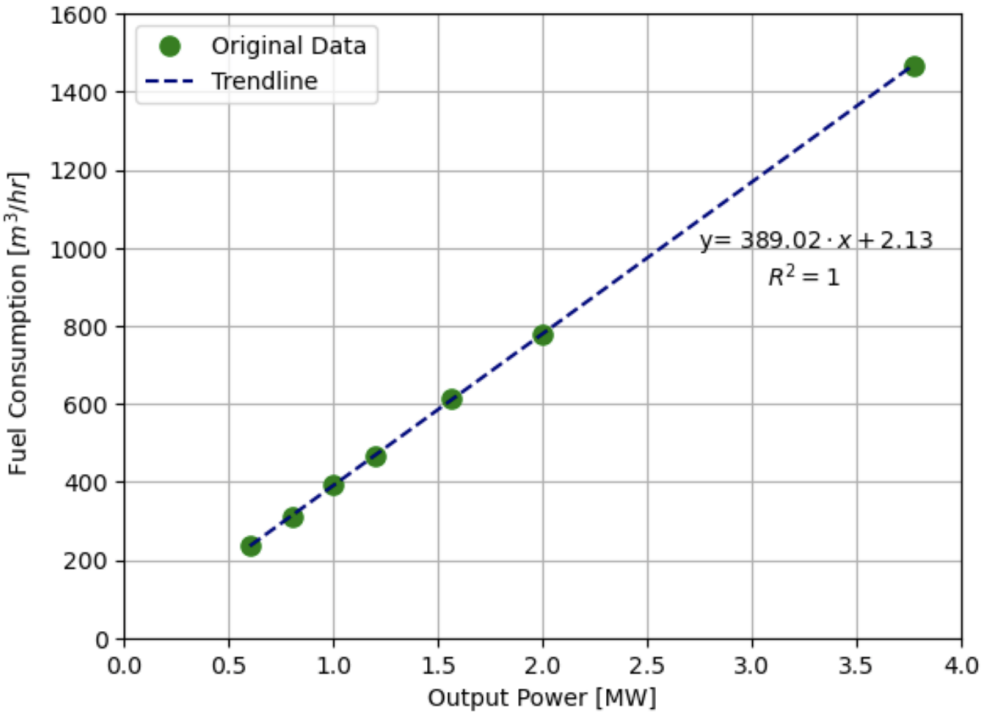

Figure E.1: Biogas Generator Fuel Curve. Own elaboration based on data from [151].

The equation obtained by the fitting was the following:

$$Fuel\ Comsuption\ [m^3/hr] = 389.0 \cdot Output\ Power\ [MW] + 2.1 \tag{E.1}$$

Where 389.0 corresponds to the slope of the curve and 2.1 to the intersection with the y-axis.

The two coefficients needed for the simulation are a_{bg} and b_{bg}. The parameter a_{bg} is the generator fuel curve intercept coefficient and corresponds to the no-load fuel consumption of the generator divided by its rated capacity [152]. For this model, the rated capacity of the generator is 1560 W [151], so the value of this parameter is:

$$a_{bg} = \frac{y - axis\ intercept}{P_{nom}} = \frac{2.13\ m^3/hr}{1.56\ MW} = 1.36\ [m^3/hr/MW] \tag{E.2}$$

The second coefficient corresponds to the generator fuel curve slope, b_{bg}, which is the marginal fuel consumption of the generator and can be directed obtained from Equation E.1 ($b_{bg} = 389.02\ [m^3/hr/MW]$)]) [152].

Battery System

Table E.4 shows the technical parameters considered for the battery storage system. In this study, it was assumed that the type of batteries used are Lithium-ion batteries since they represented over 90% of the total installed capacity for large-scale battery storage [153]. The parameters used were obtained from previous studies and are typical values for Lithium-ion batteries. In particular, for the maximum nominal capacity, the characteristics of the largest Lithium-ion battery installed in the world were considered. It corresponds to Vistra Moss Landing Energy Storage Facility, which has a capacity installed of 1,200 MWh and is located in Monterey County, California [154].

Table E.4: Battery Bank Technical Parameters.

Parameter	Value	Units	Reference
Type of Battery	Lithium-ion	-	[153]
Maximum nominal capacity (P_b^{max})	1,200	MWh	[154]
Charge efficiency (η_{charge})	95	%	[18]
Discharge efficiency ($\eta_{discharge}$)	95	%	[18]
Hourly auto-self rate (η_{auto})	0.02	%	[155]
Depth of Discharge (DoD)	90	%	[156]
Minimum state of charge (SOC_{min})	10	%	[156]
Maximum State of Charge (SOC_{max})	90	%	[18]

Electrolyser

Table E.5 shows the technical parameters considered for the electrolyzer. For this study, it was assumed that the type of electrolyzer used is alkaline since it is a mature technology, and they are the most widely deployed at present [92; 157]. The maximum nominal capacity was defined considering that for the land, there are no real projects of more than 100 MW in water electrolysis [158]. The other parameters are typical values for alkaline electrolyzers.

Table E.5: Electrolyser Technical Parameters.

Parameter	Value	Units	Reference
Type of Electrolyzer	Alkaline	-	[157]
Maximum nominal capacity (P_{el}^{max})	100	MW	[158]
Minimum Efficiency (η_{el}^{min})	43	%	[159]
Maximum Efficiency (η_{el}^{max})	69	%	[159]
Minimum load ratio (r_{min})	30	%	[160]
Hydrogen Higher Heat Value (HHV_{H_2})	39.4	kWh/kg	[87]

Hydrogen Tank

Table E.6 shows the technical parameters considered for the hydrogen tank. In this work, it was assumed that hydrogen is stored in gaseous form since it is one of the simplest, most common, and efficient storage technologies in use [161], and that the electrolyzer is directly connected to the hydrogen tank [81]. The rest of the parameters used were obtained from previous studies.

Table E.6: Hydrogen Tank Technical Parameters.

Parameter	Value	Units	Reference
Type of Storage	Compressed gas	-	[161]
Efficiency of the tank (η_{tank})	95	%	[91]
Minimum hydrogen level as a percentage of the nominal capacity (${H_2}^{min}$)	5	%	[91]
Maximum hydrogen level as a percentage of the nominal capacity (${H_2}^{min}$)	100	%	[91]

Fuel Cell

Table E.7 shows the technical parameters considered for the fuel cell. In this study, it was assumed that the type of fuel cell used is proton exchange membrane (PEM) because it has reliable performance and is commercially available at large industrial scale applications [81]. Although, other types of fuel cells with higher efficiencies could be used in the future [162]. The parameters used were obtained from previous studies and are typical values for PEM fuel cells. Specifically, for the maximum nominal capacity, the world's largest fuel cell installed characteristics were considered. It corresponds to the 59-MW Gyeonggi Green Energy park, located in Hwasung City, South Korea [163].

Table E.7: Fuel Cell Technical Parameters.

Parameter	Value	Units	Reference
Type of Fuel Cell	PEM	-	[81]
Maximum nominal capacity (P_{fc}^{max})	59	MW	[163]
Minimum Efficiency (η_{fc}^{min})	40	%	[162]
Maximum Efficiency (η_{fc}^{max})	50	%	[162]
Hydrogen Lower Heat Value (LHV_{H_2})	33.3	kWh/kg	[87]

Converters

The converters were modeled as a function of their efficiency. For this thesis, it was considered that all converter's efficiency remain constant for all time. The value used for all converters DC/DC is 96%, as most converters found in the industry [26]. On the other hand, the efficiency of the inverters is considered 90% [164].

Appendix F

Code

```
#Author: Javiera Andrea Vergara Zambrano, University of Chile
#The implemented code developed within the scope of the master thesis, "Evaluation of a solar-biogas hybrid energy system for a mining process in Chile considering technical, economic and environmental aspects". It provides the optimum design of a hybrid energy system considering three cases:

#1) Minimization of the annualcosts
#2) Minimization of the total emissions of the system
#3) Minimization of both objective functions (using the e-constraint method)

#Notes:
# This code was design with Julia 1.5.3 and JuMP 0.21.8.
# To run this code is necessary to have a valid license of Gurobi or a MLP solver.
# The CSV with the data used can be found in: https://drive.google.com/file/d/1DaN0XbpEEhnUW0jvF3eMTUlhONtecR7R/view?usp=sharing
```

USER'S INTERACTION

```
#Select k=1 for min costs, k=2 for min emissions and k3 for min costs & emissions
k=1

#Insert the relative importance weight between the objective functions (between 0 and 1)
w=0.1;

#Insert data file location
loc= "/Users/Javi/Desktop/Data/Data.csv";
```

DATA

```
# Parameters
days= 365; #days
months= 12; #months
hours= 24; #hours
time_model= days*hours; #hours
time_simulation= 1:time_model; #simulation time

#Mine Data
p_load= data[1:time_model,2] #mine load (MWh);
```

```
#PV array
g_beta= data[1:time_model,3];  #solar irradiance at tilted plane (W/m^2)
t_amb= data[1:time_model,4]; #ambient temperature (K)
g_ref= 1000; #reference  solar irradiance (W/m^2)
alpha= -0.0045; #temperature coefficient (1/K)
t_ref= 25+273.15; #temperature of reference (K)
eta_ref= 0.185; #efficiency of PV panels (-)
t_c_NOCT= 48+273.15; #cell temperature at NOCT (K)
t_a_NOCT= 20+273.15; #ambient temperature at NOCT (K)
g_NOCT= 800; #incident radiation at NOCT (W/m^2)
f= (t_c_NOCT-t_a_NOCT)/g_NOCT; #overall heat loss coefficient (K/W/m^2)
A= 2 #area of a solar panel (m^2)
PT= 0.14 #power total losses (%)

t_pv=zeros(time_model) #temperature of PV panel (K)
for t in time_simulation
    t_pv[t]= t_amb[t]+ g_beta[t]*f
end

heat_loss=zeros(time_model) #heat loss (-)
for t in time_simulation
    g= (g_beta[t]/g_ref)*[1 + alpha * (t_pv[t]-t_ref)]
    heat_loss[t]= g[1]
end

#Biogas generator
a_bg= 1.36 #fuel curve coefficient intercept (m3/hr/MW)
b_bg= 389 #fuel curve coefficient slope (m3/hr/MW)
f_bg_max= 1111 #fuel available (m3/hr)

#BESS
eta_charge= 0.95 #efficiency of charging (%)
eta_discharge= 0.95 #efficiency of discharging (%)
eta_auto= 0.0002 #hourly auto-discharge (%)
DoD= 0.9 #Depth of discharge (%)
SOC_i=0.30 # initial SOC (%)
SOC_min= 1-DoD #minimum SOC (%)
SOC_max= 0.90 #maximum SOC (%)
p_bess_max= 1200 #max BESS capacity installed (MWh)

#Fuel cell
LHV= 33.3 #hydrogen lower heat value (kWh/kg H2)
eta_fc= 0.45 #efficiency of fuel cell (%)
p_fc_max= 59 #max nominal capacity (MW)

#Electrolyzer
eta_el= 0.56 #efficiency of electrolyzer (%)
HHV= 39.4 #hydrogen higher heat value (kWh/kg H2)
p_el_max= 100 #max nominal capacity (MW)

#H2 tank
h2_min= 0.05 #min h2 tank (%)
```

```
h2_max= 1 #min h2 tank (%)
eta_tank= 0.95 #tank efficiency (%)

#Converters
eta_con= 0.96 #converters efficiency (%)
eta_in= 0.90 #inverters efficiency (%)

#Big M
M= 10^4

#Cost of intallation (annual)
CAP_pv= 0.083 #MUSD/MW-installed
CAP_bess= 0.050 #MUSD/MWh-installed
CAP_ele= 0.067 #MUSD/MW-installed
CAP_tank= 0.086 #kUSD/kg H2
CAP_fc= 0.057 #MUSD/MW-installed
CAP_bg= 0.300 #MUSD/MW-installed

#Cost of operation and maintenance (annual)
OM_pv= 0.019 #MUSD/MW-installed
OM_bess= 0.007 #MUSD/MWh-installed
OM_ele= 0.017 #MUSD/MW-installed
OM_tank= 0.020 #kUSD/kg H2
OM_fc= 0.011 #MUSD/MW-installed
OM_bg= 0.070 #MUSD/MW-installed

#Grid Costs
C_grid= 0.060 #kUSD/MWh
C_con_grid= 7.414 #kUSD/MW
C_over_grid= 6 #kUSD/MW

#Emissions
E_grid= 0.3834 #grid emission factor (ton CO2-eq/MWh)
E_biogas= 0.00021 #biogas emission factor (ton CO2-eq/MWh);

#Ideal objective values
TC_ideal= 70.36464000767008 #MUSD
TE_ideal= 82830.21471154809 #ton CO2-eq

#Non-ideal objective values
TC_non= 161.1297894149766 #MUSD
TE_non= 276577.6566629845 #ton CO2-eq/MWh;
```

MODEL

```
using JuMP, Gurobi

m = direct_model(Gurobi.Optimizer()) #Solver
JuMP.set_optimizer_attribute(m, "OutputFlag", 1)
set_time_limit_sec(m, 5500.0)

```

```
#Decision Variables
#Solar PV
@variable(m, p_pv[time_simulation]>=0) #power generated by the PV array including losses at time t (MW)
@variable(m, p_pv_nom>=0) #nominal power of the PV array (MW)
@variable(m, n_pv>=0, Int) #number of PV panels (-)
#Biogas
@variable(m, p_bg[time_simulation]>=0) #power generated by the biogas generator (MW)
@variable(m, p_bg_nom>=0) #nominal power of the biogas generator (MW)
@variable(m, f_bg[time_simulation]>=0) #fuel consumption of the biogas generator (m^3/hr )
#Grid
@variable(m, p_grid[time_simulation]>=0) #power supply by the grid (MWh)
@variable(m, p_con_grid>=0, Int) #power contracted from the grid (MW)
@variable(m, p_over[time_simulation]>=0) #overconsumption energy from the grid (MWh)
@variable(m, y[time_simulation], Bin) #binary variable that is 1 if there is energy overconsumption (-)
#BESS
@variable(m, p_charge[time_simulation]>=0) #energy charge in the BESS (MWh)
@variable(m, p_bess[time_simulation]>=0) #energy storage in the BESS (MWh)
@variable(m, p_bess_nom >=0) #nominal power of the BESS (MWh)
@variable(m, p_discharge[time_simulation]>=0) #energy discharge from the BESS (MWh)
@variable(m, z_bess[time_simulation], Bin) #binary variable that is 1 if battery is discharging (-)
#H2 electrolyser
@variable(m, p_el[time_simulation]>=0) #power consumption of the electrolyzer (MW)
@variable(m, p_el_nom>=0) #nominal power of the electrolyzer
@variable(m, q_h2[time_simulation]>=0) #hydrogen mass flow produced by the electrolyzer (kg/hr)
#H2 fuel cell
@variable(m, fc_h2[time_simulation]>=0) #h2 fuel consumption of the fuel cell (kg/hr)
@variable(m, p_fc[time_simulation]>=0) #fuel cell output power (MW)
@variable(m, p_fc_nom>=0) #nominal fuel cell output power (MW)
#H2 tank
@variable(m, h2_tank[time_simulation]>=0) #h2 tank level (kg)
@variable(m, h2_tank_nom>=0) #h2 tank nominal capacity (kg)

#Constraints
#Power balance
for t in time_simulation
  @constraint(m, p_load[t]/eta_in- p_bg[t]/eta_in- p_grid[t]/eta_in-p_pv[t]*eta_con+ p_charge[t]-p_discharge[t]+p_el[t]/eta_con-p_fc[t]*eta_con==0) #power balance ( MWh)
end

#PV array
for t in time_simulation
    @constraint(m, p_pv[t]==p_pv_nom *heat_loss[t]*(1-PT)) #power generated  by the PV array
    @constraint(m, p_pv_nom== n_pv * A * eta_ref*10^-3) #nominal power of the PV array
end
```

```
#Generator
for t in time_simulation
    @constraint(m, f_bg[t]== a_bg*p_bg_nom + b_bg*p_bg[t]) #hourly fuel consumption
    @constraint(m, f_bg[t]<=f_bg_max) #the fuel consumed is limited by the fuel available
    @constraint(m, p_bg[t]<=p_bg_nom) #nominal power of the biogas generator
end

#BESS
@constraint(m, p_bess_nom <= p_bess_max) #max capacity of the BESS installed
@constraint(m,  p_bess[1] == p_bess[time_model]) #initial/final condition
@constraint(m, p_bess[1] == SOC_i*p_bess_nom) #initial condition bess
@constraint(m, p_discharge[1]<=p_bess_nom*SOC_i)
for t in time_simulation
        @constraint(m, SOC_min* p_bess_nom<=p_bess[t]) #max state of charge
        @constraint(m, p_bess[t]<=SOC_max*p_bess_nom) #min state of charge
        @constraint(m, p_discharge[t]<=M*z_bess[t]) #if the battery is charging, the batteries
    ↪  doesn't discharge
        @constraint(m, p_charge[t]<=M*(1-z_bess[t])) #if the battery is discharging, the
    ↪ batteries doesn't charge
    if t<time_model
        @constraint(m, p_bess[t+1]==p_bess[t]*(1-eta_auto)+p_charge[t+1]*eta_charge
                            -p_discharge[t+1]/eta_discharge) #BESS power balance (MWh)
    end
end

#H2
@constraint(m,h2_tank[1]==h2_tank[time_model]) #initial/final condition
@constraint(m, p_el_nom <= p_el_max )#max capacity of the electrolyzer installed
@constraint(m, p_fc_nom<=p_fc_max) #max capacity of the fuel cell installed
for t in time_simulation
    #Electrolyzer
    @constraint(m, p_el[t]<=p_el_nom) #nominal power electrolyzer
    @constraint(m, eta_el*p_el[t]>=q_h2[t]*HHV/1000) #efficiency electrolyzer
    #Fuel Cell
    @constraint(m, p_fc[t]<=p_fc_nom) #nominal power fuel cell
    @constraint(m, eta_fc*fc_h2[t]>=p_fc[t]*1000/LHV) #efficiency fuel cell
    #H2 Tank
    @constraint(m, h2_tank[t]<= h2_tank_nom*h2_max) #max H2 tank capacity
    @constraint(m, h2_tank[t]>= h2_tank_nom*h2_min) #min H2 tank capacity
    if t<time_model
        @constraint(m, h2_tank[t+1]== h2_tank[t]+ q_h2[t+1]-fc_h2[t+1]/eta_tank) #H2
    ↪ tank balance (kg H2)
    end
end

#Grid
for t in time_simulation #overconsumption calculation as max{0, p_grid[t]-p_con_grid})
    @constraint(m, p_over[t]>=p_grid[t]-p_con_grid)
    @constraint(m, p_over[t]>=0)
    @constraint(m, p_over[t]<=(p_grid[t]-p_con_grid) + M*(1-y[t]))
    @constraint(m, p_over[t]<= M*y[t])
end
```

```
#Costs
@expression(m, cost_pv, CAP_pv*p_pv_nom+ OM_pv*p_pv_nom) #MUSD
@expression(m, cost_bg, CAP_bg*p_bg_nom + OM_bg*p_bg_nom) #MUSD
@expression(m, cost_bess, CAP_bess*p_bess_nom + OM_bess*p_bess_nom) #MUSD
@expression(m, cost_ele, CAP_ele*p_el_nom + OM_ele*p_el_nom) #MUSD
@expression(m, cost_tank,(CAP_tank*h2_tank_nom)/1000) #MUSD
@expression(m, cost_fc, CAP_fc*p_fc_nom + OM_fc*p_fc_nom) #MUSD
@expression(m, cost_grid_en, C_grid*sum(p_grid[t] for t in time_simulation)) #MUSD)
@expression(m, cost_grid_p, C_con_grid*p_con_grid*months) #MUSD)
@expression(m, cost_grid_over, C_over_grid*(sum(p_over[t] for t in time_simulation))) #
    ↪ MUSD
@expression(m, cost_grid, (cost_grid_en + cost_grid_p+cost_grid_over)/1000) #MUSD
@expression(m, TC,(cost_pv+cost_bg+cost_bess+cost_grid+cost_ele+cost_tank+cost_fc)
    ↪ ) #MUSD

#Emissions
@expression(m, Emi_grid, E_grid* sum(p_grid[t] for t in time_simulation)) #ton CO2-eq
@expression(m, Emi_biogas, E_biogas* sum(p_bg[t] for t in time_simulation)) #ton CO2-
    ↪ eq
@expression(m, TE, (Emi_biogas+Emi_grid)) #ton CO2-eq

#Objective Function
if k==1
    @objective(m, Min, TC) #min costs
elseif k==2
    @objective(m, Min, TE) #min emissions
elseif k==3
    @constraint(m, TE<=TE_non-w*(TE_non-TE_ideal)) #min costs & emissions
    @objective(m, Min, TC)
end

#Optimization
@time optimize!(m);
```

PRINT RESULTS

```
if k==1 || k==2 || k==3
    println()
    println("PV array")
    println("The number of PV panels is ", value.(n_pv))
    println("The nominal power of the PV array is ", value.(p_pv_nom), " MW")
    println()
    println("Biogas generator")
    println("The nominal power of the biogas generator is ", value.(p_bg_nom), " MW")
    println()
    println("Grid")
    println("The power contracted from the grid is ", value.(p_con_grid)," MW")
    println()
    println("BESS")
    println("The BESS capacity is ", value.(p_bess_nom), " MWh")
    println()
```

```
    println("H2 Storage")
    println("The electrolyzer capacity is ", value.(p_el_nom), " MW")
    println("The fuel cell capacity is ", value.(p_fc_nom), " MW")
    println("The H2 tank capacity is ", value.(h2_tank_nom), " kg H2")
    println()
    println("Costs")
    println("The total cost of the HRES is ", value.(TC), " MUSD")
    println("The cost PV is ", value.(cost_pv), " MUSD")
    println("The cost biogas is ", value.(cost_bg), " MUSD")
    println("The cost BESS is ", value.(cost_bess), " MUSD")
    println("The cost electrolyzer is ", value.(cost_ele), " MUSD")
    println("The cost H2 tank is ", value.(cost_tank), " MUSD")
    println("The cost fuel cell is ", value.(cost_fc), " MUSD")
    println("The cost grid is ", value.(cost_grid), " MUSD")
    println()
    println("Emissions")
    println("The total emissions are ", value.(TE), " ton CO2-eq")
else
    println()
    println("Insert a valid value of k")
end
```